Norwegian University of Life Sciences
Sciences and Technology
Building and environmental technology

Philosophiae Doctor (PhD)
Thesis 2022:77

Resolving snow challenges for increased deployment of photovoltaic systems

Løsninger på utfordringer knyttet til snø for økt utbredelse av solcelleanlegg

Iver Frimannslund

Resolving snow challenges for increased deployment of photovoltaic systems

Løsninger på utfordringer knyttet til snø for økt utbredelse av solcelleanlegg

Philosophiae Doctor (PhD) Thesis

Iver Frimannslund

Norwegian University of Life Sciences
Faculty of Science and Technology
Department of Building and Environmental Technology

Ås (2022)

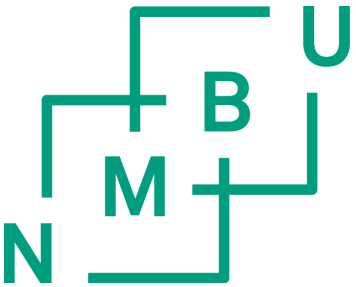

Thesis number 2022:77
ISSN 1894-6402
ISBN 978-82-575-2030-4

Abstract

Photovoltaic (PV) systems are becoming more competitive due to a cost reduction of the technology and increased electricity prices. As the technology extends to cold climates with lower irradiance, a knowledge gap in how PV systems are affected by the environment arises, which can limit PV system deployment. This thesis focuses on the impact of snow, which is perhaps the most distinguished environmental impact compared to the high irradiance climates where PV systems traditionally have been deployed. An interdisciplinary perspective is used to investigate different snow challenges connected to the deployment of PV in cold climates, and how they can be resolved.

One of the challenges explored in the thesis is the development of snowdrifts in ground mounted PV plants. This challenge is relevant for PV systems installed in exposed snowdrift climates. To document the challenge itself, field measurements of snowdrift development in a small-scale PV plant in a polar climate were performed. The study concludes that PV plants designed with established principles commonly used at lower latitudes are susceptible to snowdrift accumulation. To achieve a snowdrift resilient plant, the design of the plant itself can be adapted. This strategy is further investigated in a numerical study using Computational Fluid Dynamics and energy yield simulations to quantify the impact of changing the design parameters on the snowdrift accumulation conditions and the energy yield. It is found that all the design parameters can be adjusted to improve the snowdrift conditions, with variable effect on the yield. Based on these results, adaptions to local climate conditions can be made to increase the snowdrift resiliency of the PV plant while minimizing an adverse impact on the yield, enabling the use of ground mounted PV plants in exposed snowdrift climates.

Another of the investigated snow challenges is the use of active snow mitigation with PV systems on existing building roofs. Such systems reduce heavy snow loads so that roofs which lack structural capacity can be utilised for PV power production. In the thesis, PV snow mitigation systems are analysed in two separate studies focusing on the influence of active snow mitigation with PV systems on (i) the structural safety of building roofs, and (ii) the energy consumption and production compared to ordinary PV systems. The results provide a foundation for estimating which structures and climates PV snow mitigation systems are suitable. The research address former knowledge gaps for the use of PV snow mitigation systems and can contribute to increased utilisation of roof area for PV power production in the built environment.

Snow contributes to an uncertainty in the yield of PV systems as it is difficult to predict snow shedding from the PV modules. There are several models for estimating yield losses in PV systems based on empirical data of snow shedding, but due to being developed based on single systems, the applicability to different configurations in different snow climates are limited. With the intent of achieving a model with wider applicability, an existing snow loss model is improved by considering the influence of snow depth on the snow shedding. By applying the model to seven different PV systems in different snow

climates, the error in estimation of snow loss is reduced by 23 percentage points compared to the original model. The model contributes to reducing the uncertainty in PV yield estimations without the need for system specific empirical data of snow shedding.

The overall contribution of the work is to resolve specific snow challenges which limit the deployment of PV systems in cold climates. Additional snow challenges have been identified during the work with the thesis, and recommendations for paths for future work are suggested. With ongoing research on this topic, the limitations for PV deployment in cold climates can be resolved and PV systems can contribute to increased renewable energy production in cold climates.

Sammendrag

Reduserte produksjonskostnader og økte strømpriser øker konkurransedyktigheten til solcelleanlegg. Solcelleanlegg har vært mest utbredt i, og delvis blitt utviklet for, varme klima med mye stråling, men når solcelleanlegg sprer seg til kaldere klima begrenses bruken av teknologien av manglende kunnskap om klimapåkjenninger. En av de største forandringene i klimapåkjenninger i kalde klima kontra varme klima er påvirkningen fra snø. Denne avhandlingen omhandler hvordan snø begrenser bruk av solcelleanlegg og hvordan slike utfordringer kan løses.

En av utfordringene som undersøkes er snøfonndannelse i bakkemonterte solcelleanlegg. For å undersøke hvor utsatt solcelleanlegg er for snøfonndannelse er det gjennomført feltforsøk på et bakkemontert solkraftverk i et polart klima. Studien viser at solcelleanlegg som er designet ut ifra samme prinsipper som på lavere breddegrader gir en utforming som er svært utsatt for snøfonndannelse. En måte å redusere risikoen for snøfonndannelse på er å tilpasse designet av anlegget. For å undersøke denne tilpasningsstrategien er det gjennomført en numerisk studie som anvender fluidmekanikk- og energiytelsessimuleringer til å kvantifisere hvilken påvirkning det gir å endre utformingen av solkraftverket. Resultatene viser at alle de undersøkte designparameterne i solcelleanlegg kan tilpasses for å redusere risikoen for snøfonndannelse, men at de forskjellige designparameterne gir forskjellig påvirkning på energiytelsen. Resultatene fra disse studiene gir et grunnlag for å tilpasse utformingen av solkraftverk til klima med betydelig snødriv samtidig som ytelsen ivaretas.

En annen utfordring som undersøkes er hvordan solcelleanlegg med snøsmeltefunksjon kan benyttes på eksisterende takkonstruksjoner som ikke tåler den totale vekten av snølasten og solcelleanlegget. I avhandlingen undersøkes det hvordan slike solcelleanlegg påvirker konstruksjonssikkerheten til bygg ved å benytte statistiske metoder. Resultatene tydeliggjør påvirkningen styringen og designet av slike anlegg har på konstruksjonssikkerheten til bygg, samt hvordan forskjellige kapasitets- og lastforutsetninger påvirker utbyttet av slike anlegg. I tillegg til påvirkningen på konstruksjonssikkerhet undersøkes energibehovet og hvilken potensiell produksjonsøkning det medfører å aktivt redusere snølasten på tak i en studie som benytter en kombinasjon av numeriske verktøy. Resultatene viser hvilke type klimatiske forhold som gir lavest energibruk og høyest økning i produksjon. En sammenstilling av resultatene fra de to studiene danner et grunnlag for å vurdere hvilke konstruksjoner og klima som egner seg for å benytte solcelleanlegg med snøsmeltefunksjon. Forskningen reduserer kunnskapshull for bruken av solcelleanlegg på tak med begrenset bæreevne og kan bidra til økt utnyttelse av eksisterende takflater til solstrømproduksjon.

Den siste undersøkte utfordringen omhandler modellering av påvirkningen snø har på solcelleanleggs ytelse. En begrensing med mange eksisterende modeller for ytelsestap fra snø er at de er utviklet med empiriske data fra ett type snøklima og ikke nødvendigvis gir gode resultater når de anvendes i andre klimaforhold. Dette forsøkes å forbedres ved å

videreutvikle en eksisterende snøtapsmodell til å ta hensyn til snødybde i avsklidningen av snø fra solcellepanelene. Sammenlignet med den opprinnelige snøtapsmodellen reduseres nøyaktigheten til modellen med 23 prosentpoeng når den anvendes til syv forskjellige solcelleanlegg. Modellen kan bidra til å redusere usikkerheten til ytelsen av solcelleanlegg i forskjellige type snøklima.

Det overordnede bidraget til avhandlingen er å løse utfordringer snø gir for bruk av solcelleanlegg. Gjennom arbeidet har det blitt oppdaget ytterligere utfordringer. På bakgrunn av dette foreslås det hva som er aktuelt å fokusere på i fremtidig forskning på solcelleanlegg i klima med snø. Videre forskning på temaet kan føre til at bruken av solcelleanlegg i mindre grad hindres av snø og til å redusere klimautslipp i kalde klima.

Acknowledgements

The process of doing a PhD has been a journey and I want to thank all the people who have helped guiding me through and who have made this time period more enjoyable.

First of all, I want to thank my main supervisor, Thomas Thiis. Showing what research could be while I was a mast student become an inspiration for undertaking a PhD. Thank you for the knowledge you have shared during this period, for good company, patience and for still being an inspiration. Furthermore, I want to thank my co-supervisors for their support. Performing field measurements in Svalbard would have been a lot more difficult and a lot less pleasant hadn't it been for hospitality and Svalbard wisdom of Arne. Also, a huge thanks goes to Bjørn for the continued support and helping me in making the work relevant for the PV industry.

The laborious work in doing field measurements at a latitude of 78°N have made me humble to the efforts required to perform such tasks, and grateful for the received collective help. Thanks to UNIS and the Arctic Technology department for their efforts, to Sebastian Sykora and Tom Ringstad for help with logistics and logging equipment, and to Avinor, PowerControls and CyboEnergy for providing PV system components.

Back at the NMBU, I want to thank all friends and colleagues who I've shared my time with during the PhD period. Thanks for all the shared lunches, coffee breaks, and random corridor conversations. A special thanks goes out to the PhD students I've somewhat shared the PhD process with, such as Dag, Stergiani, Effie, Bjørn, Philip, Lars, Erlend and Veronica.

In a less professional context there are a lot of people who I want to thank. I have at times been quite focused on the PhD, and I would like to show my appreciation friends and family who have shown patience for the process. Thanks to my family, especially my parents, Gorm and Guri, as well as my sister, Trine, for always having an open door to stop by and forget all worries. An unlimited amount of thanks and love goes at to my partner, Helene, who have always been so positive throughout the PhD period. Thanks for being a good listener and all the compassion during this period. Among friends, I want to thank you for helping me to disconnect, which can be an underrated factor in succeeding with a PhD. A big thanks goes out to Henrik, Lone, Snorre, Kim, Bror, Jordal friends, Elvebakken friends, Bøler friends and all other uncategorisable friends. Looking back, I am grateful for all the experienced which have helped me grow during the PhD. Now, I am primarily just excited for the future.

List of Papers

Paper I
Frimannslund, I., Thiis, T., Aalberg, A. & Thorud, B. (2021). Polar solar power plants: investigating the potential and the design challenges. *Solar Energy*, 224: 35–42.

Paper II
Frimannslund, I., Thiis, T., Ferreira, A. & Thorud, B. (2022). Impact of solar power plant design parameters on snowdrift accumulation and energy yield. *Cold Regions Science and Technology*, 201.

Paper III
Frimannslund, I., Thiis, T., Kohler, J. & Aalberg, A. Reliability of building roofs with photovoltaic systems with active snow mitigation. Manuscript in preparation.

Paper IV
Frimannslund, I., Thiis, T., Skjøndal, V. & Marke, T. Energy demand and yield enhancement of photovoltaic snow mitigation systems. Submitted manuscript.

Paper V
Øgaard, M., Frimannslund, I., Riise, H. & Selj, J. (2022). Snow loss modelling for roof mounted photovoltaic systems: improving the Marion snow loss model. *IEEE Journal of Photovoltaics*, 12: 1005–1013.

Supplementary Paper I
Frimannslund, I. & Thiis, T. (2019). A feasibility study of photovoltaic snow mitigation systems. *Technical Transactions*, 7: 81–96.

Table of contents

1. Introduction

1.1 Motivation

A main challenge for humanity is mitigating climate change by reducing greenhouse gas emissions. Meeting this challenge involves the transition from fossil fuels to renewable energy sources, which must occur rapidly to achieve the 1.5-degree goal set in the Paris Agreement. To achieve this goal, the installed capacity of renewable energy sources must increase from 2 800 to 27 700 GW before 2050 (IRENA, 2021). The increase in capacity from renewable energy sources entails a mix of technologies to which solar power is predicted to be a major contributor.

PV technology has been developed predominantly in climates with high irradiance, which has been a key factor for its economic success. The environmental effects of these climates have, to some extent, governed the design and research of PV systems. However, with the recent development of cost reduction of PV (Kavlak et al., 2018) and an increase in electrical power prices in July 2022 (IEA, 2022), PV technology has become increasingly competitive in climates with lower irradiation. The dispersion of the PV system to cold climates influences the environmental effects PV systems are subjected to, where the impact of snow can be especially significant. The effects of snow on PV systems are manifold: snow can impact the mechanical resiliency of PV systems; limit the infrastructure on which they can be mounted; and both positively and negatively affect the yield. The effects of snow have governed the design of infrastructure in cold regions and as PV systems become increasingly prevalent in such climatic regions, it will be necessary to adapt the PV technology as well. This thesis focuses on the challenges of snow in the deployment of PV systems and how such challenges can be resolved.

Figure 1. PV plant affected by snowdrift development at the Princess Elizabeth station in Queen Maud Land, Antarctica. (SMA Solar Technology AG, 2019).

1.2 Structure of the thesis

This thesis is written in the form of a binding article comprising individual research works (i.e., papers). The binding article synthesises the individual papers and presents an overview of the research reported in them.

An attempt was made to structure the thesis in a logical manner according to the order in which the research was conducted. First, the background section presents the theories and concepts that underlie the work presented in this thesis. Subsequently, snow challenges are categorised and knowledge gaps are identified. The aims and research questions that guided the thesis are then presented. The results section provides a summary of the individual research works, all of which are related to the research questions. In the discussion section, the research questions are addressed and the implications of the findings and future work are discussed. In the last chapter, the conclusions of the thesis are presented.

The research papers are provided in full as attachments to the thesis. They include detailed information that is partly omitted from the binding article for the sake of conciseness.

2. Background

2.1 Environmental effects on PV systems

PV systems are widely impacted by the environment, which influences the system in several ways. During its lifetime, a PV system is subjected to abrupt environmental loads (Jelle, 2013; Stathopoulos et al., 2012), long-term environmental degradation (Jordan & Kurtz, 2013; Kim et al., 2021), and climatic phenomena influencing the yield (Mustafa et al., 2020; Pawluk et al., 2019). In PV projects, the influence of the environment is considered in site selection, electrical and mechanical design, performance calculations and plant maintenance planning. Knowledge of the influence of the environment on PV systems is necessary to ensure that the PV system can withstand environmental effects over its lifetime and to optimise the performance of PV systems. Such knowledge is a key factor in the successful deployment of PV systems on a global scale.

The environmental effects on a PV system vary greatly depending on the climate. In warmer climates, wind is the dominant environmental load for the mechanical resiliency of a plant, often governing the mechanical design (Stathopoulos et al., 2012). Much attention has also been directed towards dust and dirt on photovoltaic panels (Maghami et al., 2016), which is an especially important topic in arid regions with infrequent rain. Other environmental influences that are also considered in the PV industry in temperate climates are thermal stresses, seismic loads, geotechnical stability and chemical degradation.

The following sections address different topics that are relevant for the deployment of PV systems in colder climates and for the understanding of the work conducted in the thesis.

2.2 PV yield performance in cold climates

The extension of PV technology to cold climates impacts the performance of PV systems in several ways and require considering different phenomena compared to warmer climates to achieve an optimised system performance.

The lower ambient air temperatures in cold region climates have a favourable effect on the performance of PV systems. Decreasing the cell temperature results in a slightly lower photogenerated current and a more significant increase in voltage, giving the combined effect of increasing the power output by a module from 0.35–0.5% / K. The influence of climate over time on the performance of PV systems can be quantified with the performance ratio. The performance ratio is defined as the power output of a PV system in real climatic conditions compared with the power output of the system in fixed test conditions for PV modules (known as the standardised test conditions (STC)). A performance ratio of 100% equals the performance of a PV system under STC. Several previous studies have shown an indirect correlation between increasing latitude and

increasing performance ratios due to the influence of temperature (Ascencio-Vásquez et al., 2019; Bayrakci et al., 2014). In polar climates, the performance ratio can be as high as 95% and as low as 75% in arid climates around the equator (Ascencio-Vásquez et al., 2019).

In a colder climate, the prevalence of snow increases, creating several challenges and opportunities for the use of PV systems. Intuitively for many, snow can shade the module surface and decrease the received irradiance by the modules, inducing what is commonly referred to as *snow loss*. The snow loss in a PV system has a non-linear relationship with the snow-covered module area, which is due to the series connection of cells in modules and the series connections of several modules in strings, resulting in a production that is restrained by the lowest producing cell or module in the string (Woyte et al., 2003). Thus, even a partial snow coverage in a PV system can produce significant snow loss. The snow loss in a PV system is strongly associated with the climatic conditions in which the PV system is situated (Pawluk et al., 2019). However, several factors related to the design of PV systems have been shown to influence snow loss. Increasing the tilt of the modules increases the sliding of snow (Andrews et al., 2013). The frames of the modules strongly affect snow adhesion (Riley et al., 2019), and the orientation of the module (landscape/portrait) has been shown to influence snow shedding due to the connection of the strings (Burnham et al., 2019). Moreover, increasing the height of the system can ensure that sliding snow is completely transported off the module (Heidari et al., 2015). The use of bifacial modules (i.e., PV modules that produce power from irradiance received on both sides) has been shown to reduce snow loss from 16% to 2%, which is due to enhanced snow shedding caused by the heat generated by power production from irradiance received on the exposed back side (Hayibo et al., 2022). Additionally, hydro- or icephobic coatings can be applied to the module surface to reduce adhesion (Andersson et al., 2020), and active heating methods can be applied to ensure that snow slides off the modules (Husu et al., 2015).

Quantifying snow loss in PV systems is important for several reasons. Accurate snow loss modelling contributes to better yield estimates, decreasing the financial uncertainty in PV projects. Additionally, the snow alter the electrical signatures produced from PV systems which can disturb passive fault detection of PV systems based on the production data (Skomedal et al., 2021). There are several suggested models for estimating snow losses in PV systems that derive empirical coefficients for the influence on the yield based on observations of snow shedding (Pawluk et al., 2019). However, as such models often are based on observations from a limited set of configurations in certain climatic conditions and have limited applicability to systems with different configurations in different climatic conditions (Øgaard et al., 2021a). Therefore, there is a need for easy-to-use snow loss models that are applicable to a variety of systems in different climatic conditions. The need for better methods to quantify snow loss is exemplified by the Norwegian standard for the calculation of energy use in buildings, in which fixed monthly snow loss values are derived from different climate zones in Norway (Standard Norge, 2021), without consideration of system configurations and local topographical conditions.

However, snow does not only affect the yield of PV systems adversely. Freshly fallen snow has an albedo of 90% and increases the amount of reflected irradiance from the ground (Giddings & LaChapelle, 1961). This increases the potential for bifacial PV which produce power from the irradiance received on both sides of the module. The amount gained by using a bifacial module compared with a monofacial module is termed bifacial gain (Guerrero-Lemus et al., 2016). This gain has been documented to be as high as 19% in the winter months (Hayibo et al., 2022). In addition to producing power from the irradiance received on the back side, bifacial modules enhance snow shedding because of the heat generated from power production (Granlund et al., 2019). Increased PV power production due to reflective snow cover on the ground are not only relevant for bifacial PV systems, but they also positively impact the yield of façade systems.

2.3 Wind-transported snow

The aeolian processes initiated by wind can redistribute uniform snow covers to a great extent. The physics of the wind transported snow can be explained by the force the wind exerts upon a particle (Bagnold, 1941). A parameter determinative for this force is the *friction velocity* or *shear velocity*, which is the shear forces occurring at ground level formulated in terms of velocity. Particle deposition and erosion in fluid flows is can be determined by the value of the friction velocity in relation to a threshold friction velocity (Tominaga, 2018). A threshold friction velocity is the limit separating particle erosion and deposition. For friction velocities above the threshold friction velocity, particle erosion occurs, while for friction velocities below the threshold, deposition occurs. The threshold friction velocity of snow ranges from 0.07–0.25 m/s for fresh snow and 0.25–1.0 m/s for old, wind-hardened snow (Gray & Male, 1981).

Deposition of wind-transported snow typically occur in sheltered areas such as terrain depressions and the windward side of ridges (Jaedicke, 2001) or in the aerodynamic shade of objects (Thiis & Ferreira, 2014). Mounds of snow deposited by the wind is commonly referred to as snowdrifts. Snow redistribution is important in the design of infrastructure as wind can create large, ununiform loads. In the context of snow redistribution in PV plants, the literature predominantly focusses on how the presence of PV systems influence snow erosion and deposition on building roofs. Compared to an exposed roof surface, the installation of a tilted PV systems with multiple rows is generally expected to increase snow loads on building roofs. Grammou et al. (2019) and Brooks et al. (2016) used water flume simulations to investigate the drift patterns from PV systems on building roofs and showed how the wind direction in relation to the orientation of the panels influence roof snow loads. Thiis et al. (2015) and Ferreira et al. (2019) used wind tunnel measurements and numerical simulations to investigate how the configuration of the panels influenced erosion and deposition patterns. Although the PV panels generally decrease the friction velocity on roof surfaces, elevated panels leaning against the wind can potentially increase the erosion of snow on the roof (Thiis et al., 2015). To the knowledge

of the author, no previous study has investigated the redistribution of snow in ground-mounted solar power plants.

2.4 Snow load in building design

The design of buildings to withstand snow load is more developed than in the design of PV systems. This section covers how snow load is considered in building design as this can be inspiration for the design of PV systems, and as the snow load design of buildings can influence PV deployment on building roofs.

The occurrence of roof snow load is a complex process which vary significantly with local topography and with the characteristic of the roof structure (Meløysund, 2010). Structural design standards aim to give simplified provisions for estimating the roof snow loads, which involves reducing the complexity of the occurrence of snow load. In design standards such as ASCE-7, ISO4355 and EN1991-1-3, the snow load to be used in the design is commonly calculated as the ground snow load multiplied by different factors that influence the snow load on the roof. Equation 1 shows formula for calculating the roof snow load according to EN-1991-1-3 (CEN, 2003):

$$S = \mu_i C_e C_t S_k \tag{1}$$

where S is the design snow load, μ_i is the shape coefficient, C_e is the exposure coefficient, C_t is the thermal coefficient and S_k is the ground snow load (also referred to as the characteristic snow load).

Snow loads exhibit large yearly variations and are often best represented by extreme value distributions, such as a Gumbel or log-normal distribution. To determine the magnitude of the ground snow load used in a design, a value with a desired probability of being exceeded is used. The probability threshold used varies according to the standard (Croce et al., 2019). EN-1991-1-3, ASCE-7 and ISO4355 use 0.02 as the threshold, representing a return period of 50 years, which is the design working life of common building structures (CEN, 2002).

The geometric shape of the roof influences the spatial distribution of snow on it, as well as snow erosion and sliding. This is accounted for by the shape coefficient (μ_i) In Equation 1. As the distribution of snow load on the roof can be either uniform or non-uniform depending on the influence from wind and snow sliding, different load scenarios must be considered. A balanced snow load scenario accounts for the snow load distribution with little influence from wind, while unbalanced snow load scenario accounts for a redistribution of the load on the roof. The structure must be designed to withstand both load scenarios. For flat roofs, a shape coefficient of 0.8 is commonly used, indicated by Thiis and O'Rourke (2015) to be a conservative estimate.

As described in the previous section, PV panels influence aerodynamic patterns on roofs, which can increase snow loads. A proposal in the second generation of the Eurocode

on snow load on structures for a flat roof shape coefficient accounting for the presence of PV panels on the roof snow load from Formichi (2019) is given in Equation 2:

$$\mu_P = \frac{\gamma\, h}{S_k} \qquad \text{with} \qquad \mu_i \leq \mu_P \leq 1 \tag{2}$$

where μ_P is the shape coefficient in the PV system, γ is the snow density, h is the PV panel height, S_k is the ground snow load and μ_i is the shape coefficient (0.8 for flat roofs). Thus, mounting PV panels on building roofs can give a 20% increase in the design roof snow load, depending on the height of the panels compared with the height of the snowpack.

2.5 Structural reliability

The deployment of PV systems on building roofs influences the structural reliability of the building, a topic investigated in this thesis. Structural reliability is a discipline within structural engineering dealing with the optimisation of the capacity of structures to achieve a desired structural safety (Melchers & Beck, 2018). Structural reliability theory is built upon probabilistic concepts to quantify the probability of a structural failure. Limit state functions are used to in reliability analysis to quantify the probability of exceeding a given limit state, and is commonly expressed as given in Equation 3:

$$Z(X) = R - E \tag{3}$$

where $Z(X)$ is the limit state function of the basic variables, R is the structural resistance of the component and E is the load imposed on the component. The basic variables that govern R and E are represented as uncertain variables with probability distributions.

Limit state functions represent different types of limit states, including the collapse of a structure (ultimate limit states) or the disruption of normal use (serviceability limit states) (Melchers & Beck, 2018). The limit state function is solved by applying several methods, such as FORM, SORM or the Monte Carlo method, to yield the probability of structural failure (P_f). The Cornell Reliability Index (Cornell, 1971) is commonly used as a measure of structural safety, which is defined according to Equation 4:

$$\beta = -\Phi^{-1}(P_f) \tag{4}$$

where β is the reliability index and φ is the cumulative distribution function of the normal function. Structural safety levels are determined according to the building category and the consequences of a structural failure. Table 1 shows the minimum safety levels required by the Eurocodes.

Table 1. Reliability class and minimum values for β according to EN-1990 (ultimate limit states) (CEN, 2002)

Reliability class	**Minimum values of β**	
	One year reference period	50 years reference period
RC1	5.2	4.3
RC2	4.7	3.8
RC3	4.2	3.3

In structural design standards, the desired structural safety level is achieved using the load and resistance factor design (LRFD) method, where partial factors are used to scale the capacity of the structure according to the characteristics of the imposed loads and the structural material (Ravindra & Galambos, 1978). Partial factors account for uncertainty related to the respective load and material, and are commonly calibrated to achieve the desired safety requiring little resources in the design of buildings.

However, the structural safety of the building stock is not uniform, and many buildings a reliability lower than stated in current requirements. This occurs due to imperfect calibration of the partial factors (Köhler et al., 2019; Vitali et al., 2019), due to provisions changing over time, and due to provisions being adopted differently at a national level (Druķis et al., 2017; Meløysund et al., 2006). Although lower reliability than the criteria for new structures is acceptable for existing structures (Sýkora et al., 2016), many structures are in need of measures to increase the structural safety. This can be achieved by reducing the uncertainty in the structures capacity through inspection (Sykora et al., 2010), with Structural Health Monitoring (SHM), with structural reinforcement, or with snow mitigation measures for buildings in climates with snow (Diamantidis et al., 2018).

2.6 PV snow mitigation systems

The lack of structural capacity in existing structures can be a limiting factor for the deployment of PV systems. PV systems impose an additional load on roof structures, which adversely impacts structural reliability. Additionally, a roof-mounted PV system can obstruct manual snow removal on buildings that rely on such measures.

PV snow mitigation systems are intended to increase the structural reliability of existing building roofs by actively melting roof snow loads. Such systems function by monitoring the snow load on the roof with load cells installed on individual modules and initiating melting when the snow load exceeds a defined threshold limit. The technological methods used to melt snow differ. The forward bias method involves applying power to the PV system using rectifiers, which create heat production in the modules by their electrical resistance (Yan et al., 2020). Another method is to use electrical wires at the back of the PV modules (often with insulation on top) connected to a separate electrical circuit as researched by Anadol (2020) and Rahmatmand et al. (2018). Alternatively, heat can be

transferred from a liquid medium in a closed circuit at the back of the modules powered by a heat pump.

PV snow mitigation systems are commonly designed with a low angle tilt with modules facing each other so that the snow does not slide off the module surface during melting, as shown in Figure 2. Common in PV systems on large flat roofs, this configuration achieves high utilisation of the roof surface. Meltwater is removed from the roof, either passively on the roof surface to scuppers or with the use of heated gutters to avoid refreezing.

Figure 2. A typical PV snow mitigation system installed on a warehouse roof in Oslo. The system was designed by Innos (2022).

When addressing PV systems with snow melting capabilities, it is important to differentiate between systems that are designed to reduce snow loads from systems that are intended to increase the yield by enhancing snow shedding on the modules. These two uses of melting snow operate differently. When the intention is to reduce the snow load, melting is only initiated for high snow loads compared with the yield enhancement purpose, which initiates melting for small snowfalls as well. This thesis focuses on the use of a PV snow mitigation system to reduce snow loads and increase the deployment of PV systems on existing building roofs.

2.7 PV systems in polar regions

PV has long been used in Polar regions for technical installations such as weather stations and telecommunication equipment (Tin et al., 2010), but now a market for larger PV systems is emerging. In both the Arctic and in Antarctica, there are several remote settlements that traditionally have relied on fossil fuels. The energy consumption for such

settlements is often high, not only because of low temperatures but also because of the extensive use of vehicles for transportation (Tin et al., 2010).

Moreover, the transport of fuel to remote polar settlements is costly and significantly adversely impacts the levelised cost of electricity (LCOE). Renewable energy systems, such as PV systems, are commonly autonomous in operation and require little maintenance. If PV systems can be successfully deployed in a harsh polar climate, fuel dependency can be reduced, thus decreasing costs and GHG emissions (Ringkjøb et al., 2020). This was demonstrated by Merlet (2016), who estimated that a solar power plant "fuel saver" at the Norwegian research station in Antarctica covering 50% of the consumption can reduce the LCOE by 50%.

The potential for solar power in remote polar settlements is significant. Store Norske Spitsbergen Coal Company (2022) identified 1 500 off-grid settlements in the Arctic that mainly rely on fossil fuels. In Antarctica, 75 active research stations rely mainly on fossil fuels (Tin et al., 2010). In Norway, the energy supply for the largest northernmost city of Longyearbyen in Spitsbergen is currently being much debated as the coal power plant is being decommissioned and a cleaner source of energy is desired. Thus, there is a marked for PV plants in polar regions, but the use of the technology in such climatic conditions is poorly documented in research on PV systems.

3. Knowledge gaps, aims and research questions

The literature review in the previous section provided a background for understanding the challenge of snow in the deployment of photovoltaic systems. The following section categorises different types of snow challenges and identifies gaps in the knowledge about the occurrence of and solutions to such challenges. The identified knowledge gaps give a basis for stating the aims and research questions of the thesis.

3.1 Snow challenges

In this thesis, the term snow challenges refers to any obstacle to the deployment of PV systems in cold climates. These challenges are not considered permanent. Instead, compared with climates without the significant influence of snow, they require adaptation. A categorisation of the challenges is shown in Figure 3.

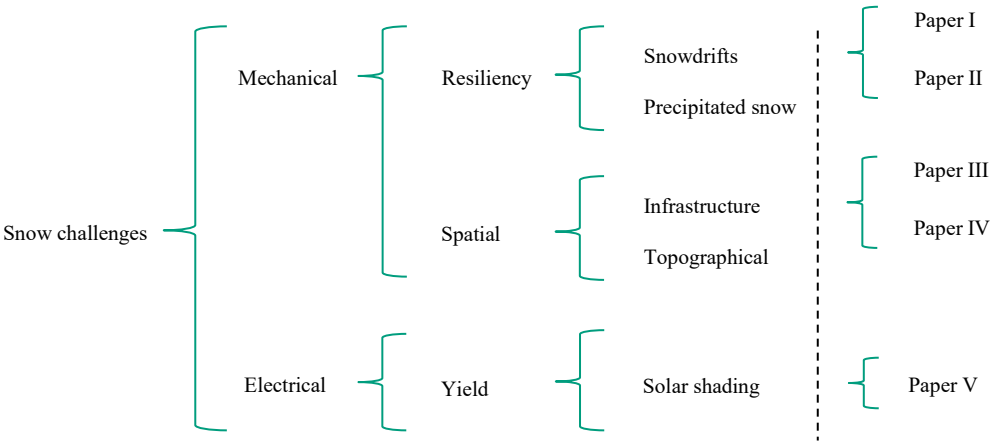

Figure 3. Snow challenges for photovoltaic (PV) systems and their relationship to the individual papers that comprise this thesis

Snow challenges were first divided into two main categories—mechanical and electrical—according to the two fields which PV design is commonly performed. Herein subdivisions are made which are defined in the following paragraphs. The categorisation focuses on snow challenges as they are currently considered in science. Other aspects, such as the communication of research to consumers or industry, which may also be a significant barrier to the deployment of PV systems, are beyond the scope of this thesis.

3.1.1 Resilience challenges

Resilience challenges occur as the load imposed from snow can damage PV systems. The resilience challenges can be resolved through improving the design and robustness of the system. A distinction is made between the resilience of PV systems against the snow loads as a result of precipitated snow, and resilience against snowdrifts. The distinction between precipitated and snowdrift loads is a simplification as snow in PV systems will be a consequence of both precipitation and redistribution, but it is conducive for the understanding of the resilience of PV systems to differentiate between the type of snow load.

Precipitated snow that is not significantly influenced by wind gives a uniform layer of snow on the downfall area. Prevalent in sheltered climates, such conditions can be related to the exposure coefficient for sheltered climates in the snow load standards of ISO and CEN. In PV systems, precipitated snow is commonly affected by sliding snow dependent on the system tilt and climatic conditions. Thus, in PV systems, precipitated snow loads either occur uniformly on the panels (common in low tilt configurations), or they may slide and build up at the underlying surface (common in high tilt configurations). Because precipitation is usually uniform over short distances, a PV system with a specific configuration can exhibit a similar loading scenario. Resilience to precipitated loads is achieved by designing solar panels and mountings with increased mechanical resistance to withstand snow loads.

Resilience to snowdrifts is relevant in climates characterised by the horizontal redistribution of snowpacks in winter. In PV systems, snowdrifts are primarily a concern in ground-mounted PV plants, as the amount of horizontally transported snow is usually significantly lower on building roofs. How PV systems influence the shape coefficient used in the design of building roofs has received attention in the literature, but knowledge of the author, no previous study has focused on snowdrifts in ground-mounted PV plants. Ground-mounted PV plants are designed differently than roof-mounted systems, as tilt is commonly increased at the expense of increased area use. Such systems often have a higher gap between the panel and the underlying surface, which increases the wind flow underneath the surface. There is a marked for PV plants in remote polar climates, but a knowledge gap exists regarding the susceptibility of PV plants designed according to established principles of snowdrift accumulation, the consequences of snowdrifts in the plant and potential solutions to the challenge.

3.1.2 Spatial challenges

Spatial challenges occur as snow may influence the available area for installing PV systems. The spatial challenges occur both for systems mounted on existing infrastructure or ground mounted systems at locations with certain topographical characteristics.

Snow can limit the deployment of photovoltaic systems on existing infrastructure with limited structural capacity. This is due to PV systems contributing with additional weight, preventing manual snow removal as well as influencing the snow erosion and passive heat transfer on building roofs. The methods used to estimate PV rooftop potential often do not consider the limitations arising from limited structural capacity (Melius et al., 2013), although this is a known challenge (Richards et al., 2011). Consequently, studies on PV rooftop potential may overestimate the available area for installation. As elaborated on in section 2.6, the use of PV snow mitigation system can be a potential solution to utilise roof area characterised by limited structural capacity. However, the impact of active snow mitigation with PV systems on the structural safety has not been analysed in the scientific literature. A part from a case-study from Diamantidis et al. (2018) analysing the use of snow load monitoring and mitigation on an existing structure, there are few relevant studies focusing on active snow mitigation on building roofs. Knowledge is lacking for the impact of PV snow mitigation system on the structural reliability, including which structures are suitable for having such systems and how the function of such systems influences the reliability. Work on the topic can also be relevant for standardisation organisations as PV snow mitigation systems are increasing in popularity and provisions on such systems can contribute to increased deployment of PV systems in the built environment with a desirable impact on the structural safety.

Another knowledge gap in the use of PV snow mitigation systems is the amount of energy used to operate such systems, as well as how active melting may influence the yield. The energy consumption and production of PV snow mitigation system is crucial for the economic competitiveness of the technology and the future of such systems. Several studies concern the use of active snow mitigation to enhance yield (Aarseth et al., 2018; Anadol, 2020; Rahmatmand et al., 2018), but no existing studies to the knowledge of the author consider the energy use of PV snow mitigation systems which aim to reduce the load. Systems which aim to improve the structural reliability of buildings initiate melting when the snow load exceeds a threshold limit, but the amounts of snow that is removed and the energy required for doing so in different climatic conditions is not documented in scientific literature. Although PV snow mitigation systems require energy to reduce the snow load, they reduce the duration of snow coverage on the modules and can produce more as well. Thus, it is not only the energy consumption of PV snow mitigation system which is an uncertainty for its economic profitability, but also the resulting yield enhancement as well. The use of active snow mitigation with PV systems is a potential solution to overcome the spatial challenges for PV systems in the built environment, but the use of the active snow mitigation feature is limited by lacking knowledge on the influence on the structural reliability as well as the influence on the energy consumption and production.

Topographical challenges occur when the impact of snow makes a topographical area less suitable for PV installation. Examples include avalanche terrain or terrain susceptible to snow accumulation, such as ground depressions and the leeward side of ridges (Jaedicke, 2001). PV systems could be designed to be resilient in such locations but

with a significant increase in cost, which would reduce their economic competitiveness. Although the extent of the reduction of available areas due to topographical challenges has not been addressed in the scientific literature, it may become a relevant topic as PV systems become increasingly prevalent in climates with snow.

3.1.3 Yield challenges

Yield limitations occur as snow can reduce the yield of PV systems due to snow covered panels. As elaborated in section 2.2, snow losses create an uncertainty in yield estimations in PV projects which is favourable to reduce for increasing the attractiveness of PV systems. Additionally, identifying snow losses can contribute to better winter-time fault detection in PV systems (Øgaard et al., 2021a). Although the influence from snow on PV systems is researched by many, there is a lack knowledge on of snow models applicable to a variety of configurations and different climatic conditions.

3.2 Aims and research questions

The main aim of this thesis is to resolve snow challenges to increase the deployment of PV systems. The focus in this thesis is directed towards three main challenges: the snowdrift resiliency of ground-mounted solar power plants; PV snow mitigation systems on existing building roofs; and snow loss modelling on roof-mounted systems. Based on the identified knowledge gaps, research questions were formulated for each topic. The following section provides the research questions and reasons for their formulation, according to the topic.

3.2.1 Snowdrift resiliency

The resiliency of ground-mounted PV plants to snowdrifts remains undocumented in the scientific literature, and there is much uncertainty regarding the feasibility of the use of ground mounted PV plants in snowdrift climates. Therefore, the susceptibility of traditional PV plants designed at lower latitudes to snowdrift accumulation is addressed in RQ1.1:

RQ1.1

How are traditional ground mounted PV plants affected by snowdrift accumulation?

If traditional ground-mounted PV plants are susceptible to snowdrift accumulation and are barriers to their deployment, then the measures necessary to achieve snowdrift resilient power plants should be investigated. Multiple strategies can be employed to

influence snowdrift conditions in solar power plants, among which adapting the design of the plant is very relevant. This gives the basis for RQ1.2:

RQ1.2

How can PV power plants be adapted to achieve resilience to snowdrift accumulation?

3.2.2 PV snow mitigation

Active snow mitigation with PV system is a structural safety measure but has not been linked to the topic of structural reliability in scientific literature. The impact of PV snow mitigation on the structural reliability of building roofs will depend on the function of the system, as well as the capacity and load conditions on the structure, which must be considered in the investigation. This is addressed in RQ2.1:

RQ2.1

How does PV snow mitigation systems influence the structural reliability of existing roofs?

The potential for PV snow mitigation systems to utilise unused roof area with limited structural capacity strongly depends on the energy required to melt snow. Additionally, PV systems which melt snow can produce more due to decreasing the duration of the modules being covered by snow. The influence of using energy to melt snow and the resulting enhanced production have not been previously investigated in the scientific literature, which is addressed by RQ2.2:

RQ2.2

How does the snow mitigation function influence the energy balance of PV systems?

The performance of PV snow mitigation systems is sensitive to the climatic conditions. The climatic conditions can impact the feasibility of reducing the load, the energy use of the system, and the influence the system has on the reliability. Assessing the climatic performance of the system is essential to indicate where the use of PV snow mitigation systems are suitable, and in which climatic conditions they should be avoided.

Such information is useful for assessing the geographical potential of PV snow mitigation systems, as addressed by RQ2.3:

RQ2.3

What types of climates are suitable for the use of PV snow mitigation systems?

3.2.3 Snow loss modelling

Because existing snow loss models are based on measurements performed under limited climatic conditions and a limited variety of PV configurations, there is a need for snow loss models with broader applicability. Models that consider local climate and system-specific configuration can increase the accuracy of snow loss models applied to different PV projects under different climatic conditions. This is addressed in RQ3.1:

RQ3.1

How can snow loss models be improved to capture local climate?

4. Methodology

The thesis comprises individual studies that address specific research questions. In total, five research questions were addressed in five separate papers, as shown in Figure 4.

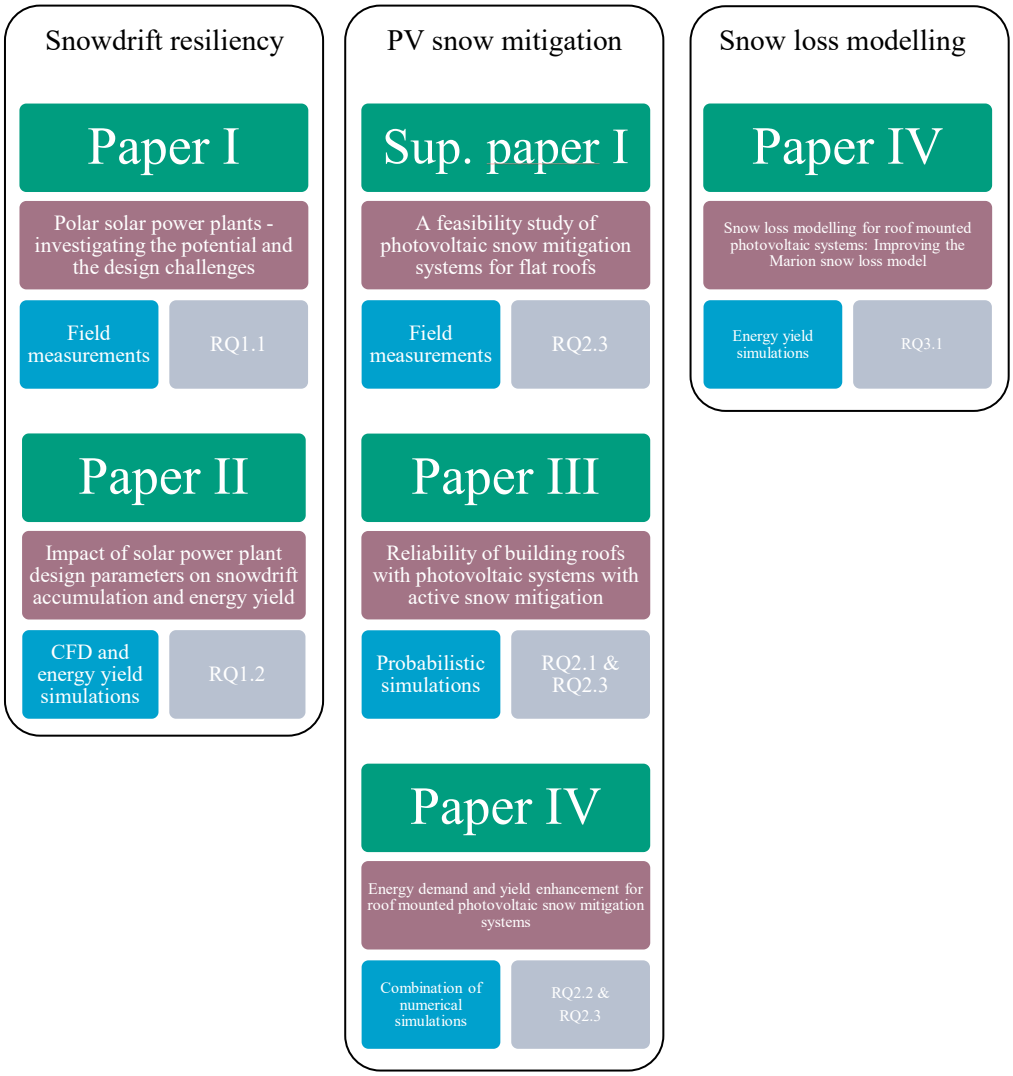

Figure 4. Overview of the individual papers, including their titles (red), methods (blue) and research questions (grey), organised by topic.

Various methods were used to address the research questions as shown in Figure 4. Paper I, "Polar solar power plants: investigating the potential and design challenges", aims to address RQ1.1, "How are traditional solar power plants affected by snowdrift accumulation?" For this purpose, field measurements were considered suitable as this would showcase the occurrence of the real phenomenon and could serve as a basis for future studies on the topic.

Paper II, "Impact of solar power plant design parameters on snowdrift accumulation and energy yield", was built on the findings from Paper I. Paper II aims to address RQ1.2: "How can photovoltaic power plants be adapted to achieve resilience against snowdrift accumulation?" Numerical simulations were chosen as the method in this study, which allowed for an efficient investigation of a variety of design adaptions. Two numerical tools were applied: computational fluid dynamic (CFD) simulations to quantify the snowdrift accumulation conditions in the plant; energy yield simulations to quantify the influence of an adaption on yield. The results reported in Paper I were used to validate both the CFD method and the energy yield simulation method.

Paper III, "Reliability of building roofs with photovoltaic systems with active snow mitigation", addressed RQ2.1: "How do PV snow mitigation systems influence the structural reliability of building roofs?" A structural reliability analysis was conducted, in which the influence of a PV snow mitigation system on the reliability of a structural component was modelled with limit state functions, which were solved using Monte Carlo simulations. This method was chosen because it is suitable for evaluating the impact of PV snow mitigation systems on structures with varying capacity and load conditions. Additionally, in this modelling approach, the influence of the function of the PV snow mitigation system could be isolated, indicating the degree to which the system could be improved to increase structural reliability.

Paper IV, "Energy demand and yield enhancement for roof-mounted photovoltaic snow mitigation system", addresses RQ2.2: "How does the use of active snow mitigation with PV systems influence its energy balance?" Because the energy demand for PV snow mitigation systems is likely to be time-variant depending on the infrequency of heavy snow loads, evaluating the energy demand over long periods was considered beneficial. The study combined the energy balance snow model (EBSM), which estimated the power consumption of PV snow mitigation system, with PV yield simulations, which estimated the yield enhancement from decreased snow cover on the modules. Probabilistic methods were also applied to determine the return period of snow loads in different climates.

Paper V, "Snow loss modelling for roof-mounted photovoltaic systems: improving the Marion snow loss model", addresses RQ3.1: "How can snow loss models be improved to capture local climate". As many existing snow loss models have limited applicability to a range of systems in different climatic conditions, this study sought to improve one of the most prominent existing models by considering additional climatic parameters. PV yield simulations were used to estimate snow loss, and the results were compared with the measured snow loss to indicate the accuracy of the model.

4.1 Interdisciplinarity

The nature of the research problems required an interdisciplinary perspective on the multiple aspects of the problem, which resulted in a research methodology that combined several known methods to address complex problems. The complexity of the methodology is related to the interdisciplinarity of the study, as illustrated in Figure 5.

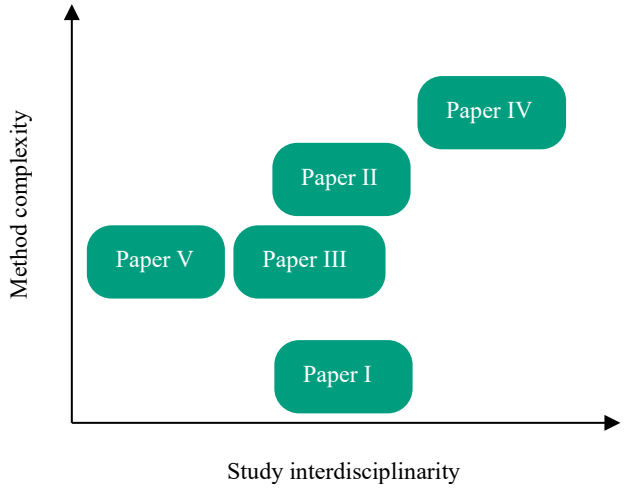

Figure 5. Interdisciplinarity of the study in relation to the complexity of the methodology

The interdisciplinary method can be challenging for readers, depending on their backgrounds. An attempt was made to adequately present the research problem and the applied method while maintaining sufficient depth in the various scientific fields in which the studies were conducted.

4.2 Validation

Validation of the findings have been important in all the conducted studies. The studies using numerical simulations are validated when possible to ensure the applicability of the method. As the research topics are not widely covered in literature, lack of data for validation have been a challenge, but sought to be overcome by connecting field measurement results to the numerical simulations. In Paper II, the methodology was validated using the results of the field measurements performed in Paper I. The reliability analysis in Paper III is not validated which is not uncommon for theoretical reliability analysis. In Paper IV, the method was validated using data collected from a commercial PV snow mitigation system. Paper V focus on the accuracy of a theoretical model compared with field measurement data from commercial PV systems and is essentially a validation study in itself.

5. Results

This chapter summarises the main findings and conclusions reported in the individual papers. The complete papers are provided in Annex A of the thesis.

5.1 Summary of Paper I, “*Polar solar power plants – Investigating the potential and the design challenges”*

Paper I field measurements are used to investigate the occurrence of snowdrifts in ground-mounted solar power plants. The measurements were conducted in the high Arctic of Spitsbergen in the Adventdalen Valley in proximity to Longyearbyen. The valley serves as a funnel for regional weather systems, giving a uniform wind direction blowing up or down the valley. A mock-up solar power plant was built on the valley floor with the intent of documenting the development of the snowdrifts. The power plant was built of wood, as it is the form rather than the material which is important for the development of the snowdrifts. Established design principles were used govern the design of the plant. The plant was facing south and the tilt and pitch were adjusted according to the solar geometry. Three PV modules were installed on the mock-up plant and connected to an inverter with individual MPPTs for each module. The modules were both monofacial and bifacial: two monofacial modules were installed facing opposite directions (one facing the ground and one facing the sky) and one bifacial module was installed with the same tilt angle. The data presented in the paper is from two years with four conducted snow depth measurements and one year with logged power production measurements.

The results of the snowdrift measurements are shown in Figure 6. The accumulation of snowdrifts increased according to the time of exposure in the field. The accumulation occurred mainly leeward of the PV arrays. Snowdrifts on the windward side in the prevailing wind direction were also observed, but they may have been caused by an irregular wind direction blowing up instead of down the valley. During the measurements, the snowdrifts did not achieve a steady state, and they increased in size with the time of exposure in the field. The snowdrifts partially buried the system, shading the panel surface and imposing a load on the array. The results indicated that a solar power plant designed with established design principles is susceptible to snowdrift accumulation in snowdrift climates.

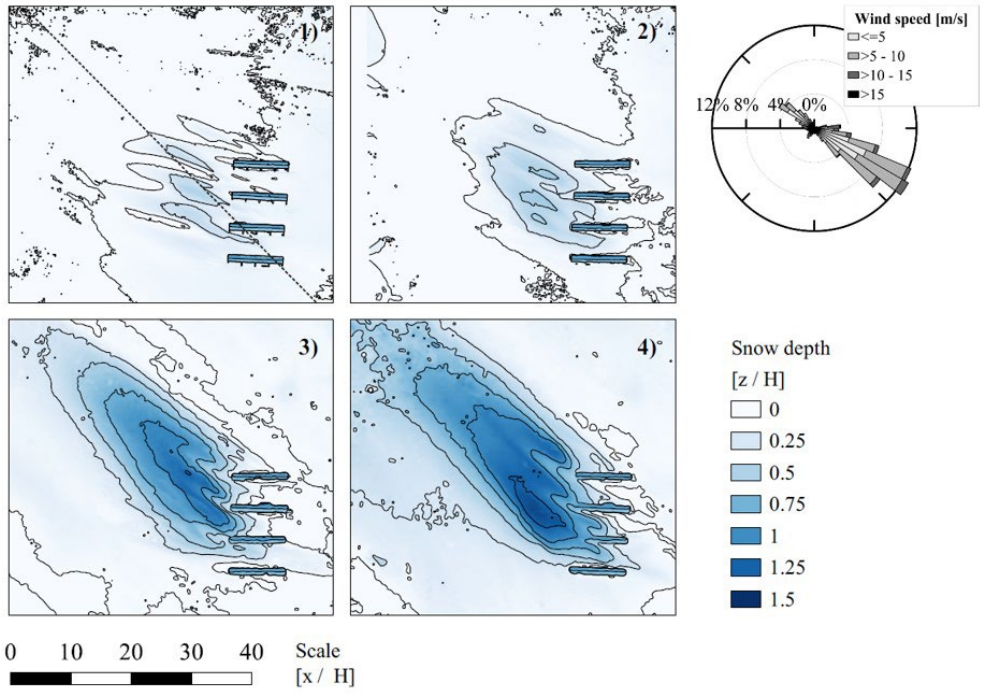

Figure 6. Snow depth in relation to panel height (H = 1.3 m) for the four measurements. The wind rose shows the statistical wind conditions at the field site.

An important finding of the study was the similarity between snowdrifts produced by PV arrays and snowdrifts produced by snow fences. The shape of the snowdrifts viewed in a cross-section perpendicular to the wind direction exhibited a strong similarity to a 50% porous snow fence (Tabler, 2003). This similarity indicated that snow fence theory can be applied to single PV arrays. Thus, the configuration parameters of PV system design can be applied to the properties of snow fences to indicate the impact of design adaptions on snowdrift accumulation. The application of snow fence theory to PV systems indicated that the accumulation could be reduced by reducing the panel tilt, increasing the gap-to-ground and adjusting the orientation of the arrays parallel to the wind direction. However, snow fences differ from PV systems in the array configuration of the latter, which include several rows of PV panels with shorter gaps (the pitch) between. This property of PV systems is not applicable to snow fence theory as snow fences are usually installed with much larger gaps so that the flow field can redevelop between them.

The results of PV power production showed a favourable influence by the polar climate. The yield of a theoretical bifacial module with an 80% bifacial factor showed a bifacial gain of 14.7%. The gains were significantly higher in spring during snow cover, which were sharply reduced as the snow melted. In Figure 7, the production profiles

indicate the characteristics of bifacial power production according to season, with increased daytime peaks in spring and midnight power production in summer.

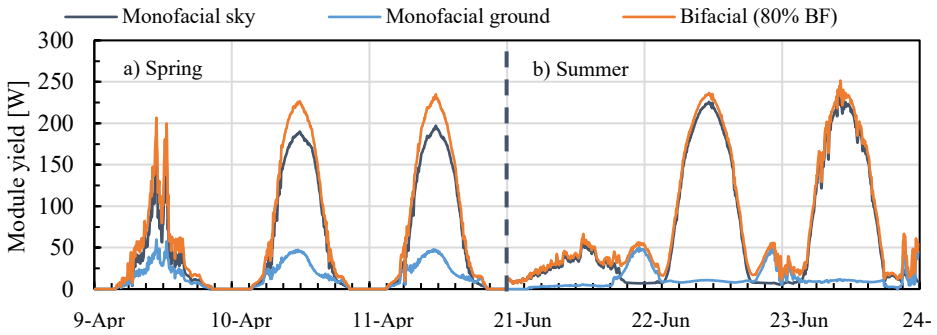

Figure 7. Production profiles on three consecutive days of modules in summer and spring

The performance ratio was calculated to determine the performance of the monofacial module under polar conditions. The performance ratio is given as the production of the system normalised by production under STC conditions for the same amount of irradiance. For the monofacial panel facing the sky, it was measured to be 92.5%, which is likely an under-estimation as it was only measured in between July and October where the influence of springtime power production was omitted. Logged backsheet temperatures significantly below the STC temperature indicated that the high-performance ratio was positively affected by low temperatures. The overall yield of the monofacial module was measured at 670 kWh/kWp/year, but as irradiance in the year the measurements were conducted was lower than the yearly average, the measured specific yield is likely an underestimation of the long-term average.

The study concludes that measures are necessary to achieve snowdrift resilient PV power plants in snowdrift climates. One way to achieve this goal is to adapt the design of the plant. However, this adapting the design of the plant can impact the yield. Thus, the challenge for PV plants in polar climates is to consider two distinctive design criteria, which may conflict if they are considered individually. The results from the power production demonstrate the potential for PV in Polar climates, which has several favourable characteristics compared to more temperate climates.

5.2 Summary of Paper II, *"Impact of solar power plant design parameters on snowdrift accumulation and energy yield"*

In Paper II, numerical simulations were used to investigate how the configuration of solar power plants could be adapted to increase resilience against snowdrift accumulation and how this adaption would influence the yield of the plant. CFD simulations were used to evaluate snowdrift accumulation conditions with friction velocity as a proxy, while energy yield simulations were used to evaluate the yield represented by the specific yield. The study quantifies the sensitivity of five solar power plant design parameters with respect to snowdrift accumulation and yield. Performance was quantified in relation to the base case design of a traditionally designed solar power plant constituting 15 rows with a footprint of 105 × 105 m. A parameter adjustment was applied to the base case, and the performance was re-evaluated. The sensitivity was then calculated as the performance of the case subjected to a parameter adjustment in relation to the performance of the base case. The investigated design parameters were panel tilt, pitch (distance between rows), gap-to-ground, orientation of the plant in relation to the wind direction, and the scale of the system. Figure 8 shows the parameters, and Table 2 shows the range of the parameters.

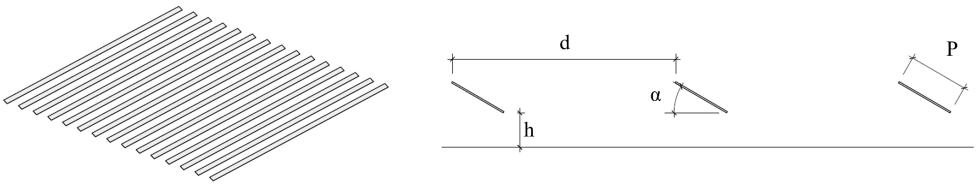

Figure 8. The parameters: panel tilt (α), pitch (d) and gap-to-ground (h). P is the panel length. The base case consists of 15 rows.

Table 2. Variation range of each parameter. The configuration of the base case is marked with an underline.

Wind Direction / Azimuth [°]	**Tilt [°]**	**Gap-to-ground [m]**	**Pitch [m]**	**Scale**
0	10	0.5	5	0.5
30	30	1.0	7.5	1.0
60	50	1.5	10	2.0
90	70	2.0	12.5	
120	90	2.5	15	
150				
180				

5.2 Summary of Paper II, “Impact of solar power plant design parameters on snowdrift accumulation and energy yield”

The simulation method was investigated in a validation study before it was applied to the study object. The validation of the CFD simulations is comprised by a comparison of measured and simulated shear stress using different turbulence models, as well as a comparison of the distribution of friction velocity with the measured snow depth from the field measurements presented in Paper I. The results from the validation is omitted from the summary but can be found in the full paper in Annex A. The energy yield simulations were validated by comparing the simulated yield of the system with the same configuration reported in Paper I with the measured yield from Paper I. A good fit is achieved, but as the irradiance is higher in the simulations, it is concluded that the simulation method likely under-estimates the yield. However, as the focus is on the relative influence of the design parameter (i.e., sensitivity), the underestimation is of little significance.

The influence of the adjusting the design parameters on snowdrift accumulation conditions is shown in Figure 9. The influence on the specific yield was calculated in a similar manner, but it is omitted here for the sake of conciseness.

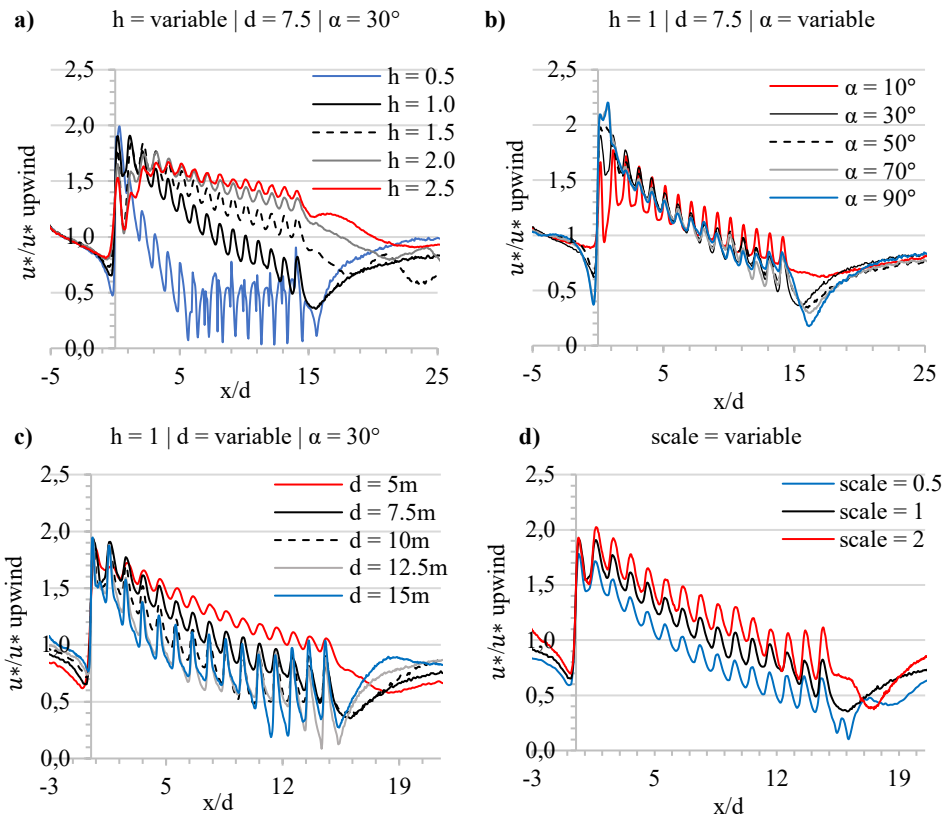

Figure 9. Normalised friction velocity for (a) gap-to-ground, (b) tilt, c) pitch and (d) system scale.

The sensitivity of the parameters was then quantified as the performance with the parameter adjustment in relation to the performance of the base case, as given by Equation 5 and Equation 6. The sensitivity parameters for both the snowdrift accumulation conditions represented by the friction velocity) and the specific yield is shown in Figure 10.

$$u_{*rel} = \frac{\bar{u}_{*(parameter)}}{\bar{u}_{*(base-case)}} \tag{5}$$

$$SY_{rel} = \frac{SY_{(parameter)}}{SY_{(base-case)}} \tag{6}$$

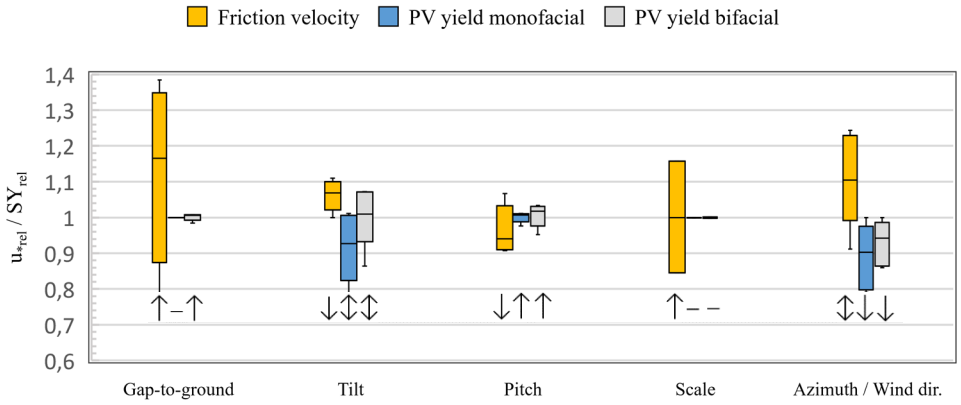

Figure 10. Impact of the five investigated parameters on friction velocity and specific yield. The arrows signify whether an increase in the parameter of the base case produced a positive or negative response to $\mathbf{u_{*rel}}$ or $\mathbf{SY_{rel}}$. The two-headed arrows indicate an ambiguous response, while a dash signifies an insignificant response.

For high values of u_{*rel} or SY_{rel} a change in the parameter can increase the performance compared to the base case. Increased u_{*rel} reduce the risk of snowdrift accumulation, while increased SY_{rel} signifies increased yield. The span of the bars in Figure 10 indicates the range of responses from adjusting the parameter and is thus the quantified sensitivity of the parameter. Figure 10 shows that all the investigated parameters can be adjusted to improve the snowdrift accumulation conditions and that the influence on the yield is variable. Only two parameters that improves the accumulation conditions have a positive or insignificant influence on the energy yield; that is, increasing the gap-to-ground, or increasing the system scale. The three remaining parameters can be adjusted to improve the accumulation conditions, but will result in a trade-off in the yield of the plant.

In the full paper, a discussion is made on the influence of the base-case configuration on the results, which remains an uncertainty in the uncovered sensitivity.

However, the impact of the parameter adjustments on the snowdrift accumulation conditions are compared with snow fence theory (Tabler (2003) as well as a CFD study on wind forces in solar power plants (Shademan et al. (2014), which are in conjunction with the findings of this study, thus reassuring the validity of the results.

The uncovered results can be applied to solar power plant projects to indicate the effects of adjusting design parameters to increase snowdrift resiliency. The design adjustments necessary to achieve a snowdrift resilient power plant depends on local climatic conditions and are likely to differ depending on location and plant size. Investigating the effect of adjusting multiple parameters in real climatic conditions is suggested as a relevant focus for future work.

5.3 Summary of Paper III, *"Reliability of building roofs with PV systems with active snow mitigation"*

The aim of the Paper III is to quantify the influence of PV snow mitigation systems on the structural reliability of building roofs. This is investigated by constructing a limit state function for the ultimate limit state of a simply supported beam and implementing the influence of a PV snow mitigation system on the load variables. Monte Carlo simulations are used to solve the limit state functions, giving the resulting reliability index of the component.

To isolate the influence from the added weight of the PV system from the influence from snow melting, three different limit state functions representing three different load scenarios are formulated: a roof without a PV system (Equation 7), a roof with a PV system without mitigation (Equation 8), and a roof with a PV system with active snow mitigation (Equation 9). The distribution of the variables is given in Table 3.

$$Z(X) = \theta_R W_{pl} f_y - \frac{\theta_E L^2}{8} [\gamma_{steel} A_s + gb + \mu_i bS] \tag{7}$$

$$Z(X) = \theta_R W_{pl} f_y - \frac{\theta_E L^2}{8} [\gamma_{steel} A_s + gb + g_{PV} b + \mu_i bS] \tag{8}$$

$$Z(X) = \theta_R W_{pl} f_y - \frac{\theta_E L^2}{8} [\gamma_{steel} A_s + gb + g_{PV} b + \mu_i bS^*] \tag{9}$$

In the limit state function representing a roof beam with active snow mitigation (Equation 9), the snow load influenced by mitigation (S*) is a censored variable of the annual maximum snow load S. The snow load influenced by mitigation (S*) is defined by several other variables which account for the function of the system. These variables consider the limit for when the snow load is reduced, how much of the area that the snow load is

reduced, the probability of successfully reducing the load. For a full overview of how the function of the snow mitigation is implemented, see the full Paper in Annex A.

Table 3. Variable definitions for the limit state functions.

Symbol	Input	Distribution	Mean	CoV	Source
W_{pl}	Section modulus	DET	-	-	
γ_{steel}	Steel density	DET	77	-	
L	Beam span	DET	12	-	
b	Beam spacing	DET	7	-	
A_s	Beam cross-section area	DET	-	-	
f_y	Yield strength	LogNormal	0.283	0.05	(CEN, 2022)
g	Permanent load	Normal	1	0.1	(CEN, 2022)
g_{PV}	Weight of PV	Normal	0.2	0.05	
μ_i	Shape coefficient	LogNormal	0.66	0.16	(CEN, 2021)
S	Snow load (1-year)	Gumbel	Variable	0.51	(CEN, 2022)
S^*	Snow load w. mitigation	*	Variable	-	
θ_R	Resistance unc.	LogNormal	1.15	0.055	(CEN, 2022)
θ_E	Permanent load unc.	LogNormal	1	0.05	(CEN, 2022)

The focus in the study is on structures with a lower capacity than in the current requirements, which are the types of structures which PV snow mitigation systems are commonly mounted on. To represent such structures, the limit state functions are applied to structures with varying capacity and snow load. The capacity is determined according to Eurocode 1991-1-1 but with a lower characteristic snow load than the 50-year snow load of the snow load distribution applied in the limit state function. The factor defining the relationship between the 50-year snow load and the snow load used in the design was termed the capacity ratio ω. The snow load in the limit state function is varied between so that the 50-year load is between 0.5-9.0 kN/m^2.

The model is used to show three main results: how the magnitude of snow load and under-design ratio influence the reliability; the sensitivity of the reliability to the function of the system and the influence of the system function on snow load reduction amounts. In this summary, only the first two results are given in short. The influence of the snow load and under design ratio on the reliability index (β) for the three different load scenarios is shown in Figure 11.

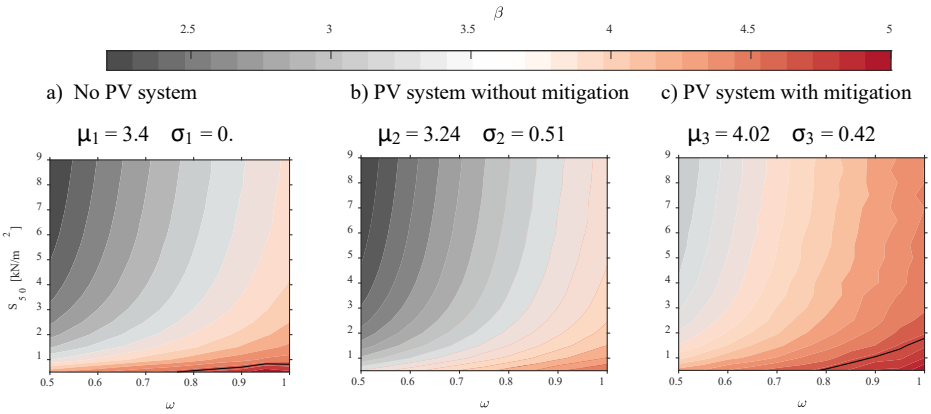

Figure 11. Reliability index (β) with varying snow loads (S_{50}) and capacity ratios (ω): (a) building without a PV system, (b) building with a PV system without snow mitigation, and (c) building with a PV system with snow mitigation.

Figure 11 shows that the load from the PV system reduces the reliability index with an average of 0.16 while a PV system with active snow mitigation on average increases the reliability index by 0.62. For all the investigated load and capacity combinations, the impact of active snow mitigation compensates for the increase in load from the system. The modelled impact of the PV snow mitigation system is most significant in structures with a low capacity ratio and high snow loads. It is the least significant for structures with low snow loads as the load increase from the PV system becomes relatively larger. However, Figure 11 is made with fixed snow load reduction variables which are investigated separately in a sensitivity analysis. For a full elaboration on how the snow reduction variables, see the full paper in Annex A. The results of this analysis are shown in Figure 12.

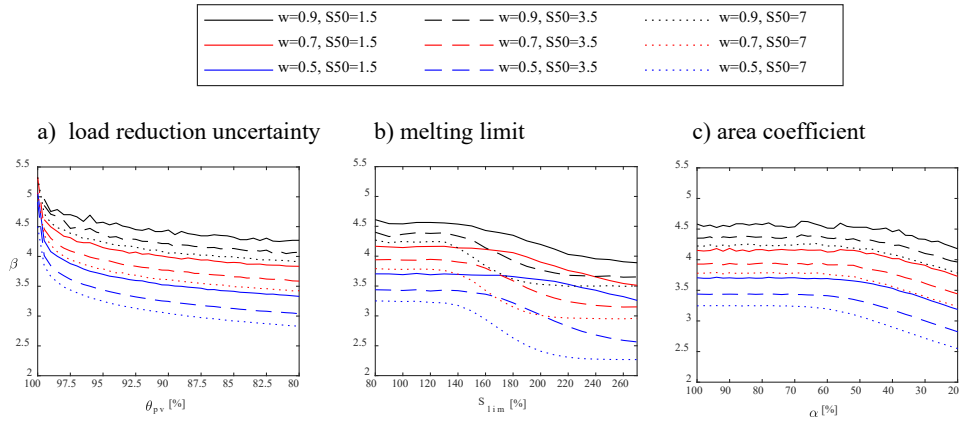

Figure 12. Sensitivity of the reliability index (β) to a) the probability of successful load reduction (θ_{pv}) and b) melting limit (S_{lim}) and c) melting area coefficient (α).

The influence from the load reduction uncertainty is shown Figure 12a. This variable comprises all factors that can prevent sufficient load reduction, where a value of 100% represents a guaranteed reduction. This variable has a significant impact on reliability, giving an exponential increase towards a load reduction uncertainty of 100%. The impact of this variable highlights the necessity for designing reliable PV snow mitigation system. The next investigated variable is the melting limit which determines for which snow load value the load should be reduced. A melting limit of 100% indicates that the load is reduced at the load the structure is designed to withstand (excluding the influence from the partial factors). Figure 12b shows that the melting limit does not impact the reliability if it is below 120%. This indicates that there is a potential for postponing the load reduction above the design load for the roof to reduce the snow load reduction amounts (which is investigated more in detail in the full paper). A similar influence is for the coverage of PV panels on the roof (represented by the area coefficient in Figure 12c), but this was perhaps less relevant than increasing the melting limit, as a high utilisation of PV panels on the roof surface is desirable for roof mounted PV system.

The modelling approach demonstrates the influence of active snow mitigation with PV systems on the structural reliability of building roofs. The results can be used to optimise PV snow mitigation systems to reduce the snow load reduction amounts while achieving a desired structural safety. It is also relevant for standardisation organisations as provisions for the use of snow mitigation systems can contribute to increasing the reliability of existing structures while producing renewable energy. Provisions allowing for reducing the design snow load used for buildings equipped with active snow mitigation systems exists in ISO4355 Annex F “Snow loads on roofs with snow control”(ISO, 2013). However, the provisions are lacking in addressing how such systems should be controlled and operated to achieve a satisfying structural reliability.

5.4 Summary of Paper IV *"Energy demand and yield enhancement for roof mounted photovoltaic snow mitigation systems"*

Paper IV investigates the influence of active snow mitigation on the energy balance of PV systems. In this study, an adapted energy balance snow model (EBSM) is used to simulate the energy consumption from PV snow mitigation and coupled with a PV yield simulation to estimate the power production. Figure 13 shows the outline of the methodology.

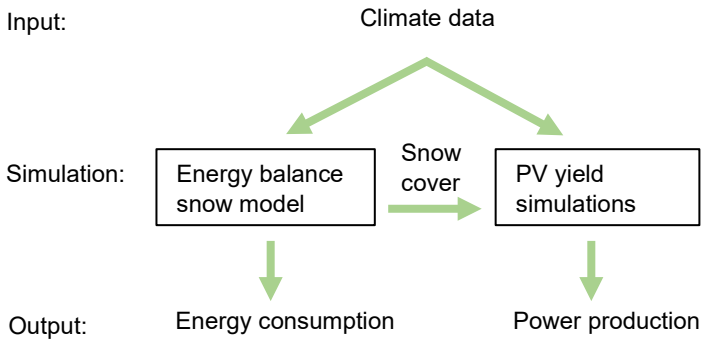

Figure 13. Outline of the study methodology.

EBSMs are numerical models that simulate the snow water equivalent (SWE) based on climatic data. The model determines whether the precipitation falls as rain or snow and calculates the energy fluxes between the snowpack and the environment to estimate the accumulation or ablation of the snowpack. The EBSM used in this model is the ESCIMO-model by Marke et al. (2016) which is adapted to induce a heat flux from the PV panels when the snow exceeds a threshold limit. From this model the energy use and the snow cover duration on the PV system is estimated. The snow cover duration is then implemented in a PV energy yield simulation to determine how the reduced snow cover duration can enhance the yield of PV systems.

As input data to the adapted EBSM model, the ERA5-reanalysis dataset is used (Hersbach, 2018). This dataset provides continuous hourly data from 1979 to the present day in a grid of 0.25°x0.25°. Four locations are investigated in the study: Tromsø, Oslo, Munich and Davos. These locations are chosen based their different snow and irradiance characteristics, giving insight into the PV snow mitigation system's energy balance in different climatic conditions.

To define the melting limits, the return period snow loads for the four locations without heat flux from the PV system is simulated. The annual maximum snow loads from the 41 years is fitted to a distribution using the Akaike Information Criterion (Akaike, 2011) and the return period snow loads of 30, 20 10 and 5 years is calculated. These return

periods are then used to define the threshold for when the heat flux is applied in the adapted EBSM. The return period concept is used to define the threshold loads, as the study is focused on existing buildings which are under-designed with respect to snow load. Different return period snow loads have historically been used in national design standards, giving a building stock with a variable capacity for snow load (Croce et al., 2019; Meløysund et al., 2006).

The simulation method overcomes the difficulty of estimating the long-term energy consumption and production of PV snow mitigation systems, which can be difficult to determine with field measurements due to the infrequency of heavy snow loads. The model can easily be applied to any snow load climate with simple climatic data, which also overcomes the limitations of wide climatic representability.

The results on the simulated energy consumption, yield enhancement and net effect on the energy balance of PV systems is shown in Figure 14.

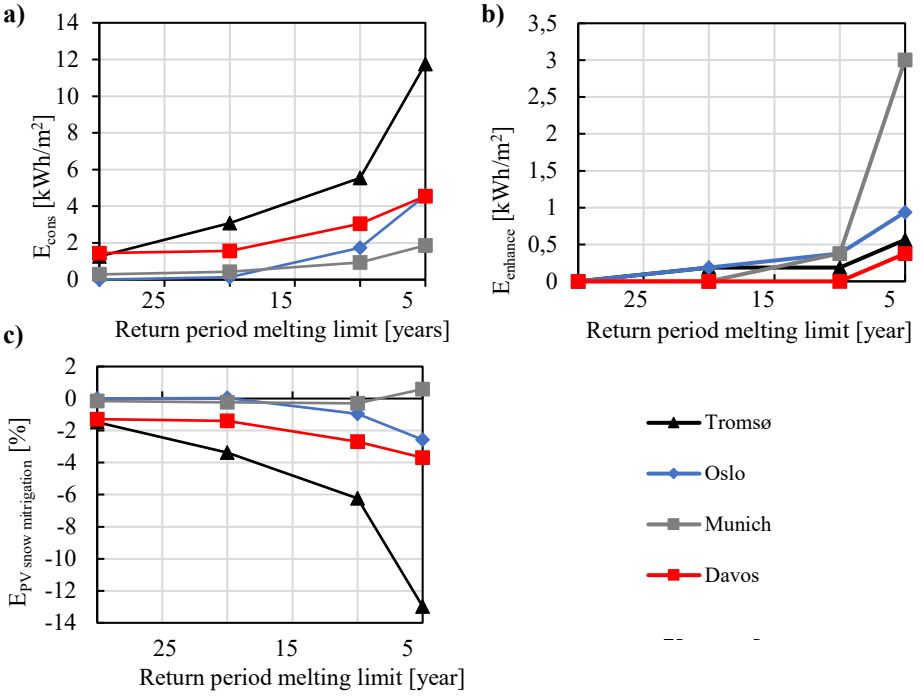

Figure 14. Simulated results of the a) average energy consumption per year (E_{cons}), b) yield enhancement ($E_{enhance}$), and c) net impact on the energy balance compared to a system without mitigation. The results are produced for the return period melting limits of 30, 20, 10 and 5 years.

As shown in Figure 14a, the average energy consumption increases with decreasing melting limit due to more snow being melted on the roof. The difference in energy consumption

between the climates is a result of several mechanisms. The amount of snow removed from the roof is dependent on the occurrence of snow load which differs largely in magnitude and frequency depending on the location. Additionally, the normalised energy amounts required to melt snow is dependent on climate, which are significantly smaller for warmer climates such as Oslo and Munich compared to Tromsø and Davos. If ranging the average energy consumption for all the melting limits from highest to lowest, the order becomes the following: Tromsø, Davis, Oslo and Munich. This indicates as expected that cold climates with high snow loads give a large energy consumption for active snow mitigation systems.

The yield enhancement in Figure 14b is generally small in magnitude (<1 kWh/m^2), except for the 5-year return period melting limit in Munich, where there is a gain of 3 kWh/m^2. The significant energy gain in Munich occurs due to the 5-year return period melting limit being so low that almost all the snow is removed from the roof and significant energy gains occur in all the winter months.

Figure 14c shows the net influence of energy consumption and yield enhancement of the PV snow mitigation function for different melting thresholds. A general trend is an increasing negative impact with decreasing melting limits. The most negative impact (-13%) occurs in the five-year return period melting limit in Tromsø. However, for the 5-year return period melting limit in Munich, the yield enhancement exceeds the energy production and a positive influence of +0.6% is achieved. This indicates that PV snow mitigation systems which are operated to reduce maximum snow loads will likely have a negative influence on the energy balance compared to ordinary PV systems, although in small snow load climates, small gains can be achieved. Thus, PV snow mitigation systems are likely more economic competitive in small snow load climates than high snow load climates.

In the discussion section of the paper, the uncertainties in the study are discussed. The method is comprehensive and involves several steps which each come with an inherent uncertainty. Most prominent is the neglection of snow erosion and roof heat loss in the EBSM model, coarse spatial resolution of the ERA5 climate data, suboptimal temporal resolution of the snow loss in the yield simulations and simplified operation of the PV snow mitigation system.

Despite its uncertainties, the study contributes with quantifying the long-term energy balance of PV snow mitigation system in different climatic conditions and demonstrating several mechanisms contributing to the energy balance of such systems. In general, the study indicates that PV snow mitigation systems are more economic competitive in warmer, low snow load climates. In such climates, less snow is removed from the roof, the efficiency of the system is higher, and the yield enhancement is more significant. Warm climates with low snow loads are often at lower latitudes, where PV systems are more competitive. Thus, the energy required to reduce snow loads is not a significant barrier for the use of PV snow mitigation systems in low snow load climates.

5.5 Summary of Paper V *"Snow loss modelling for roof mounted photovoltaic systems: Improving the Marion snow loss model"*

Paper V quantifies the accuracy of a snow loss model by comparing simulated snow loss with measured snow loss for a variety of PV systems in Norway. A previous study by Øgaard et al. (2021a) identified that among four existing snow loss models, the snow loss model by Marion et al. (2013) (here referred to as "*the Marion snow loss model"*) performed the best, but can be improved by considering snow depth and system configuration. However, this finding was based on limited data, and a broader application of the improved Marion snow loss model is needed to verify its accuracy. This study compares the accuracy of the improved model with the original model, for eight different PV systems in Norway, with several years of yield measurements.

To quantify the accuracy of the snow loss model, the modelled snow loss in eight PV systems is compared with the measured snow loss. Both measured and modelled snow loss is quantified by comparing the expected output of a PV system without snow, with the actual output of the PV system. The quantification of the measured snow loss involves separating the snow loss from other loss mechanisms. In this study, the separation of loss mechanisms is performed according to the methodology presented by Øgaard et al. (2021b). The eight analysed PV systems are given in Table 4.

Table 4. Details of the analyzed systems. The climate zone is according to the Köppen-Geiger climate classification (Kottek et al., 2006).

System	Position (°)	Tilt (°)	Climate zone	Analysis period
Commercial, flat roof systems				
C1a	59.6, 10.7	10	Dfb	2015-01 – 2021-06
C1b	59.6, 10.7	10	Dfb	2017-01 – 2021-06
C2	60.9, 10.9	10	Dfb	2018-01 – 2021-06
C3	60.4, 5.5	10	Cfb	2018-01 – 2021-06
Residential, tilted roof systems				
R1	60.8, 11.1	26	Dfb	2019-01 – 2021-06
R2	61.3, 10.2	24	Dfc	2018-01 – 2021-06
R3	60.9, 11.0	40	Dfb	2019-01 – 2021-06
R4a/b	61.1, 10.5	35	Dfb	2018-01 – 2020-12
R5	60.8, 10.6	38	Dfc	2019-01 – 2021-06

5.5 Summary of Paper V "Snow loss modelling for roof mounted photovoltaic systems: Improving the Marion snow loss model"

The following paragraphs presents the methodology for modelling the snow loss. The PV yield simulations are performed with the System Advisor Model (SAM) in Python (Ryberg & Freeman, 2015), which uses hourly meteorological data to estimate the power output of a PV system with defined characteristics with the single diode model. The snow loss model is coupled to this simulation. Additional to the climatic data already used in the PV yield simulation, the snow loss model requires data of snow depth on the roof or the ground. Snow sliding from PV modules commonly contribute to snow being cleared of the module surface before snow is cleared from the roof or ground. In the Marion snow loss model, snow sliding occurs when the conditions in Equation 10 are met and the snow sliding amount is calculated in accordance to Equation 11:

$$T_{amb} > G_{POA}/m \tag{10}$$

$$Snow\ slide\ amount = sc * \sin(tilt) \tag{11}$$

where T_{amb} is the ambient temperature, G_{POA} is the Plane of Array irradiance, m is an empirically defined value of -80 W/m^{2}K. The snow slide amount is the fraction of the total row height which is cleared from snow, sc is an empirical snow clearing coefficient and tilt is the inclination of the module compared to a horizontal plane. In the original Marion model, sc was found to give the best results for a constant value of 0.2. However, by accounting for snow depth in the determination of sc, the accuracy of the model can be improved. Here, a snow depth dependent sc is implemented, being equal to 0.4 when snow depth < 3 cm and sc = 0.06 when snow depth > 3 cm. A snow depth dependent clearing coefficient can better represent the occurrence of interference from the roof for low tilt systems, where the build-up of snow on the bottom of the module prevents snow being entirely cleared from the module. A snow depth dependent sc was also found to be suitable for the residential systems on roofs with significant tilts and is employed in the same manner for all the investigated systems.

The yield simulation in SAM enables to differentiate between the substrings in the modules. In this study, a partially covered module substring is simplified to be fully shaded. The model differentiates between portrait or landscape orientation.

The modelled snow loss is estimated using ambient temperature and irradiance data from nearby meteorological weather stations (Norsk Klimaservicesenter, 2021). The snow depth data is taken from the seNorge snow model which estimates SWE for Norway in a 1x1 km resolution based on numerical simulations (Saloranta, 2016). To estimate snow depth, the model uses a snow density model. The seNorge model estimates ground snow depth, and no conversion to roof snow depth is made.

The Mean Absolute Error (MAE) of the simulated snow loss for different values of the snow clearing coefficient are shown in Figure 15. A general trend is that the MAE decrease with decreasing snow clearing coefficient, but discrepancies are evident for single systems. The variable snow clearing coefficient gives the lowest average MAE if one is to

be chosen for all the systems. The average snow loss error less than 11%, which is 23 percentage points lower than the sc of 0.2 used in the original Marion model.

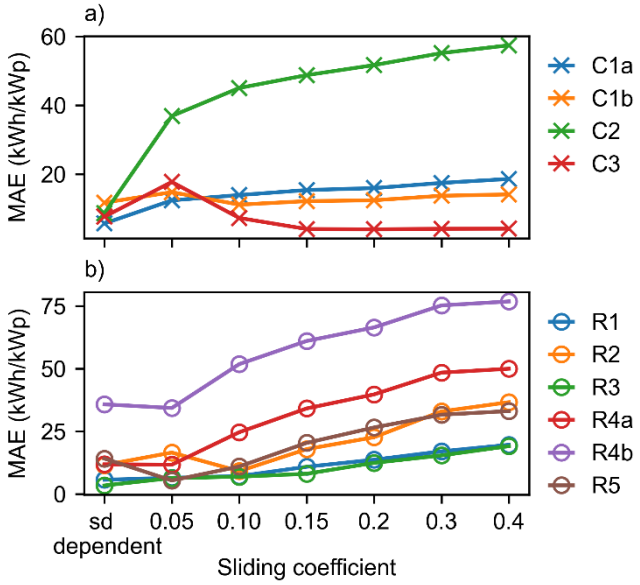

Figure 15. Mean absolute error of the simulated snow loss with varying clearing coefficient for a) the commercial systems and b) the residential systems.

A discussion is made on the factors contributing to the uncertainties in the study. In general modelling the influence of snow on PV systems based on limited meteorological data is challenging due to the sensitivity of the snow cover to local climatic conditions. The most significant uncertainties in the study are believed to arise from the simplification that all modules on a roof are covered snow with an equal depth, that partially covered strings are regarded as fully covered, uncertainties in the snow depth data used as input to the model and the lack of conversion from ground to roof snow loads.

Nonetheless, the inclusion of snow depth in the snow clearing coefficient of the snow loss model significantly reduces the error in the snow loss estimation. The advantage of the model is its applicability to systems with different configurations in different climatic conditions. The improved snow loss model contributes to increased accuracy in short-and long-term PV yield estimations, as well as better winter-time fault detection in PV systems.

6. Discussion

In this section, the findings of the individual research papers are connected to the research questions. The chapter is divided by topic to provide a confined discussion.

6.1 Research questions

RQ1.1

How are traditional ground mounted PV plants affected by snowdrift accumulation?

Based on the findings reported in Paper I, it may be concluded that PV plants designed with established principles commonly used in warmer climates are susceptible to snowdrift accumulation. The field measurements showed that snowdrifts in the plant jeopardised its mechanical resiliency as they increased to cover the arrays. The snowdrifts did not show signs of achieving a steady state, indicating that they would continue to increase with more horizontal snow transport.

Paper I only investigates the snowdrifts developing from one specific solar power plant configuration in under certain climatic conditions and requires a reasoning for the validity of the results to different types of configurations and climates. Paper II contributes to the matter of influence of configuration where the effect of adjusting the design parameters is quantified. The results from Paper II show that configurations which are not adjusted beyond what qualifies as normal configuration properties, snowdrift accumulation is likely to occur. For example, traditional solar power plants commonly have gaps > 1.0 m, which is likely not sufficient to avoid snowdrift accumulation. Based on this it is argued that the conclusion that traditional solar power plants are susceptible and adversely affected by snowdrifts can be extended to design configurations beyond the one investigated in Paper I.

The severity of the snowdrift accumulation will depend on the climate. The wind direction during snow transport will influence the shape of the snowdrifts. The local exposure, the wind speed and snow conditions will influence the magnitude of horizontal snow transport, impacting the growth rate and size of the snowdrifts. Thus, snowdrifts in solar power plants can occur widely different than exhibit in Paper I, and the nature of the accumulation will differ depending on the climatic conditions of the location.

RQ1.2

How can PV plants be adapted to achieve resilience against snowdrift accumulation?

The research question is addressed in Paper II, which shows that all PV plant design parameters (including tilt, pitch, gap-to-ground, orientation and scale) can be adjusted to increase the snowdrift resiliency with a variable impact on the yield of the plant. The influence of the parameters is summarised as the following:

- Increasing the gap-to-ground significantly increase the snowdrift resilience and the effect on energy yield is insignificant for monofacial modules and positive for bifacial modules.
- Reducing the panel tilt increases the snowdrift resiliency in the windward and leeward zone and has an adverse effect on the specific yield.
- Reducing the pitch increases the snowdrift resiliency, but reduces yield as shading between rows increases.
- Increasing the scale of the system (a proportional scaling of all geometric properties) increases the snowdrift resiliency and has in insignificant influence on the specific yield
- Adjusting the azimuth to achieve a prevailing wind direction closer to parallel to the rows significantly increase the snowdrift resiliency but will reduce the yield if the azimuth deviates from true south on the northern hemisphere or north on the southern hemisphere.

The study quantifies the impact of adjusting the design parameters, but the magnitude of design adjustments to achieve a snowdrift resilient plant is not suggested. This is due to that the desired adaption will depend on the climatic conditions of the location and PV system characteristics. The results from the study can be applied in PV projects to suggest suitable adjustment for the type of system and climatic conditions.

One limitation of the thesis regarding the snowdrift resiliency of solar power plants is the lack of an evaluation of the different strategies to achieve snowdrift resilient PV plants. Adapting the design of a plant to avoid snowdrifts is only one strategy through which a snowdrift resilient plant can be achieved. In that sense, there is a missing link between Paper I and Paper II, where after identifying the design challenge in Paper I, Paper II goes forward to investigate a specific strategy without considering other possibilities. The strategy in focus in Paper II can be classified as a non-deposition strategy, as it aims to avoid any snowdrifts in the plant area. Deposition strategies would involve depositing snow in designated areas where it would not adversely impact the PV plant. This could be achieved with the use of traditional snow fences or with PV arrays designed similar to snow

fences to deposit snow (i.e. power-producing snow fences). The reason for the focus on the non-deposition strategy in Paper II was due to its applicability to different snowdrift climates and PV plants of different size. If no snow is deposited in the plant, the magnitude of horizontal snow flux becomes less relevant. To the contrary, a deposition strategy must consider the magnitude of transported snow and the length of the melting season, as the snow storage capacity may be filled. In Antarctica where the melting season can be short or even non-existent, deposition strategies may be less favourable. However, for climates with less significant horizontal redistribution of snow and with significant melting seasons, depositions strategies may be more favourable. The evaluation of different strategies should consider the influence of plant size in addition to climate and is a suggested topic for future work on the snowdrift resiliency of PV plants.

Important for the understanding of Paper I and Paper II is that the studies consider the development of snowdrifts in climates characterised by little precipitation. This is representable for typical polar climatic condition where precipitation is scarce but the horizontal redistribution of the snowpack can be significant (Grzegorz, 2010). Understanding the occurrence of snowdrifts in isolation (in climates with little precipitation) is useful before continuing to consider hybrid scenarios with a combination of precipitated snow and redistribution. Investigating such hybrid scenarios is also more complex and require more advanced models considering the temporal build of the snow pack in combination with influence from wind, such as presented by Gamble et al. (1992) or Zhou et al. (2018).

RQ2.1

How does PV snow mitigation systems influence the structural reliability of existing roofs?

This topic is addressed in Paper III using probabilistic simulations to quantify the impact of active snow mitigation with PV systems on the reliability of a structural component. To address the question, it must be recognised that the influence of the PV snow mitigation system on the structural reliability depends on the capacity and load conditions of the structure, as well as on the function of the system. For well-functioning systems with a probability of reducing the load of 95%, the impact on the reliability is significantly positive (an average increase of the reliability index β by 0.62), meaning that the increase in load from the PV system is compensated by a reduction of the snow load. However, the reliability is shown to be very sensitive to the probability of reducing the load. It is difficult to suggest a realistic value for the probability of load reduction, as this variable has an epistemic nature, indicating that its true value cannot be known, only the uncertainty in its approximation can be reduced. Thus, RQ2.1 is adressed with a highly theoretical study indicating the influence of PV snow mitigation systems presupposing different conditions,

but its actual impact in real conditions require more data on the probability of load reduction.

RQ2.2

How does the snow mitigation function influence the energy balance of PV systems?

This research question is addressed in Paper IV, using numerical tools to quantify the energy consumption and yield enhancement of PV snow mitigation systems. In general, the energy balance is shown to vary significantly with climate as this impacts the reduction amounts, the energy efficiency of the system and the yield enhancement. In low snow load climates, less snow is removed from the roof and a higher energy efficiency of the system is obtained (likely due to low snow load climates on average being warmer). The yield enhancement is close to negligible for climates with significant snow loads, but can be significant for low snow load climates with low melting limits. A simplified conclusion of the study is that climates with significant snow loads (50-year return period load >1 kN/m^2) will have a negative net influence on the energy balance, while low snow loads climates (50-year return period load < 1 kN/m^2) will have a close to insignificant impact on the net energy balance compared to an ordinary PV system. This conclusion presumes a correlation between the magnitude of snow load and the mean ambient wintertime air temperature which is not valid in all climates. More studies on the topic will over time contribute to determining the validity of the findings presented here.

RQ2.3

What types of climates are suitable for the use of PV snow mitigation systems?

Addressing this research questions require that the performance of the system with respect to different performance criteria is considered. The question is addressed by synthesising the results from Supplementary Paper I focusing on the feasibility of load reduction, Paper III focusing on the influence of the reliability, and Paper IV focusing on the energy balance of PV snow mitigation systems.

In terms of the ability to melt snow and transport the meltwater off the roof, the findings from Supplementary Paper I indicate that temperature and wind exposure influence the feasibility of load reduction. Based on field measurements of snow load reduction with PV snow mitigation systems, it is argued that the risk of meltwater to refreeze or to be absorbed by the snowpack is higher in cold climates. Melting in temperatures above freezing is associated with low risk, as the probability of refreezing is eliminated and the

potential for water saturation of the snow decreases. This indicates that temperate climates gives less risk of not successfully reducing the load than cold continental or polar climates.

Regarding the influence of climate on how PV snow mitigation system impacts the structural reliability the only parameter which directly concerns climate in Paper III is the magnitude of the snow load. In this study it is shown that the PV snow mitigation system has a more significant (positive) impact on structures experiencing higher snow load. However, in the factor which accounts for the probability of successful load reduction is shown to have a strong impact on the reliability. This factor will be influenced by climatic conditions which reduce the ability to mitigate the snow load, which (as is argued in the previous paragraph) is negatively impacted by cold climate. Thus, colder climates may give a less positive impact on the reliability.

The energy required to operate PV snow mitigation systems is investigated in Paper IV. Here it is shown that the energy used to melt a kilogram of snow (i.e. the efficiency of the system) is over double in the coldest investigated climate (Tromsø) compared to the warmest investigated climate (Munich). Furthermore, the climates with the higher snow loads have significantly higher total energy use than the low snow load climates. The yield enhancement is also more significant in low snow load climates than the high snow load climates. Overall, in terms of energy, the PV snow mitigation system is more favourable in warm climates with low snow loads than cold climates with high snow loads.

Synthesising the findings on the influence of climate on the performance of PV snow mitigation systems suggest that such systems are most suitable for warm climates with low snow loads due to the being more likely to successfully reducing the load and requiring less energy in operation. However, the increase in load from the PV system has a more significant negative impact on the reliability for structures designed for lower loads. This is the only mechanism that make PV snow mitigation systems more suitable for low snow load climates, but it does not outweigh the positive performance of the system in warmer, low snow load climates to change the conclusion of the climatic suitability of such systems.

RQ3.1

How can snow loss models be improved to capture local climate?

The basis for formulating this research question is that many existing snow loss models have limited applicability to different system configurations and climatic conditions (Øgaard et al., 2021a). Snow shedding from PV modules is previously observed to be influenced by the piling up of snow on the roof causing ground interference, which has is more significant for thicker snowpacks than thinner ones. In Paper V, the accuracy of snow

loss modelling is improved by considering the influence of snow depth on the snow clearance of the modules. The mean average error of the snow loss is reduced by 23% compared to the existing Marion snow loss model.

6.2 Future work

In this thesis, the research questions addressed specific knowledge gaps in how snow is a challenge for the deployment of PV systems. With these questions partly answered, the perspective of the candidate on future work on snow challenges is given.

Regarding the challenge of the mechanical resilience of PV systems to snow, this thesis contributes to the scientific body of knowledge of snowdrifts in ground-mounted solar power plants. The research focused on the isolated occurrence of snowdrifts in climates with little precipitation, which is typical in polar regions. However, in many climates, snow distribution in solar power plants is a consequence of substantial amounts of precipitated snow combined with redistributions of the snowpack. In Norway, concessions applications for ground mounted PV plants (both fixed tilt and tracker systems) up to 100 MWp in climates with characteristic snow loads up to 4.5 kN/m^2 is being assessed by the Norwegian Water and Energy Resource Directorate (2022). How snow is distributed in high snow load climates also influenced by redistribution is not very well known and is crucial for the resiliency of such systems. Better estimates of the snow load in such design scenarios can contribute to ensuring the performance of the PV system during its working lifetime and contribute on reducing use of resources in the mechanical design of such systems. This is a recommended research topic in future work.

The spatial challenges for PV systems mounted on existing infrastructure is in this thesis investigated with a focus on the use of PV snow mitigation systems. However, other methods than actively mitigating snow may suffice to increase the deployment of PV systems on existing infrastructure. Diamantidis et al. (2018) demonstrated the value of measuring the roof snow load for reducing the uncertainties related to its occurrence and the associated need for snow removal. The concept of reducing the uncertainties of the buildings reliability can contribute to determining if the reliability is sufficient and whether measures are needed (Sykora et al., 2010). That a structure lacks in capacity with respect to snow load does not necessarily mean that snow load mitigation measures are necessary. Thus, other methods reducing the uncertainties in the imposed load and the structural capacity of the building can be sufficient for to utilise indisposed roof surfaces for PV purposes. If the reliability proves too low after reducing the load and capacity uncertainties, other measures than reducing the snow load can be performed, such as evacuating the building in case of a heavy snow load. Exploring the different paths to increasing PV deployment on existing structures within the field of structural reliability is a recommended topic for future work.

7. Conclusions and future work

The thesis investigates a multitude of snow challenges which are identified as knowledge gaps for the deployment of PV systems. The overall aim has been to contribute to resolving these challenges by focusing on a selection of these challenges. Revisiting the snow challenges in Figure 3 allows for evaluating what has been accomplished with the work in the thesis and what remains as relevant topics for future work.

How snow is a challenge for the mechanical resiliency of PV plants is investigated in this thesis with a focus on the occurrence of snowdrifts in ground mounted solar power plants. The conducted work has contributed with documentation of how snowdrifts are a challenge for the resiliency of PV plants, the necessity for adaptions to achieve snowdrift resilient power plants, a connection to the existing theory of snow fences, as well as quantifying the impact of design adaptions on the snowdrift conditions and energy yield. The results are relevant for climates with little precipitation and significant redistribution such as Polar climates. Future work on the mechanical resiliency of PV plants against snow should focus on snow loads which are a combination of precipitation and redistribution as this is becoming very relevant for the deployment of PV systems in more continental climates.

The spatial snow challenges are investigated with a focus on the use of PV snow mitigation systems to increase PV deployment on existing building roofs. The work contributes with demonstrating the influence of PV snow mitigation systems on the structural reliability of buildings, as well as quantifying the energy use and yield enhancement of such systems. Based on the results of the studies that comprise this thesis, the PV snow mitigation system is considered the most suitable in warm climates that experience low snow loads. Such climatic characteristics increase the probability of successfully reducing the load and have the least unfavourable impact on the energy balance of PV systems.

The thesis contributes to the challenges of snow to the yield of PV systems by improving an existing model for estimating snow loss on roof-mounted PV systems. The model is improved by accounting for the influence of snow depth, increasing the applicability of the snow loss model to different snow climates. Comparing simulated snow loss with measured snow loss gives a mean absolute error of 11% compared to 34% for the model not considering snow depth. In general, the knowledge on snow losses in PV systems is found to be significantly more developed than other snow challenges.

The following five points provide a brief summary of the thesis and demonstrate its contribution to the literature:

- Snow creates challenges for the deployment of PV system by influencing the mechanical resiliency of PV systems, the available area for installation and the yield of PV systems.

- Ground mounted PV plants optimised for power production are susceptible to snowdrift accumulation, but resiliency against snowdrifts can be obtained by adapting the design of the plant to control the snowdrift accumulation conditions.
- PV snow mitigation systems have the potential of increasing PV deployment on existing building roofs by enhancing the structural reliability. The load reduction capabilities and the energy consumption of such systems strongly depend on climate.
- A snow load model is improved to better capture the effect of local climate by considering the influence of snow depth and system configuration on the snow shedding.
- The thesis contributes to resolving the different snow challenges with an interdisciplinary perspective and suggest future research paths which contributes to resolving remaining snow challenges.

References

Aarseth, B. B., Øgaard, M. B., Zhu, J., Strömberg, T., Tsanakas, J. A., Selj, J. H. & Marstein, E. S. (2018). Mitigating Snow on Rooftop PV Systems for Higher Energy Yield and Safer Roofs. *EU PVSEC 2018: 35th European Photovoltaic Solar Energy Conference and Exhibition*, Brusells.

Akaike, H. (2011). Akaike's Information Criterion. In Lovric, M. (ed.) *International Encyclopedia of Statistical Science*, pp. 25-25. Berlin, Heidelberg: Springer Berlin Heidelberg.

Anadol, M. A. (2020). Snow melting on photovoltaic module surface heated with transparent resistive wires embedded in polyvinyl butyral interlayer. *Solar Energy*, 212: 101-112. doi: https://doi.org/10.1016/j.solener.2020.10.073.

Andersson, P.-O., Jelle, B. & Zhang, Z. (2020). Avoiding snow and ice accretion on building integrated photovoltaics – challenges, strategies, and opportunities. *Solar Energy Materials and Solar Cells*, 206: 1-12. doi: 10.1016/j.solmat.2019.110306.

Andrews, R., Pollard, A. & Pearce, J. (2013). The Effects of Snowfall on Solar Photovoltaic Performance. *Solar Energy*, 92: 84-97. doi: 10.1016/j.solener.2013.02.014.

Ascencio-Vásquez, J., Brecl, K. & Topič, M. (2019). Methodology of Köppen-Geiger-Photovoltaic climate classification and implications to worldwide mapping of PV system performance. *Solar Energy*, 191: 672-685. doi: https://doi.org/10.1016/j.solener.2019.08.072.

Bagnold, R. (1941). *The Physics of Blown Sand and Desert Dunes*: London: Methuen.

Bayrakci, M., Choi, Y. & Brownson, J. R. S. (2014). Temperature Dependent Power Modeling of Photovoltaics. *Energy Procedia*, 57: 745-754. doi: https://doi.org/10.1016/j.egypro.2014.10.282.

Burnham, L., Riley, D. & Braid, J. (2019). Design considerations for photovoltaic systems deployed in snowy climates. *37th European Photovoltaic Solar Energy Conference and Exhibition*, pp. 1626 - 1631.

CEN. (2002). *Eurocode - Basis of Structural Design*. Annex B - Management of Structural Reliability for Construction Works.

CEN. (2003). *Eurocode 1, actions on structures—Part 1-3: General actions—Snow loads*. Brussels, Belgium.

CEN. (2021). *SC1.T6; Final Draft "Interdependence of climatic actions"; Background document "Probabilistic basis for determination of partial safety factors and load combination factors";*: 1-317.

CEN. (2022). *CEN/TC 250/SC 10/AHG "Reliability background" Report Draft version May 2022*.

Cornell, C. A. (1971). First order uncertainty analysis of soil deformation and stability. *Proceedings of the First conference on Applications of Statistics and Probability to Soil and Structural Engineering*, Hong Kong.

Croce, P., Formichi, P., Landi, F. & Marsili, F. (2019). Harmonized European ground snow load map: Analysis and comparison of national provisions. *Cold Regions Science and Technology*, 168: 102875. doi: https://doi.org/10.1016/j.coldregions.2019.102875.

Diamantidis, D., Sykora, M. & Lenzi, D. (2018). Optimising Monitoring: Standards, Reliability Basis and Application to Assessment of Roof Snow Load Risks. *Structural Engineering International*, 28 (3): 269-279. doi: 10.1080/10168664.2018.1462131.

Druķis, P., Gaile, L., Valtere, K., Pakrastiņš, L. & Goremikins, V. (2017). Study of structural reliability of existing concrete structures. *IOP Conference Series: Materials Science and Engineering*, 251: 012087. doi: 10.1088/1757-899x/251/1/012087.

Formichi, P. (2019). *PT-Paper CEN/TC250/SC1, PT Doc_N_035_Rev_02*. snow loads in 2nd intermediate draft, prEN 1991-1-3. 43rd Meeting, Paris.

Gamble, S. L., Kochanski, W. W. & Irwin, P. A. (1992). Finite area element snow loading prediction - applications and advancements. *Journal of Wind Engineering and Industrial Aerodynamics*, 42 (1): 1537-1548. doi: https://doi.org/10.1016/0167-6105(92)90162-4.

Giddings, J. C. & LaChapelle, E. (1961). Diffusion theory applied to radiant energy distribution and albedo of snow. *Journal of Geophysical Research (1896-1977)*, 66 (1): 181-189. doi: https://doi.org/10.1029/JZ066i001p00181.

Granlund, A., Narvesjö, J. & Malou Petersson, A. (2019, 2019). The Influence of Module Tilt on Snow Shadowing of Frameless Bifacial Modules. *36th European Photovoltaic Solar Energy Conference and Exhibition, Marseille, September 9-13, 2019*, pp. 1650-1654.

Gray, D. M. & Male, D. H. (1981). *Handbook of snow : principles, processes, management & use*. Toronto; New York: Pergamon Press.

Grzegorz, R. (2010). Climate: Polar. In Warf, B. (ed.) vol. 2 *Encyclopedio of Geography*: SAGE publications.

Guerrero-Lemus, R., Vega, R., Kim, T., Kimm, A. & Shephard, L. E. (2016). Bifacial solar photovoltaics – A technology review. *Renewable and Sustainable Energy Reviews*, 60: 1533-1549. doi: https://doi.org/10.1016/j.rser.2016.03.041.

Hayibo, K. S., Petsiuk, A., Mayville, P., Brown, L. & Pearce, J. M. (2022). Monofacial vs bifacial solar photovoltaic systems in snowy environments. *Renewable Energy*, 193: 657-668. doi: https://doi.org/10.1016/j.renene.2022.05.050.

Heidari, N., Gwamuri, J., Townsend, T. & Pearce, J. M. (2015). Impact of Snow and Ground Interference on Photovoltaic Electric System Performance. *IEEE Journal of Photovoltaics*, 5 (6): 1680-1685. doi: 10.1109/JPHOTOV.2015.2466448.

Hersbach, H., Bell, B., Berrisford, P., Biavati, G., Horányi, A., Muñoz Sabater, J., Nicolas, J., Peubey, C., Radu, R., Rozum, I., Schepers, D., Simmons, A., Soci, C., Dee, D.,

Thépaut, J-N. (2018). *ERA5 hourly data on single levels from 1979 to present.* Copernicus Climate Change Service (C3S) Climate Data Store (CDS) (ed.).

Husu, A. G., Stan, M. F., Cobianu, C., Fidel, N. & Nedelcu, O. (2015, 11-12 June 2015). An inedited solution to increase the energy efficiency of photovoltaic panels for regions with snow. *2015 13th International Conference on Engineering of Modern Electric Systems (EMES)*.

IEA. (2022). *Electricity Market Report - July 2022*. Paris: IEA.

Innos. (2022). *Innos AS*. Available at: www.innos.no (accessed: 18.01.2022).

IRENA. (2021). *World Energy Transitions Outlook: 1.5°C Pathway*. Abu Dhabi: International Renewable Energy Agency.

ISO. (2013). *ISO 4355 Bases for design of structures, Determination of snow loads on roofs*: ISO. p. 42.

Jaedicke, C. (2001). *Drifting snow and snow accumulation in complex terrain*: University of Bergen.

Jelle, B. P. (2013). The challenge of removing snow downfall on photovoltaic solar cell roofs in order to maximize solar energy efficiency—Research opportunities for the future. *Energy and Buildings*, 67: 334-351. doi: https://doi.org/10.1016/j.enbuild.2013.08.010.

Jordan, D. & Kurtz, S. (2013). Photovoltaic Degradation Rates—an Analytical Review. *Progress in Photovoltaics: Research and Applications*, 21. doi: 10.1002/pip.1182.

Kavlak, G., McNerney, J. & Trancik, J. E. (2018). Evaluating the causes of cost reduction in photovoltaic modules. *Energy Policy*, 123: 700-710. doi: https://doi.org/10.1016/j.enpol.2018.08.015.

Kim, J., Rabelo, M., Padi, S. P., Yousuf, H., Cho, E.-C. & Yi, J. (2021). A Review of the Degradation of Photovoltaic Modules for Life Expectancy. *Energies*, 14 (14): 4278.

Kottek, M., Grieser, J., Beck, C., Rudolf, B. & Rubel, F. (2006). World Map of the Köppen-Geiger Climate Classification Updated. *Meteorologische Zeitschrift*, 15: 259-263. doi: 10.1127/0941-2948/2006/0130.

Köhler, J., Sørensen, D., John & Baravalle, M. (2019). Calibration of existing semi-probabilistic design codes. *13th International Conference on Applications of Statistics and Probability in Civil Engineering*, Seoul, South Korea.

Maghami, M. R., Hizam, H., Gomes, C., Radzi, M. A., Rezadad, M. I. & Hajighorbani, S. (2016). Power loss due to soiling on solar panel: A review. *Renewable and Sustainable Energy Reviews*, 59: 1307-1316. doi: https://doi.org/10.1016/j.rser.2016.01.044.

Marion, B., Schaefer, R., Caine, H. & Sanchez, G. (2013). Measured and modeled photovoltaic system energy losses from snow for Colorado and Wisconsin locations. *Solar Energy*, 97: 112-121. doi: https://doi.org/10.1016/j.solener.2013.07.029.

Marke, T., Mair, E., Förster, K., Hanzer, F., Garvelmann, J., Pohl, S., Warscher, M. & Strasser, U. (2016). ESCIMO.spread (v2): Parameterization of a spreadsheet-based energy balance snow model for inside-canopy conditions. *Geoscientific Model Development*, 9: 633-646. doi: 10.5194/gmd-9-633-2016.

Melchers, R. E. & Beck, A. T. (2018). *Structural Reliability Analysis and Prediction*. Third Edition ed.: John Wiley & Sons Ltd.

Melius, J., Margolis, R. & Ong, S. (2013). *Estimating Rooftop Suitability for PV: A Review of Methods, Patents, and Validation Techniques*. United States: Medium: ED; Size: 35 p. doi: 10.2172/1117057.

Meløysund, V., Lisø, K. R., Siem, J. & Apeland, K. (2006). Increased Snow Loads and Wind Actions on Existing Buildings: Reliability of the Norwegian Building Stock. *Journal of Structural Engineering*, 132 (11): 1813-1820. doi: doi:10.1061/(ASCE)0733-9445(2006)132:11(1813).

Meløysund, V. (2010). *Prediction of local snow loads on roofs*. Trondheim: Norwegian University of Science and Technology.

Merlet, S. T., Thomas; Thorud, Bjørn; Olsen, Espen; Nyhus, Jostein. (2016). Challenges of PV Generation in Polar Regions. Case Study: the Norwegian Research Station "Troll" in Antarctica. *32nd European Photovoltaic Solar Energy Conference and Exhibition*.

Mustafa, R., Gomaa, Dhaifullah, M. & Rezk, H. (2020). Environmental Impacts on the Performance of Solar Photovoltaic Systems. *Sustainability*, 12: 608. doi: 10.3390/su12020608.

Norsk Klimaservicesenter. (2021). *Observasjoner og værstatistikk*. Available at: https://seklima.met.no/ (accessed: 25.06.2021).

Norwegian Water and Energy Resource Directorate. (2022). *Konsesjonssaker*. Available at: https://www.nve.no/konsesjon/konsesjonssaker/ (accessed: 31.08.22).

Pawluk, R., Chen, Y. & She, Y. (2019). Photovoltaic electricity generation loss due to snow – A literature review on influence factors, estimation, and mitigation. *Renewable and Sustainable Energy Reviews*, 107: 171-182. doi: 10.1016/j.rser.2018.12.031.

Rahmatmand, A., Harrison, S. J. & Oosthuizen, P. H. (2018). An experimental investigation of snow removal from photovoltaic solar panels by electrical heating. *Solar Energy*, 171: 811-826. doi: https://doi.org/10.1016/j.solener.2018.07.015.

Ravindra, M. K. & Galambos, T. V. (1978). Load and Resistance Factor Design for Steel. *Journal of the Structural Division*, 104 (9): 1337-1353. doi: doi:10.1061/JSDEAG.0004981.

Richards, E. H., Schindel, K., Bosiljevac, T., Dwyer, S. F., Lindau, W. & Harper, A. (2011). *Structural considerations for solar installers : an approach for small, simplified solar installations or retrofits*. United States. doi: 10.2172/1034886.

Riley, D., Burnham, L., Walker, B. & Pearce, J. (2019). Differences in Snow Shedding in Photovoltaic Systems with Framed and Frameless Modules. *IEEE 46th Photovoltaic Specialists Conference (PVSC)*, pp. 0558-0561.

Ringkjøb, H.-K., Haugan, P. M. & Nybø, A. (2020). Transitioning remote Arctic settlements to renewable energy systems – A modelling study of Longyearbyen, Svalbard. *Applied Energy*, 258: 114079. doi: https://doi.org/10.1016/j.apenergy.2019.114079.

Ryberg, D. & Freeman, J. (2015). *Integration, Validation, and Application of a PV Snow Coverage Model in SAM*. United States: Medium: ED; Size: 24 p. doi: 10.2172/1225466.

Saloranta, T. M. (2016). Operational snow mapping with simplified data assimilation using the seNorge snow model. *Journal of Hydrology*, 538: 314-325. doi: https://doi.org/10.1016/j.jhydrol.2016.03.061.

Shademan, M., Barron, R., Balachandar, R. & Hangan, H. (2014). Numerical simulation of wind loading on ground-mounted solar panels at different flow configuration. *Canadian Journal of Civil Engineering*. doi: 10.1139/cjce-2013-0537.

Skomedal, Å. F., Øgaard, M. B., Haug, H. & Marstein, E. S. (2021). Robust and Fast Detection of Small Power Losses in Large-Scale PV Systems. *IEEE Journal of Photovoltaics*, 11 (3): 819-826. doi: 10.1109/JPHOTOV.2021.3060732.

SMA Solar Technology AG. (2019). *Upgrades for emissions-free research station in Antarctica*. Available at: https://www.sma-sunny.com/en/upgrades-for-emissions-free-research-station-in-antarctica/.

Standard Norge. (2021). *SN-NSPEK 3031:2021*. Energy performance of buildings — Calculation of energy needs and energy supply.

Stathopoulos, T., Zisis, I. & Xypnitou, E. (2012). Wind Loads on Solar Collectors: A Review. In *Structures Congress 2012*, pp. 1169-1179.

Store Norske Spitsbergen Coal Company. (2022). *Omstilling til Fornybar Energi i Arktis*. Available at: https://www.snsk.no/energi/om-energi.

Sykora, M., Holický, M., Jung, K., Thiis, T., Flø, A. & Kvaal, K. (2010). *Structural assessment of industrial heritage buildings*: Czech Technical University in Prague, Klokner Institute.

Sýkora, M., Diamantidis, D., Holický, M. & Jung, K. (2016). Target reliability for existing structures considering economic and societal aspects. *Structure and Infrastructure Engineering*, 13: 1-14. doi: 10.1080/15732479.2016.1198394.

Tabler, R., D. (2003). *Controlling Blowing and Drifting Snow with Snow Fences and Road Design*. Niwot, Colorado: 345.

Thiis, T. & Ferreira, A. (2014). Sheltering effect and snow deposition in arrays of vertical pillars. *Environmental Fluid Mechanics*, 15. doi: 10.1007/s10652-014-9356-1.

Thiis, T., Ferreira, A., Molnar, M. & Erichsen, A. (2015). Characterisation of shear stress distribution on a flat roof with solar collectors. *Czasopismo techniczne*.

Thiis, T. K. & O'Rourke, M. (2015). Model for Snow Loading on Gable Roofs. *Journal of Structural Engineering*, 141 (12): 04015051. doi: doi:10.1061/(ASCE)ST.1943-541X.0001286.

Tin, T., Sovacool, B. K., Blake, D., Magill, P., El Naggar, S., Lidstrom, S., Ishizawa, K. & Berte, J. (2010). Energy efficiency and renewable energy under extreme conditions: Case studies from Antarctica. *Renewable Energy*, 35 (8): 1715-1723. doi: https://doi.org/10.1016/j.renene.2009.10.020.

Tominaga, Y. (2018). Computational fluid dynamics simulation of snowdrift around buildings: Past achievements and future perspectives. *Cold Regions Science and Technology*, 150: 2-14. doi: https://doi.org/10.1016/j.coldregions.2017.05.004.

Vitali, N., Rózsás, Á. & Sýkora, M. (2019). Calibrating Partial Factors – Methodology, Input Data and Case Study of Steel Structures. *Periodica Polytechnica Civil Engineering*, 63. doi: 10.3311/PPci.12822.

Woyte, A., Nijs, J. & Belmans, R. (2003). Partial shadowing of photovoltaic arrays with different system configurations: literature review and field test results. *Solar Energy*, 74 (3): 217-233. doi: https://doi.org/10.1016/S0038-092X(03)00155-5.

Yan, C., Qu, M., Chen, Y. & Feng, M. (2020). Snow removal method for self-heating of photovoltaic panels and its feasibility study. *Solar Energy*, 206: 374-380. doi: https://doi.org/10.1016/j.solener.2020.04.064.

Zhou, X., Zhang, Y. & Gu, M. (2018). Coupling a snowmelt model with a snowdrift model for the study of snow distribution on roofs. *Journal of Wind Engineering and Industrial Aerodynamics*, 182: 235-251. doi: https://doi.org/10.1016/j.jweia.2018.09.014.

Øgaard, M. B., Aarseth, B. L., Skomedal, Å. F., Riise, H. N., Sartori, S. & Selj, J. H. (2021a). Identifying snow in photovoltaic monitoring data for improved snow loss modeling and snow detection. *Solar Energy*, 223: 238-247. doi: https://doi.org/10.1016/j.solener.2021.05.023.

Øgaard, M. B., Riise, H. N. & Selj, J. H. (2021b). Estimation of Snow Loss for Photovoltaic Plants in Norway. *38th European Photovoltaic Solar Energy Conference and Exhibition*.

Paper I

Polar solar power plants – Investigating the potential and the design challenges

Frimannslund, I., Thiis, T., Aalberg, A. & Thorud, B.

Published in Solar Energy 224 (2021)

https://doi.org/10.1016/j.solener.2021.05.069

Solar Energy 224 (2021) 35–42

Contents lists available at ScienceDirect

Solar Energy

journal homepage: www.elsevier.com/locate/solener

Polar solar power plants – Investigating the potential and the design challenges

Iver Frimannslund [a,*], Thomas Thiis [a], Arne Aalberg [b], Bjørn Thorud [c]

[a] Norwegian University of Life Sciences, Department of Building- and Environmental Technology, NO-1432 Ås, Norway
[b] University Centre in Svalbard, Department of Arctic Technology, NO-9171 Longyearbyen, Svalbard and Jan Mayen
[c] Multiconsult ASA, Department of Solar, Smart-grid and Storage, NO-0276 Oslo, Norway

ARTICLE INFO

Keywords:
Snow
Energy yield
Bifacial
Module temperature
Snowdrifts
Snow fence

ABSTRACT

The potential for power production and the climatic effects imposed on ground mounted solar power plants in Polar climates are scarcely documented and limit the use of solar power in Polar regions. The study investigates the potential and the design challenges of Polar solar power plants through field measurements of a small-scale solar power plant with modules facing both sky and ground in Adventdalen, Svalbard. The climate is characterized by significant horizontal redistribution of snow due to little shelter and strong winds, causing snowdrifts to develop in the aerodynamic shade of the PV arrays. In this study we show that snowdrifts pose a significant challenge for solar power plants in Polar climates as they can grow to cover the plant, resulting in reduced power production and an imposed mechanical load on the PV arrays. The snowdrifts produced by the PV arrays exhibit a similarity with that produced by porous snow fences and it is argued that snow fence theory can be applied to PV arrays to control the accumulation. The results from solar power production indicates that the module yield is enhanced by the low temperatures as a seasonal performance ratio of 92.5% in combination with below-STC backsheet temperatures are measured. The bifacial gain displays a strong seasonal variation due to the presence snow cover and averages 14.7% annually. The findings indicate that the Polar climate enhance the module performance and that an adaption of solar power plant design is necessary for the system to be resilient to snowdrift development.

1. Introduction

In the past, the use large-scale solar power plants have been limited to climates defined by an abundance of irradiance often referred to as the "Sunbelt" (Wang, 2019). As the prices for solar power have decreased, solar power is becoming competitive also at higher latitudes. The dispersion of large-scale solar power plants has continued past the Sunbelt, and in the future, the decrease of solar power price is expected to continue, potentially further increasing the competitiveness of the technology (ITRPV, 2020).

The competitiveness of solar power at higher latitudes is not only hinged upon decreased production costs, but also at the performance of solar modules due to the characteristics of high latitude climates. A favourable characteristic is the influence of temperature on solar cell efficiency (Duffie & Beckman, 2013). A decrease in cell temperature increases the solar cell voltage and slightly decreases the current, but the net outcome is an increased power output of approximately 0.35–0.5% per kelvin. The performance ratio describes the power output of a solar system compared to the power produced in Standard Test Conditions (STC) and is a measure of the efficiency of the system. In general it is found that the performance ratio increases with latitude due to the influence of temperature dependency on solar cells (Bayrakci et al., 2014).

Additionally, the reflected irradiance due to the high albedo of snow can increase the irradiance collected by a solar module. Bifacial solar modules produce power from the irradiance received on both sides of the module and can significantly increase the power output of solar modules in high-albedo climates (Guerrero-Lemus et al., 2016; Sun et al., 2017; Wittmer & Mermoud, 2018). To describe the net surplus of produced energy from a bifacial module, the bifacial gain (also referred to as "the gain efficiency product") is a factor calculated as the increased power output of a bifacial module compared to a monofacial module with the same configuration (Guerrero-Lemus et al., 2016). Schmid and Reise (2015) used numerical simulations to investigate the bifacial gain for various configuration and albedo values and found a variation from 5 to 24% annually. The combination of low temperatures and ground reflected irradiance increases the performance of solar power

* Corresponding author.

https://doi.org/10.1016/j.solener.2021.05.069
Received 7 December 2020; Received in revised form 21 May 2021; Accepted 23 May 2021
Available online 5 June 2021

normalized to the incoming global horizontal irradiance (Dubey et al., 2013; Sun et al., 2017; Wang, 2019).

Solar power production can thus be more effective in Polar regions and several studies also indicate that there is a market for solar power in the Arctic and the Antarctic. Polar settlements which rely on fossil fuels as the main energy supply are documented to have high fuel cost due to the transportation of the fuel to the remote settlements (Nazarova et al., 2019; Tin et al., 2010). The Russian Government has declared that the high dependence on imported fossil fuels, high energy intensity and high levelized cost of electricity are problematic areas of the development in the Arctic (Nazarova et al., 2019). Similarly, research stations in Antarctica experience the same challenges as fuel is commonly shipped by boat from the mainland and then by overland vehicles for inland stations (Tin et al., 2010). In a case study of a solar power plant "fuel saver" for the Troll research station in Antarctica, it was estimated that a solar power plant covering 50% of the consumption has a Return-On-Investment of 6 years due to a 50% reduction of the LCOE (S. Merlet, 2016). Reduced solar irradiation in the Polar regions as compared to the "Sunbelt" region is thus compensated by increased efficiency resulting from low temperatures and high albedo. The competitiveness of solar PV is further strengthened by the high fuel costs of the existing solutions.

The yield of PV systems in Polar regions is scarcely documented in scientific literature but a few examples document both measured and simulated performance. The yield should be compared carefully as it is strongly influenced by the configuration of the system as well as local shading conditions. In Antarctica, the Syowa station has 55 kW of ground mounted solar modules installed with a steep tilt and a 60° azimuth from true north both east and west with a reported specific yield of 800 kWh/kWp/year (Tin et al., 2010). In the Arctic, a specific yield of 621 kWh/kWp/year is reported for a 13.8 kW roof mounted system in Longyearbyen with a south-east azimuth and an approximate tilt of 20° (Svalbards Miljøvernfond, 2013). For the same location, Ringkjøb et al. (2020) simulated a specific yield of 672 kWh/kWp/year for a 30° south facing fixed tilt system. The simulations were performed using the Global Solar Energy Estimator (GSEE) simulation code (Pfenninger & Staffell, 2016) and MERRA-2 climate data (Gelaro et al., 2017).

The implementation of solar power systems to Polar regions must confront the climatic effects imposed by snow and ice. Snow on the modules is unfavorable as it shades the module surface resulting in a power generation loss and imposes a mechanical load on the module (Andenæs et al., 2018). An increased module tilt increases the probability of snow shedding and can reduce the snow shading losses and the snow load (Andrews et al., 2013; Granlund et al., 2019). Such studies are relevant for topographies less influenced by wind where the snow cover is dominated by vertical precipitation but are not necessarily applicable to windy, unsheltered areas dominated by horizontal redistribution of snow. The Polar tundra and Polar ice-cap climate from Köppen Geiger climate classification (Kottek et al., 2006) commonly have little vegetation to shelter from the wind, and little precipitation as well (Grzegorz, 2010). Although the annual precipitation is typically low in Polar regions, the horizontal snow-flux due to the combination of exposed terrain and high wind speeds can be large in magnitude (Mellor, 1965). The redistribution of snow is caused by snow eroding from exposed areas and accumulating in sheltered areas, creating snowdrifts. The formation of snowdrifts can be considered as a direct consequence of the aerodynamic shade from objects or terrain where the shear stress on the snow particles is reduced below a threshold limit (Thiis & Ferreira, 2014). To reduce snowdrifts in unwanted areas, the design of infrastructure in Polar regions is commonly adapted to control where snow is deposited and eroded (Thiis & Gjessing, 1999; Tominaga, 2018). Snow fences can be implemented as a measure to retain the snow in upwind accumulations zones.

In this study, it is argued that the theory of the properties of snow fences can be applied to ground mounted PV arrays. Tabler (2003) has extensively studied how the properties of snow fences influence the snowdrift shape and storage capacity. His findings include that the length and height of fully developed snowdrifts are approximately proportional to the fence height (Tabler, 1980a). This allows to use scaled models for investigating the snowdrifts produced by larger snow fences (Tabler, 1980b). Further he showed that the inclination of snow fences has the effect of displacing the nose of the snowdrift and changing both length and storage capacity (Tabler, 2003). An inclination leaning with the wind displaces the nose of the drift upwind and increases length and the storage capacity while an inclination into the wind produces the opposite result as wind is forced underneath the snow fence. However, inclining the snow fence reduces the fence height which has the effect of reducing the storage capacity. Similarly, the bottom gap of snow fences influences the storage capacity as well. A bottom gap of 10–15% of the total height of the fence is considered optimal, while increasing the gap beyond this height reduces the depth and storage capacity of the drifts

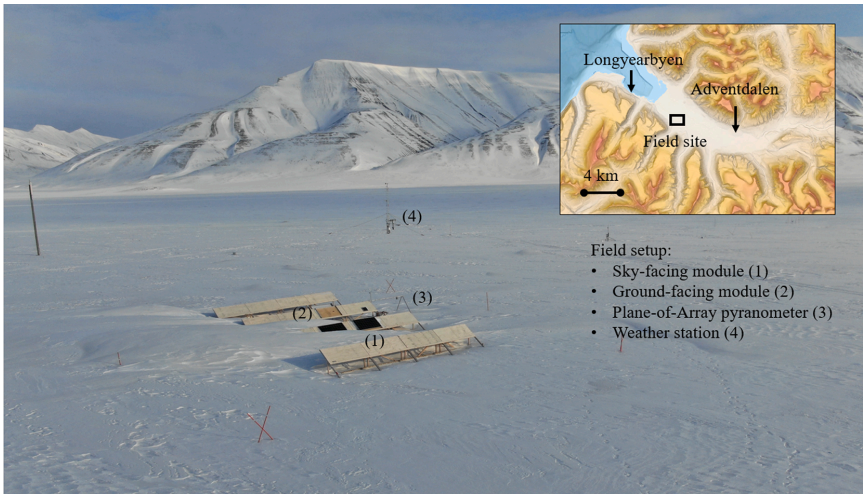

Fig. 1. Field setup and site location. Four 10 m long PV mock-up rows are placed at the valley floor in Adventdalen. PV modules are mounted on the rows and a weather station and a Plane-of-Array pyranometer are installed in proximity to the setup.

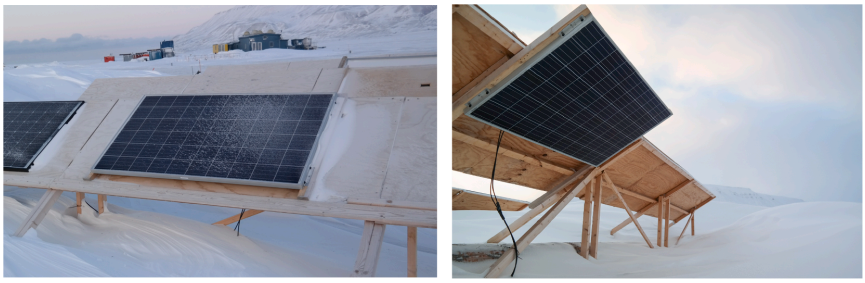

Fig. 2. Module installation with a sky-facing module (left) and a ground-facing module (right). The modules are lifted 2 cm from the wooden surface to allow for ventilation on the backside.

and displaces the nose of the drift further downwind. The profile of a snowdrift measured parallel to the wind is independent of incident wind directions (referred to as "attack angles" by Tabler) between 45 and 90° in relation to the longitudinal alignment of the fence (Tabler, 1980a). However, the cross-section area and length of the snowdrift vary with wind direction and can be expressed as the sine of the attack angle multiplied by the cross-section area or length formed by a wind direction perpendicular to the snow fence (Tabler, 2003). These properties of snow fences are connected to the properties of PV arrays and are discussed in Section 4.

For redistribution of snow in solar power systems the existing research mostly concern the influence of solar power system on roof snow loads. Ferreira et al. (2019) used wind tunnel experiments and numerical simulation to study the friction velocity on a roof surface with solar panel arrays and found that the arrays differentiate the friction velocity at roof surfaces and that the bottom gap and wind direction in relation to the system azimuth is determinative for the accumulation conditions. Brooks et al. (2014) and Grammou et al. (2019) used water flume simulations to investigate aerodynamical drift patterns on low tilt roof mounted systems and found that the drift patterns were influenced by the presence of the arrays.

This study investigates the power production potential and the climatic effects imposed on a small-scale ground mounted mock-up solar power plant in the Adventdalen valley in Svalbard. The climate in the valley is characterized by low precipitation (213 mm annually on average) and strong winds from a uniform direction (Gallet et al., 2019). The upwind distance capable of transporting snow (fetch) is large enough so that the horizontal snow flux is only limited by the evaporation of the wind-blown snow (Tabler, 2003). Several snowdrift studies have previously been performed at the same location (Jaedicke, 2001; Thiis & Gjessing, 1999). As the latitude of the site is 78° North, the seasonal variations in solar irradiance are significant. Midnight sun and wintertime darkness each occur for approximately four months of the year, with a transition between the two extremes of only two months. At summer solstice, the solar altitude is 35.2° midday (south), and 11.8° at midnight (north).

2. Field measurement setup

The investigated solar power plant in this study is a fixed tilt system constituting of four mock-up rows made of 2x3″ spruce beams and plywood with solar modules mounted on top as shown in Fig. 1. This section presents the specification of the field measurement setup.

2.1. PV design layout

Established principles of PV plant design are used to determine the configuration of the arrays. The system has a south facing azimuth to maximize the yield. Although the optimal tilt to maximize received solar irradiance in a collector plane is 50°, an angle of 30° was chosen to increase the ground cover ratio. Simulations with PVsyst indicate a 5% irradiance reduction by adjusting the tilt from 50° to 30° (PVsyst SA, 2020). The rows are spaced to avoid interrow shading for a solar altitude higher than 10°, resulting in a pitch of 5.5 m. The total height of the system is 1.3 m and the effective bottom gap between array and ground is approximately 0.65 m. Solid timber poles (length = 12 m, diameter = 20–30 cm) are used as ballast for the arrays to secure for high wind speeds. The beams are partially covered by snow and ice in wintertime. The gross surface of each array is 1.2x10 m, allowing for standard sized module (1x1.6 m) to be placed in landscape orientation.

2.2. PV modules and inverter

Two monofacial modules are installed on the 30° wooden rack in opposite directions as shown in Fig. 2: one facing the sky and one facing the ground. A bifacial module was installed as well but was covered by the snowdrifts during the beginning of the production season and suffered significant power production losses. Both monofacial modules are installed at the middle rows to provide similar shading conditions. The ground-facing module is elevated slightly above the mock-up arrays to

Table 1
Snowdrift measurement data. Days of snowdrift development represent the number of days in the field with a potential of snow redistribution, with the first day of such conditions estimated to be the 1st of October. H is the height of the system and is equal to 1.3 m.

Event	Date	Days of snowdrift development	Drift length / H	Maximum snow depth / H	Volume [m^3]
Installation	12.03.19	0	–	–	–
Measurement 1	21.03.19	12	17	0.53	34.3
Measurement 2	10.05.19	60	22	0.58	130.6
Measurement 3	21.02.20	143	45	1.27	778.8
Measurement 4	07.04.20	189	50	1.38	1007.6

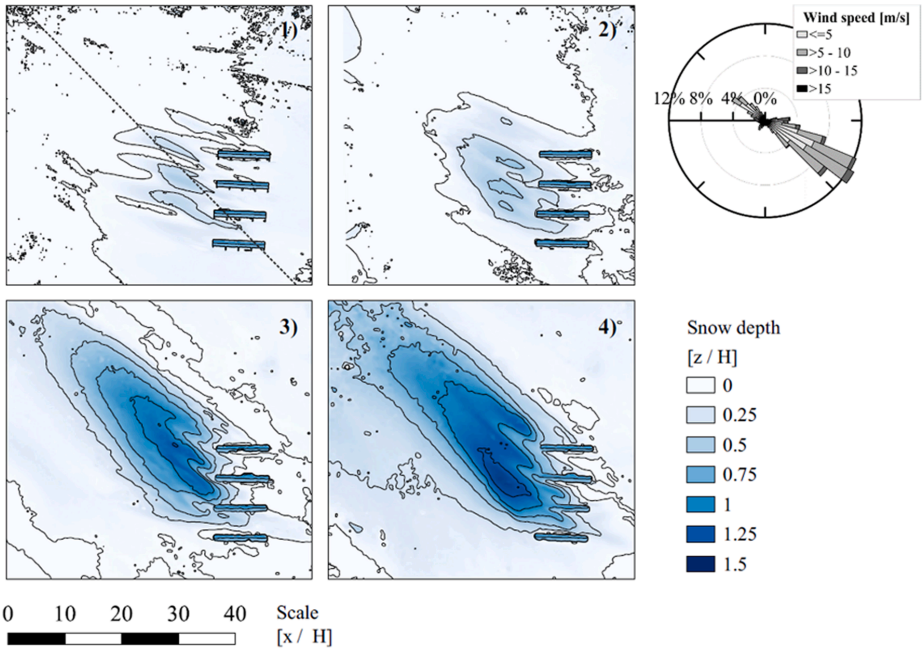

Fig. 3. Map displaying the snow depth for measurement 1–4. The wind rose in the upper right corner displays the wind conditions at the site. The dashed line in measurement 1 marks a cross-section of the snowdrifts displayed in Fig. 4.

reduce the effect of shading from the rack. The distance from the ground to the bottom of the panel is approximately 1.0 m. Plane-of-Array irradiance (POA) and reflected Plane-of-Array irradiance (POA_r) are logged with a pyranometer outside of the plant. Additionally, a backsheet temperature sensor was installed on the sky-facing module. To measure the power produced by the modules, current and voltage of each module are logged with a sample rate of 10 s with a Campbell Scientific CR1000X datalogger. The voltage and current are measured on the DC-side from the inverter.

The monofacial modules are of the type JKM265P by Jinko Solar with a rated performance of 265 W_p at STC. The inverter and built-in MPPT is the CI-Mini-1200H from CyboEnergy (CyboEnergy, 2020). The inverter is made for off-grid purposes and produces variable AC-voltage for heating elements. As the site offers no grid connection possibilities, the inverter is suitable for the setup as the load from the modules is consumed on-site by heating cables. The inverter displayed a variable capability to accurately detect the MPP of the modules. To compensate for the variability of the inverter, the results were filtered to obtain the maximum value in 2-minute intervals. The same filtration on the irradiance data increases the annual Plane-of-Array irradiance less than 5%. In general, snow was not removed from the modules throughout the season. However, the modules were cleaned after soiling events caused by a nearby road.

3. Results

3.1. Solar power plant snowdrifts

Short time after the installation of the solar power plant in the field, snowdrifts were observed in the leeward side of the plant. To document the development of the snowdrifts, photogrammetry was used to construct 3D models of the snowdrifts at different timesteps. A total of four measurements were performed over two winters. The snow drifts melted entirely between the winters. Table 1 shows key numbers from the measurements, while Fig. 3 virtually display the snowdrift depth for all four measurements. The results are presented in relation to the total

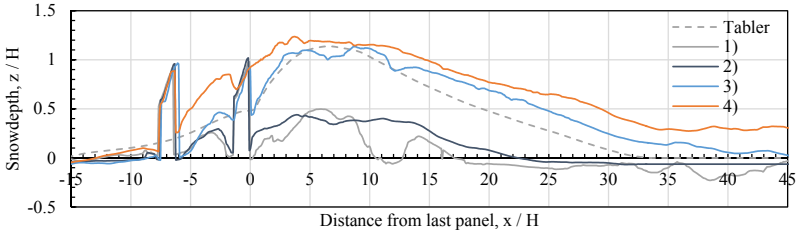

Fig. 4. Snowdrift height and length in relation to the PV height for measurement 1–4. The dashed line marks equilibrium drifts from a 3.8 m tall 50% porous snow fence (Tabler, 1989).

Fig. 5. An aerial photography displays the scale of the snowdrifts at measurement 3.

height of the array (equal to 1.3 m).

The results show an increase of drift length, height and volume with the time of exposure in the field. The accumulation mainly occurs at the leeward side of the PV arrays corresponding to the prevailing wind direction. On measurement 3 and 4, the height of the drifts exceeds the height of the arrays. In measurement 4, the snowdrifts extend onto the arrays and close the gap for the second southernmost array.

A cross-section parallel to the prevailing wind direction (indicated by the dashed line in Fig. 3) is displayed in Fig. 4. The cross section of the snowdrifts produced by the PV arrays is compared with the cross section of snowdrifts produced by a 3.8 m tall 50% porous snow fence. Fig. 4 shows that the snowdrifts from the PV arrays exhbit a similarity with snowdrifts from the snow fence.

To provide a better sense of scale to the drifts, an aerial photography from measurement 3 shows the size of the drifts in relation to passing snow-mobile transport in Fig. 5.

Table 2
Module yield for the monofacial sky- and ground-facing modules. A theoretical bifacial yield with 80% bifaciality factor is calculated from the monofacial modules yield. The bifacial gain is calculated as the relative difference in production to the sky-facing module.

Module	Annual production [kWh]	Specific yield [kWh/kWp/year]	Performance ratio* [%]	Bifacial gain [%]
Mono. sky	177.6	670.0	92.5	–
Mono. ground	32.6	122.9	–	–
Bifacial	203.7	768.3	–	14.7

* The performance ratio is calculated in an interval from July to October due to an error with the Plane-Of-Array pyranometer.

3.2. Solar power production

Solar power production began in 5th of March and ended the 19th of October. A few days at the very beginning of the season was missed due to a malfunction of the logging system. However, the influence on the total production is small due to weak irradiance in the early season. The annual yield of the system is shown in Table 2. A theoretical bifacial yield is calculated as the sum of the yield of the sky-facing module and 80% of the ground-facing module. It thus represents a bifacial module with an 80% Bifaciality factor (Guerrero-Lemus et al., 2016).

Irradiance measurements from the nearby weather stations show that the irradiance in 2020 was 7.9% lower than the annual average from the last 5 years of complete irradiance datasets. If the yield is scaled proportional to the irradiance, a long-term average specific yield of 727.8 and 834.6 kWh/kWp/year is obtained for the sky-facing module and the bifacial module respectively.

The performance of the ground-facing module in relation to the sky-facing module displays a strong seasonal variation due to the seasonal variations in snow cover and irradiance. Fig. 6 shows the seasonal variation of the relative performance.

Here it can be seen that the relative performance of the ground-

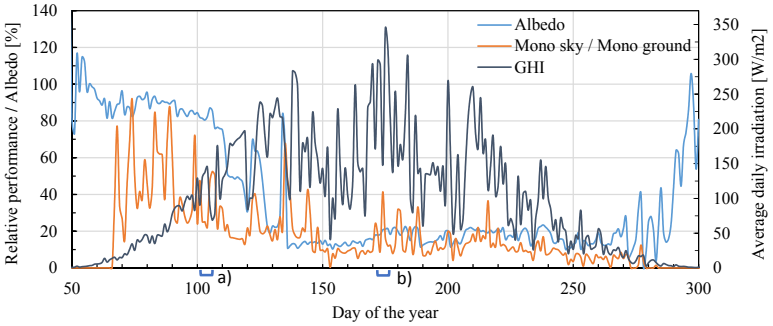

Fig. 6. Relative performance of the ground-facing module in relation to the sky-facing module compared with albedo and global horizontal irradiance. The graph is produced with daily average data.

Table 3
Seasonal variations in the production of the sky- and ground-facing module in relation to the presence of the snow cover.

Snow cover status	Production monofacial-sky [Wh/day]	Production monofacial-ground [Wh/day]	Sky-facing module / Ground-facing module [%]
During snow cover	525.0	196.2	37.4
After snow cover	828.8	129.0	15.6

facing module is reduced around day 110 due to the melting of the snow cover. The performance of the modules in relation to the presence of the snow cover is quantified in Table 3.. Here it can be seen that the production of the ground-facing module is higher before the melting of snow cover although the incoming global horizontal irradiance is weaker. Daily production profiles from three consecutive days in summer and spring in Fig. 7 illustrates this phenomenon. In spring, the performance of the bifacial module is increased by a significant contribution of rear-side irradiance and reach the same production peak as in summer although the global horizontal irradiance is weaker. In summer, the contribution from the ground reflected irradiance is less and makes up a small part of the total power production. However, the bifacial module has a secondary production peak at midnight due to irradiance on the backside of the module. The midnight production is not only caused by ground-reflected irradiance, but from direct irradiance from the north as well. This phenomenon enables uninterrupted power production in summer.

The backsheet temperature of the monofacial sky-facing module was logged during the entire year. Fig. 8 shows a scatterplot of the backsheet temperature in relation to the module yield. A trend of increasing temperature with increasing yield is evident, as is expected due to the heat produced from the PV module during operation. Most of the power production occur well below STC-temperature.

4. Discussion

The development of snowdrifts in a solar power plant is an undesired phenomenon that can limit power production and impose a mechanical load on the PV arrays. The solar power plant investigated in this study was designed with established principles of solar power plant design commonly used at lower latitudes and resulted in a development of snowdrifts in the Adventdalen climate. The accumulation was severe and partially buried one array towards the end of the second winter. The constant development of the snowdrifts during the measurements indicates that no equilibrium state of the snowdrifts is achieved, and that the accumulation is likely to continue. This is also likely for the fourth measurement where the gap beneath one of the PV arrays is closed by the snowdrift. The closing of the gap changes the flow field and is likely to prolong the accumulation and a potential equilibrium-state snowdrift. The results suggest that for a solar power plant to be sustainable in Polar

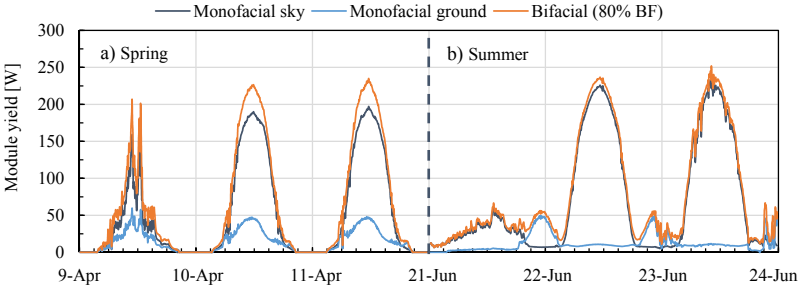

Fig. 7. Production profiles from three consecutive days for the monofacial sky-facing module, monofacial downward-facing module and a theoretical bifacial module with an 80% bifaciality factor.

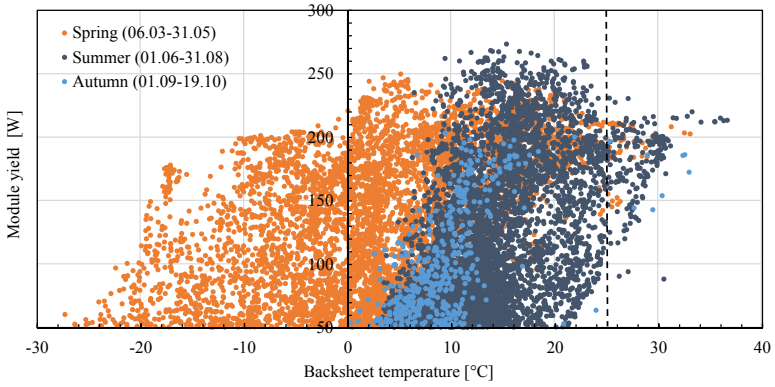

Fig. 8. Backsheet temperature in relation to the yield of the monofacial sky-facing panel from 5-minute average data. The dashed line marks the STC-module temperature.

regions, the plant should be adapted to be resilient against snowdrift development.

As snowdrifts are a direct consequence of the aerodynamic shade from objects and terrain, a modification of the design of the solar power plant can be used to control snow accumulation and erosion in the plant. In this study, the snowdrifts produced from the PV arrays exhibit a strong similarity with snowdrifts produced by porous snow fences. The development of the snowdrifts viewed as a cross-section parallel to the wind direction, shown in Fig. 4, is very similar to experimental studies on snow fences performed by Tabler (2003). The similarity indicates that snow fence theory can be applied to PV arrays and used to control snowdrift accumulation in solar power plants. The design can be adapted so that snow is deposited in designated areas (as with snow fences) or so that the deposition is minimized. How to adapt snow fences to maximize snow deposition is thoroughly documented in research, but how similar structures can be adapted to minimize the accumulation is seldom investigated and is the topic of the discussion to follow.

Several findings from snow fence studies can be connected to the properties of solar power plants. As the snow drift cross section area and length decrease with the sine of the wind direction (where 90° is perpendicular) (Tabler, 2003), an attack angle parallel to PV arrays is favourable to reduce snow accumulation. Shifting the azimuth of the plant can thus be used to reduce snow accumulation in climates with uniform wind directions such as in Adventdalen. However, the influence of the rack itself should be taken into account in such cases. The finding also indicates that if the attack angle in the field measurement setup was 90° instead of 30-45°, the length and cross section area of the snowdrifts could increase by up to 50%. The empirical expression from Tabler is valid for single snow fences, but it could be argued that the effect on several consecutive PV arrays would only propagate the accumulation.

The effect of snow fence inclination and bottom gap on snow drifts documented by Tabler (2003) can also be applied to the PV arrays. A strong inclination of snow fences reduces the net height of the fence and the resulting snow storage capacity. Strongly inclining the PV arrays while maintaining a bottom gap is therefore likely to reduce the storage capacity of the PV produced snow drifts. An empirical expression from Tabler (1994) shows that the relationship of the bottom gap and total height should be equal to 0.75 to avoid any snow storage. For the configuration of the power plant in Adventdalen, this implies that the gap between the array and the ground should be equal to 1.8 m. This is almost three times the gap as used in the field measurement setup. For a single array, this expression is likely conservative as it does not take into account the inclination of the array. However, the effect of several consecutive arrays can have an adverse effect on the accumulation conditions.

The knowledge from snow fence design indicates that the azimuth, array tilt and bottom gap of PV arrays can be adjusted to minimize snow accumulation in the plant. Additionally, the distance between the arrays is likely to influence the accumulation. The properties discussed here are likely applicable to PV arrays of varying size as the snowdrifts produced by snow fences are approximately proportional to the height of a snow fence (Tabler, 1980b). Scaling the PV array properties (including the array surface, the distance between arrays and the bottom gap) will, therefore, likely produce a similar result as shown in this study.

Changing the configuration of the plant will influence yield and costs of the system. The design of ground mounted solar power plants in climates with high snow redistribution should balance between designing a system with high energy yield and a system is optimized for snowdrift accumulation. The latter is necessary to provide a climate robust system ensuring the long-term sustainability of the system. The challenge lies in optimizing for two very different design criteria where an optimization of one can have an unfavorable effect on the other.

A specific yield of 670 and 768.3 kWh/kWp/year was measured for the sky-facing module and a theoretical bifacial module respectively. However, the irradiance in 2020 was 7.9% lower than average and indicates that the measured specific yield is likely underestimated compared with a long-term average. If the yield is scaled proportional to the irradiance, a long-term average specific yield of 727.8 and 834.6 kWh/kWp/year is obtained. Scaling the yield proportional with the irradiance does not consider the effect of increased module temperature and may slightly overestimate the module yield. Ringkjøb et al. (2020) reported a specific yield of 672 kWh/kWp/year for a monofacial module with numerical simulations of a system with the same configuration and same location as in the field measurements. However, the irradiance used in the numerical simulations was 11.9% higher than the measured irradiance at the field site in 2020. The discrepancies between simulated and measured yield may arise from differences in system specifications or from inaccurate estimation of the module performance.

A performance ratio of 92.5% was measured between July and October for the sky-facing module. As mentioned, the performance ratio is the performance of the system in the field compared to the performance at STC and is influenced by the system quality, module temperature, shading conditions and other factors. Performance ratios above 90% is considered high and signifies a well-performing system (Reich et al., 2012). The measured backsheet temperature shown in Fig. 8 indicates that the cell temperature is well below STC-temperature for the majority of the season. The measured backsheet temperature data supports that low cell temperature is likely to have a strong influence on the measured performance ratio. As the performance ratio in this study is only calculated from July-October and measured temperatures are the lowest in spring, an all-year performance ratio is likely to exceed the reported performance ratio. It is important to note that the produced power is logged on the DC-side and therefore does not take into account the conversion efficiency of the inverter.

A bifacial gain of 14.7% was calculated for a theoretical bifacial module with 80% bifaciality factor. The bifaciality factor is commonly in the range of 60–95% (Tian Shen et al., 2019). The simplification of taking the sum of the production of two monofacial modules does not take into account the non-symmetrical layout of a bifacial cell or the effect of double side glazing on the optical losses and temperature (Halm et al., 2014; Hubner et al., 1997; Janssen et al., 2017). Additionally, the ground-facing module only received irradiance on the front side of the module (facing the ground) which contributes to artificially low module temperatures during operation. However, the measured bifacial gain of 14.7% is high and encourages the use of bifacial modules in Polar regions. As the bifacial gain is a system specific property that is influenced by configuration and albedo, a higher bifacial gain can be achieved for climates with a higher average albedo or for designs with a more favourable configuration than the case investigated.

Polar ice cap climates are defined by the warmest average monthly temperature not exceeding 0 °C (Kottek et al., 2006). In such climates, the snow cover is constant, providing a high albedo the entire power production season. With a bifacial solar power system configured to utilize the reflected irradiance in combination with a climate contributing to low cell temperatures, the efficiency of a solar power system can potentially be higher than any place on earth. However, if snowdrifts develop in the system, they will not melt. The presence of snow over consecutive years theoretically signifies the formation of a glacier. The potential benefits of Polar solar power plants can therefore be high but preconditions a system resilient to snowdrift development.

5. Conclusion

The small-scale power plant in Adventdalen produced snowdrifts jeopardizing the functionality of the system. To ensure the resilience of solar power plants in snow drift climates, the design should be adapted to snowdrift development. This can be performed by adapting the configuration of the PV arrays so that snow is deposited in designated areas or so that the deposition is minimized. In this study, it is found that snowdrifts produced by the PV arrays exhibit a strong similarity with snowdrifts produced by snow fences. The similarity indicate that principles of snow fence design can be applied to PV arrays. Research on

snow fence theory imply that several properties of the PV arrays can be adjusted to control the snow accumulation. The properties which can be adjusted includes the azimuth of the plant, the tilt of the arrays and the gap between the array and the ground. In addition, the effect of several consecutive PV arrays must also be accounted for. The results from PV power production show a specific yield of 670 kWh/kWp/year for the sky-facing module but may not be representative of a long-term average due to annual variations in irradiance. The performance ratio is a metric normalized to the POA-irradiance and was measured at 92.5% for the sky-facing module. The logged backsheet temperature of the module indicates a positive contribution from low temperatures. The climate is favourable for bifacial power production due to a significant contribution from ground reflected irradiance. A theoretical bifacial yield is calculated from the yield of the monofacial modules, representing a bifacial module with 80% bifaciality factor. The bifacial gain is measured to be 14.7% and the contribution of rear side irradiance is shown to vary with the seasons due to the presence of the snow cover. The findings highlight the potential of solar power production in Polar climates as well as the design challenge due to snowdrift development from the system. An adaption of the design of solar power plants which ensures high yield and snowdrift resilience should be performed to enable the dispersion of ground mounted solar power plants to Polar regions.

Declaration of Competing Interest

The authors declare that they have no known competing financial interests or personal relationships that could have appeared to influence the work reported in this paper.

References

Andenæs, E., Jelle, B., Ramlo, K., Kolås, T., Selj, J., Foss, S., 2018. The influence of snow and ice coverage on the energy generation from photovoltaic solar cells. Sol. Energy 159, 318–328. https://doi.org/10.1016/j.solener.2017.10.078.

Andrews, R., Pollard, A., Pearce, J., 2013. The effects of snowfall on solar photovoltaic performance. Sol. Energy 92, 84–97. https://doi.org/10.1016/j.solener.2013.02.014.

Bayrakci, M., Choi, Y., Brownson, J.R.S., 2014. Temperature dependent power modeling of photovoltaics. Energy Procedia 57, 745–754. https://doi.org/10.1016/j.egypro.2014.10.282.

Brooks, A., Gamble, S., Dale, J., Gibbons, M., 2014. Determining Snow Loads on Buildings with Solar Arrays. International Structural Specialty Conference, Halifax, NS.

CyboEnergy, 2020. Available at: http://www.cyboenergy.com/ (accessed: 12.11.2020).

Dubey, S., Sarvaiya, J.N., Seshadri, B., 2013. Temperature dependent photovoltaic (PV) efficiency and its effect on PV production in the world – a review. Energy Procedia 33, 311–321. https://doi.org/10.1016/j.egypro.2013.05.072.

Duffie, J.A., Beckman, W.A., 2013. Design of photovoltaic systems. Solar Engineering of Thermal Processes. John Wiley & Sons Inc, Hoboken, New Jersey.

Ferreira, A., Thiis, T., A. Freire, N., M.C., Ferreira, A., 2019. A wind tunnel and numerical study on the surface friction distribution on a flat roof with solar panels. Environ. Fluid Mech., 19. doi: 10.1007/s10652-018-9641-5.

Gallet, J.-C., Björkman, M., Borstad, C., Hodson, A., Jacobi, H.W., Larose, C., Luks, B., Spolaor, A., Urazgildeeva, A., Zdanowicz, C., 2019. Snow research in Svalbard: current status and knowledge gaps.

Gelaro, R., McCarty, W., Suárez, M., Todling, R., Molod, A., Takacs, L., Randles, C., Darmenov, A., Bosilovich, M., Reichle, R., et al., 2017. The modern-era retrospective analysis for research and applications, version 2 (MERRA-2). J. Clim. 30 https://doi.org/10.1175/JCLI-D-16-0758.1.

Grammou, N., Pertermann, I., Puthli, R., 2019. Snow loads on flat roofs with elevated solar panel arrays. Steel Construction 12 (4), 364–371. https://doi.org/10.1002/stco.201900031.

Granlund, A., Narvesjö, J., Malou Petersson, A., 2019, 2019. The Influence of Module Tilt on Snow Shadowing of Frameless Bifacial Modules. 36th European Photovoltaic Solar Energy Conference and Exhibition, Marseille, September 9-13, 2019, pp. 1650-1654.

Grzegorz, R., 2010. Climate: Polar. In: Warf, B. (Ed.), Encyclopedio of Geography. SAGE Publications.

Guerrero-Lemus, R., Vega, R., Kim, T., Kimm, A., Shephard, L.E., 2016. Bifacial solar photovoltaics – A technology review. Renew. Sustain. Energy Rev. 60, 1533–1549. https://doi.org/10.1016/j.rser.2016.03.041.

Halm, A., Aulehla, S., Schneider, A., Mihailetchi, V., Roescu, R., Galbiati, G., Libal, J., Kopecek, R., 2014. Encapsulation losses for ribbon contacted N-type IBC solar cells. Proceedings of the 29th European Photovoltaic Solar Energy Conference and Exhibition.

Hubner, A., Aberle, A. & Hezel, R. (1997, 29 Sept.-3 Oct. 1997). Temperature behavior of monofacial and bifacial silicon solar cells. Conference Record of the Twenty Sixth IEEE Photovoltaic Specialists Conference - 1997.

ITRPV, 2020. International Technology Roadmap for Photovoltaic.

Jaedicke, C., 2001. Drifting snow and snow accumulation in complex terrain. University of Bergen.

Janssen, G.J.M., Tool, K.C.J., Kossen, E.J., Van Aken, B.B., Carr, A.J., Romijn, I.G., 2017. Aspects of bifacial cell efficiency. Energy Procedia 124, 76–83. https://doi.org/10.1016/j.egypro.2017.09.334.

Kottek, M., Grieser, J., Beck, C., Rudolf, B., Rubel, F., 2006. World Map of the Köppen-Geiger Climate Classification Updated. Meteorol. Z. 15, 259–263. https://doi.org/10.1127/0941-2948/2006/0130.

Mellor, M., 1965. Cold Regions Science and Engineering Part III, Section A3c. Hanover, New Hampshire.

Nazarova, Y., Sopilko, N., Kulakov, A., Shatalova, I., Myasnikova, O., Bondarchuk, N., 2019. Feasibility study of renewable energy deployment scenarios in remote arctic communities. Int. J. Energy Econ. Policy 9, 330–335. https://doi.org/10.32479/ijeep.7343.

Pfenninger, S., Staffell, I., 2016. Long-term patterns of European PV output using 30 years of validated hourly reanalysis and satellite data. Energy 114, 1251–1265. https://doi.org/10.1016/j.energy.2016.08.060.

PVsyst SA, 2020. PVsyst. route du Bois-de-Bay 107, Satigny, Switzerland.

Reich, N., Müller, B., Armbruster, A., van Sark, W., Kiefer, K., Reise, C., 2012. Performance ratio revisited: is PR > 90% realistic? Prog. Photovoltaics Res. Appl. 20, 717–726. https://doi.org/10.1002/pip.1219.

Ringkjøb, H.-K., Haugan, P.M., Nybø, A., 2020. Transitioning remote Arctic settlements to renewable energy systems – A modelling study of Longyearbyen, Svalbard. Appl. Energy 258, 114079. https://doi.org/10.1016/j.apenergy.2019.114079.

S. Merlet, T. T., B. Thorud, E. Olsen, J. Nyhus. (2016). Challenges of PV Generation in Polar Regions. Case Study: the Norwegian Research Station "Troll" in Antarctica. 32nd European Photovoltaic Solar Energy Conference and Exhibition.

Schmid, A., Reise, C., 2015. Realistic Yield Expectations for Bifacial PV Systems - An Assessment of Announced, Predicted and Observed Benefits. 31st European Photovoltaic Solar Energy Conference and Exhibition.

Sun, X., Khan, M., Deline, C., Alam, M., 2017. Optimization and performance of bifacial solar modules: a global perspective. Appl. Energy 212. https://doi.org/10.1016/j.apenergy.2017.12.041.

Svalbards Miljøvernfond, 2013. Sluttrapport - publikumsvennlig, 3/36 Bygningsintegrert solenergianlegg – Etablering i Elvesletta Syd.

Tabler, R.D., 1994. Design guidelines for the control of blowing and drifting snow. Strategic Highway Research Program.

Tabler, R.D., 2003. Controlling Blowing and Drifting Snow with Snow Fences and Road Design. Niwot, Colorado.

Tabler, R.D., 1980a. Geometry and density of drifts formed by snow fences. J. Glaciol. 26 (94), 405–419. https://doi.org/10.3189/S0022143000010935.

Tabler, R.D., 1980b. Self-similarity of wind profiles in blowing snow allows outdoor modeling. J. Glaciol. 26 (94), 421–434. https://doi.org/10.3189/S0022143000010947.

Tabler, R. D. (1989). Snow fence technology: State of the art. First International Conference on Snow Engineering, Santa Barbara, California.

Thiis, T., Ferreira, A., 2014. Sheltering effect and snow deposition in arrays of vertical pillars. Environ. Fluid Mech. 15 https://doi.org/10.1007/s10652-014-9356-1.

Thiis, T.K., Gjessing, Y., 1999. Large-scale measurements of snowdrifts around flat-roofed and single-pitch-roofed buildings. Cold Reg. Sci. Technol. 30 (1), 175–181. https://doi.org/10.1016/S0165-232X(99)00021-X.

Tian Shen, L., Pravettoni, M., Deline, C., Stein, J., Kopecek, R., Singh, J.P., Luo, W., Wang, Y., Aberle, A., Khoo, Y.S., 2019. A review of crystalline silicon bifacial photovoltaic performance characterisation and simulation. Energy Environ. Sci. 12 https://doi.org/10.1039/C8EE02184H.

Tin, T., Sovacool, B.K., Blake, D., Magill, P., El Naggar, S., Lidstrom, S., Ishizawa, K., Berte, J., 2010. Energy efficiency and renewable energy under extreme conditions: Case studies from Antarctica. Renewable Energy 35 (8), 1715–1723. https://doi.org/10.1016/j.renene.2009.10.020.

Tominaga, Y., 2018. Computational fluid dynamics simulation of snowdrift around buildings: Past achievements and future perspectives. Cold Reg. Sci. Technol. 150, 2–14. https://doi.org/10.1016/j.coldregions.2017.05.004.

Wang, Z., 2019. Chapter 2 - The Solar Resource and Meteorological Parameters. In: Wang, Z. (Ed.), Design of Solar Thermal Power Plants. Academic Press, pp. 47–115.

Wittmer, B., Mermoud, A., 2018. Yield Simulations for Horizontal Axis Trackers with Bifacial PV Modules in PVsyst. 35th European Photovoltaic Solar Energy Conference and Exhibition.

Paper II

Impact of solar power plant design parameters on snowdrift accumulation and energy yield

Frimannslund, I., Thiis, T., Ferreira, A. & Thorud, B.

Published in Cold Regions Science and Technology 201, (2022).

https://doi.org/10.1016/j.coldregions.2022.103613

Cold Regions Science and Technology 201 (2022) 103613

Contents lists available at ScienceDirect

Cold Regions Science and Technology

journal homepage: www.elsevier.com/locate/coldregions

Impact of solar power plant design parameters on snowdrift accumulation and energy yield

Iver Frimannslund [a,*], Thomas Thiis [a], Almerindo D. Ferreira [b], Bjørn Thorud [c]

[a] Norwegian University of Life Science, Department of Building- and Environmental Technology, NO-1432 Ås, Norway
[b] University of Coimbra, Department of Mechanical Engineering, ADAI-LAETA, 3030-788 Coimbra, Portugal
[c] Multiconsult ASA, Department of Solar, Smart-Grid and Storage, NO-0276 Oslo, Norway

ARTICLE INFO

Keywords:
Snowdrift
Photovoltaic systems
Climate adaption
Energy yield
Sensitivity analysis

ABSTRACT

Solar power plants designed in accordance with established design principles are influenced by snowdrift accumulation in Polar climates. A strategy to avoid snowdrifts in the plant is to adapt the design of the plant itself. To provide a background for the adaptation of solar power plants to Polar climates, the effect of performing parameter adjustments on the snow accumulation conditions as well as the plant yield should be quantified. This study uses Computational Fluid Dynamic (CFD) and energy yield simulations, validated with field measurements, to investigate the sensitivity of snowdrift accumulation and energy yield to solar power plant design parameters. The investigated parameters include the panel tilt, the row spacing, the gap-to-ground, the system scale and the azimuth/wind direction. Here it is shown that the investigated design parameters exhibit a large variation in sensitivity and that only two parameter adjustments which reduce the risk of snowdrift accumulation increase or have an insignificant impact on the energy yield, namely increasing the gap-to-ground and the system scale. Tilt, pitch and azimuth adjustments can reduce the risk of snowdrift accumulation but for a trade-off in energy yield. As the snowdrift accumulation conditions depend on the local snow and wind climate and PV system characteristics such as plant size, the design adjustments should be performed for the specific design scenario. This study provides a background for adjusting the design of the plant to the local climate to increase the snowdrift resilience while minimizing adverse effects on the system yield.

1. Introduction

Photovoltaic (PV) power has been used for decades in Polar regions to provide power for technical installations such as weather stations or telecommunication equipment (Tin et al., 2010). The Polar climate have severable favourable characteristics for solar power production, namely the effect of increased solar cell voltage with decreasing temperature, and high-albedo providing significant amounts of ground-reflected irradiance which can be utilized by bifacial solar panels (Frimannslund et al., 2021). In recent times, the decreased costs of solar power systems make solar power a competitive energy supply for Polar settlements as well. Remote Polar settlements have traditionally relied on imported fossil fuels, which has been documented to produce a high Levelized Cost of Electricity (LCOE) due to significant fuel transportation expenses (Dou et al., 2019; Obara et al., 2013; Tin et al., 2010). In Antarctica, research stations positioned along the coast or on the inland ice rely on fuel supply by boat or overland transport. A case study of the Troll research station in Antarctica estimates that the LCOE can be halved by a solar power plant "fuel saver" which covers 50% of the consumption (S. Merlet, 2016).

However, the success of solar power plants in Polar climates relies upon resilience against environmental loads from wind, snow, and ice. In a field measurements study of a small-scale fixed tilt ground-mounted power plant in Arctic island of Spitsbergen, the development of snowdrifts in the plant is shown to jeopardize the functionality of the system, as the snowdrifts both shade the solar panels and impose a mechanical load (Frimannslund et al., 2021). Snowdrifts build from the ground up and should be viewed as a separate phenomenon to precipitated snow on solar panels as studied by several (Andenæs et al., 2018; Pawluk et al., 2019). The snowdrift problem may also be relevant for lower latitude climates with a significant horizontal redistribution of snow such as the plains of Wyoming or Mongolia which already rely on snowdrift precaution measures in infrastructure design. As the snowdrifts are a consequence of the aerodynamic shade of the plant, and an adaption of

* Corresponding author.
E-mail address: iver.frimannslund@nmbu.no (I. Frimannslund).

https://doi.org/10.1016/j.coldregions.2022.103613
Received 18 October 2021; Received in revised form 8 April 2022; Accepted 6 June 2022
Available online 9 June 2022

the plant itself can be used to control the snowdrift accumulation. Experimental studies of rooftop solar power plant systems show the orientation of the panels in relation to the wind direction is strongly influential on the accumulation conditions on the roof (Brooks et al., 2014; Ferreira et al., 2019; Thiis et al., 2015). Additionally, a similarity between snowdrifts from snow fences and from rows of PV panels also suggest that snow fence theory can be applied to single rows of solar panels, indicating that shifting the inclination of the panels, the gap-to-ground and the orientation of the plant (azimuth) can be used to reduce the risk of snowdrift accumulation in solar power plants (Frimannslund et al., 2021). However, the effectiveness of performing design adjustments of the solar power plant to reduce the impact of snowdrift accumulation remains unquantified. Furthermore, a change in solar power plant design will influence the energy yield of the plant, and it is unfavourable to perform adjustments which increase the snowdrift resilience, but significantly reduce the power production. To clarify the consequence of changing the design of solar power plants to increase snowdrift resiliency, this study performs a sensitivity analysis of solar power plant design parameters on snowdrift accumulation and energy yield using numerical simulations. The focus is on fixed tilt systems which is the most common type of solar power plant design (VDMA, 2020).

The snowdrift accumulation conditions are assessed by using the friction velocity as a proxy for the snow accumulation conditions. The friction velocity [m/s] determines the force exerted on a particle at ground level and is strongly indicative of both accumulation and deposition of air-blown snow particles. A threshold friction velocity value is commonly applied to describe the boundary for which below, snow accumulates, or above, snow erodes. It is documented to be in the range of 0.07–0.25 m/s for fresh snow, and 0.25–1.0 m/s for old wind-hardened snow (Gray and Male, 1981). A friction velocity below the threshold limit in combination with a horizontal snow flux will over time result in the development of a snowdrift (Mellor, 1965).

Computational Fluid Dynamic (CFD) simulations enables simulating the flow field around structures and to evaluate the conditions for snowdrift accumulation. This can be performed using either single- or double-phase CFD simulations. Single-phase CFD simulation encompasses only one fluid in the domain, while double-phase simulations additionally include a particle fraction in the domain which can be used to simulate particle deposition over time. Although single-phase simulations cannot reveal the spatial and temporal development of snowdrifts, such simulations can indicate which areas are susceptible to initial accumulation by quantifying the friction velocity. A consequence of excluding the particle fraction in the simulation is the neglection of momentum exchange occurring between the air and the particles (Bintanja and Van Den Broeke, 1995), but this effect is shown to be small in magnitude for low wind speeds (Jie and Huang, 2009). Time-averaged (mean) friction velocity can be estimated using Reynolds Averaged Navier Stokes (RANS) simulations. Large Eddy Simulations can provide time-resolved solutions capturing particle erosion and deposition from burst activity (Brito et al., 2020) but is computational expensive.

2. Method

This study investigates the sensitivity of solar power plant design parameters on the snowdrift accumulation conditions and energy yield. CFD-simulations are used to determine the friction velocity in the plant, used as a proxy indicative of the snowdrift accumulation conditions. Similarly, energy yield simulations are used to determine the specific yield of the plant. The sensitivity analysis is performed in relation to one specific solar power plant design configuration referred to as the base-case. An incremental change of a solar power plant design parameter is applied to the base-case geometry to indicate the effect of a parameter adjustment. The investigated design parameters include panel tilt (α), spacing between the rows (d), gap-to-ground (h), scale and the azimuth/wind direction. One parameter adjustment is performed at the time to yield the isolated effect of the adjustment. The investigated parameters are illustrated in Fig. 1 and the range of parameter adjustments are shown in Table 1.

The azimuth of solar power plants is commonly south-facing on the northern hemisphere and north-facing on the southern hemisphere to maximize yield. If the azimuth of the plant is shifted, so is the incident angle of the wind. An adjustment of the azimuth parameter in this study thus signifies a change in wind direction in the CFD simulations or a change in the orientation of the plant in relation to true south/north in the energy yield simulations. The parameter is investigated in a range between 0 and 180 covering a full rotation of the plant the base-case geometry is symmetrical on the axis perpendicular to the PV arrays.

The range of the tilt parameter is based on modules commonly having a tilt no $<10^{\circ}$ in order to enhance self-cleaning from rain

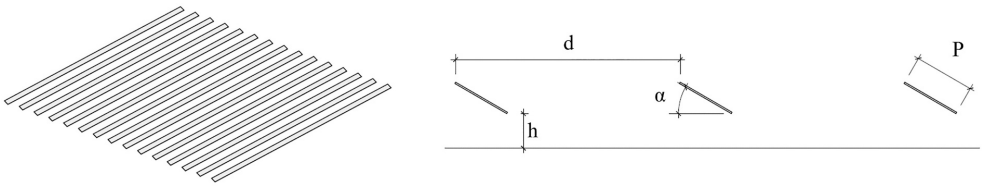

Fig. 1. Illustration of the parameters: panel tilt (α), pitch (d) and gap-to-ground (h). P is the panel length. The base-case constitutes of a total of 15 rows, providing a quadratic footprint of 105 × 105 m.

Table 1
The table shows the variation range for each parameter. The configuration of the base-case is marked by an underline. The default panel length (P) is 2 m.

Parameter	Wind Direction / Azimuth [°]	Tilt [°]	Gap-to-ground [m]	Pitch [m]	Scale
Dimensions in CFD simulation	3D	2D	2D	2D	2D
Parameter adjustments	0	10	0.5	5	0.5
	30	30	1	7.5	1
	60	50	1.5	10	2
	90	70	2	12.5	
	120	90	2.5	15	
	150				
	180				

(Kaldellis and Kapsali, 2011), and a maximum tilt of 90° where tilts above this will face the ground more than the sky. Common gap-to-ground of fixed tilt ground-mounted solar power plants is below 1 m. Here, the minimum distance is set to 0.5 m increased to a maximum distance of 2.5 m representing a very tall system. The pitch of solar power plants is normally optimized as a function of the tilt and the solar geometry to balance ground-cover-ratio and shading on the panels (Sánchez-Carbajal and Rodrigo, 2019). Here, the minimum pitch of 5 m represents a dense system affected by shading losses and the maximum pitch of 15 m represents a system with a very low ground-cover-ratio.

The scale parameter comprises a proportional scaling according to the scale factor in Table 1 of all geometric parameters (panel length, pitch and gap-to-ground). This is included as PV systems are built with a varying number of PV panels per row and it is of interest to investigate if this can influence the accumulation conditions. Here, the minimum scale of 0.5 represents a system where each row has one panel in landscape $P = 1$ m, while the maximum scale of 2 represents a system with four panels in landscape $P = 4$ m (or two in portrait). The pitch and the gap-to-ground is scaled as well to achieve similar shading conditions.

2.1. Snowdrift accumulation evaluation

2.1.1. CFD simulations

This study uses single-phase, RANS simulations to determine the friction velocity in and around the solar power plant. Single-phase simulations do not include suspended snow particles in the computational domain and will not reveal the temporal development of snowdrifts, but the method is sufficient to indicate which areas are susceptible to initial accumulation. This method is considered suitable for a sensitivity analysis as the working theory in this study is that no snow should accumulate between the rows in a solar power plant. This is due to that if snowdrifts fill the gap beneath the rows, the accumulation can propagate, and is therefore considered a high-risk strategy. If no snow should accumulate inside the plant, determining the friction velocity with single-phase simulation indicates which areas are susceptible to accumulation and is a sufficient proxy to compare the snow accumulation conditions in the plant. The relation between the friction velocity and snowdrift accumulation is further investigated in section 2.1.3.

The CFD simulations are performed in ANSYS CFX. All the wind-PV simulations use a consistent numerical method and consistent boundary conditions. The domain is sized according to guidelines from the Architectural Institute of Japan (Tominaga et al., 2008). For all 2D simulations, the distance from the inlet to the first panel is 40 m, the distance from the last panel to the outlet is 100 m and the domain has a height of 30 m. The 3D simulations use the same domain size as a minimum and a distance from the end of the PV row to the lateral sides of the domain of 57 m. A logarithmic wind profile is used at the inlet with a wind speed of 10 m/s at 10 m height and an average static pressure outlet of 0 Pa. A turbulence intensity of 5% is used and a no-slip condition is applied to the ground with no roughness.

A k-ω SST turbulence model is used, with an automatic wall-function switching between numerically resolving the viscous sublayer and modelling it through wall functions depending on the values of y^+ (a non-dimensional measurement of distance from the ground to the first cell). The mesh constitutes of tetrahedral elements with inflation layers on the ground and around the solar panels.

2.1.2. Turbulence model validation

To indicate the validity of the simulation method, results from wind tunnel measurements from Ferreira et al. (2019) are compared with numerical simulations. The shear stress along the top of the box was measured using Irwin probes (Irwin, 1981) and used to calculate a non-dimensional friction coefficient (C_f), yielded by Eq. 1.

$$C_f = \frac{\tau_w}{\frac{1}{2}\rho U_0^2} \tag{1}$$

where τ_w is the shear stress, ρ is the density of the air and U_0 is the undisturbed wind velocity. The investigated geometry is a rectangular box shown in Fig. 2a). A comprehensive validation study is performed by Ferreira et al. (2019) where simulations using various turbulence models and grid refinements to achieve the best fit. The present study extends the validation study by introducing a k-ω SST turbulence model with an automatic wall function. The results are illustrated in Fig. 2b).

Here, the SST turbulence model with the automatic wall function provides a consistent fit with the experimental results, although the friction coefficient remains slightly overestimated over the box top. The modelled friction coefficient from the SST turbulence model by Ferreira et al., 2019 is more centered on the experimental data but have larger local variations with over- and underestimates. The largest discrepancies occur at the beginning and the end of the box surface where recirculation zones occur, for which the Irwin probes cannot accurately determine the shear stress. As the simulation method is sensitive to y^+, the average y^+ is kept between 5 and 8 for all the wind-PV simulations.

To accurately model fluid flow around PV panels capturing the effect of flow separation is crucial. The validation case geometry does not induce flow separation with a suspended object in the domain, but still experience flow separation at the leading edge of the roof and reattachment downwind on the roof (Lim et al., 2009). Capturing the effect of flow separation is thus necessary to model the shear stress on a rectangular box which is achieved sufficiently in the validation case.

2.1.3. Snowdrift - friction velocity validation

In addition to validating the choice of turbulence model, it is of interest to investigate how the distribution of friction velocity matches

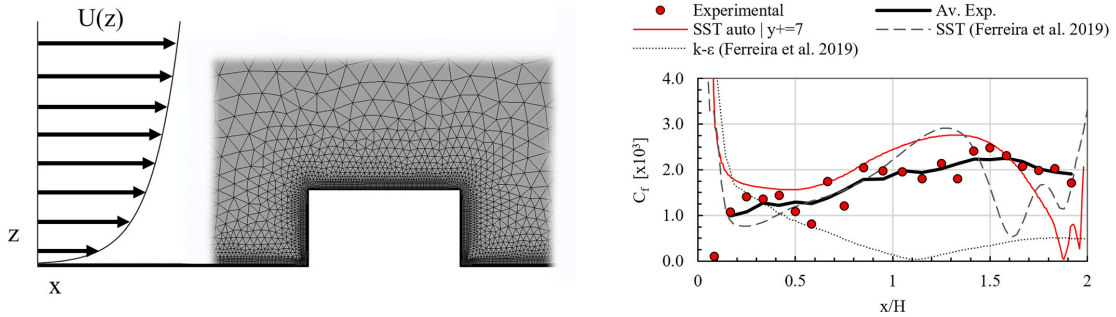

Fig. 2. a) The geometry in the validation study is a rectangular box where the friction coefficient is studied along the top surface. b) Comparison of simulated and experimental results of the friction coefficient. The experimental results and simulations with dashed lines are from Ferreira et al. (2019).

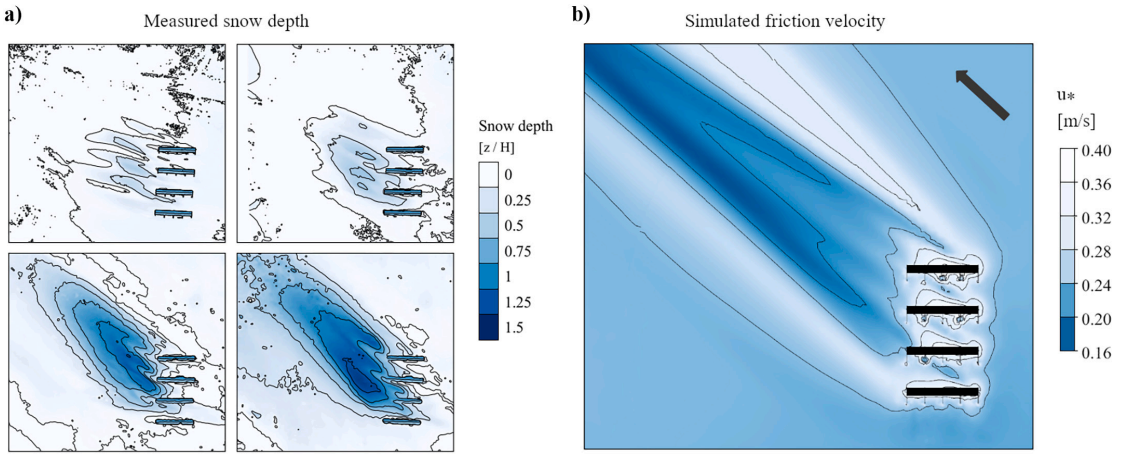

Fig. 3. a) Snowdrift depth from field measurements in four timesteps b) Friction velocity from numerical simulations. The arrow signifies the simulated the wind direction.

with snowdrifts from field measurements. To investigate this, simulated friction velocity is compared with snowdrifts from a small-scale solar power plant exposed in a Polar climate (Frimannslund et al., 2021). The geometry of the PV plant is a downscaled version of the base-case geometry presented in Table 1 (the panel surface (P) is set to 1.22 m). The prevailing wind direction in the measurements is at a 45–60° angle to the rows (where 0° is facing the front of the panels) and is set to 45° in the simulations. Fig. 3 shows the spatial distribution of friction velocity results compared with the snow depth.

The results show that there is a good agreement between the areas with low friction velocity and areas with accumulated snow. The area with low friction velocity is quite elongated leeward and matches the more fully developed snowdrifts better than the early-stage development. This phenomenon is likely to arise from that the saltation of snow particles ceases at the first encountered zone with a friction velocity lower than the threshold, resulting in an initial accumulation in the zones closer to the PV rows. As the deposition progresses, the accumulation continues downwind to produce longer snowdrifts. This development is evident in the field measurement results from Frimannslund et al. (2021) and is in agreement with experimental results from Tabler (2003) of the stepwise development of a snowdrift produced from a porous snow fence. The phenomenon indicates that when analyzing the friction velocity, the upwind minimum value with friction velocity below threshold indicates where snow will begin to accumulate rather than the lowest values of friction velocity. It is difficult to determine where this initial deposition zone will be as threshold friction velocity of snow is a dynamic property dependent physical snow characteristics i.e. particle size and moisture content (Schmidt, 1980) and as the friction velocity varies with wind speed. In Fig. 3, a friction velocity of 0.24 m/s provides an approximate fit with the snowdrifts in the field measurements.

2.2. Energy yield simulations

Energy yield simulations are used to determine the sensitivity of PV plant design parameters with the specific yield as a proxy indicative of the performance. The specific yield is defined as the annual production of a system normalized to the installed capacity of the system and has the unit of kWh/kWp/year. It is a measure of how well the system performs in the respective climate and is frequently used for comparing design system alternatives in power plant engineering. Modern yield prediction tools are accurate in estimating the PV performance, with the largest uncertainty in the simulations being the irradiance data (Urraca et al., 2018).

In this study, the energy yield and snowdrift accumulation are evaluated separately. This is performed as the goal of the adaption is to avoid snowdrifts in the solar power plant, so that the snowdrifts themselves will not influence the resiliency or yield of the plant. The influence of precipitated snow on solar panels is neither considered in the energy yield simulations as existing studies on snow the influence of precipitated snow on solar power production may be less suitable for windy Polar climates where snow cover on solar panels is significantly affected by wind erosion. More research on the influence of snow on power production in Polar climates can indicate the validity of this simplification.

The energy yield simulations are performed in PVsyst 7.1 (PVsyst SA, 2020). Both mono- and bifacial modules are investigated. All modules are Si-monocrystalline solar modules from PVsyst's generic module selection. Bifacial modules commonly have a bifaciality factor (the power output of the back compared to the front) of 60–95% (Tian Shen et al., 2019) and are here chosen to have a bifaciality factor of 80%. A 500 kW string inverter with a maximum conversion efficiency of 98.5% from PVsyst's generic selection is used. The array is sized to achieve a ratio between array to inverter power of approximately 1.2. The electrical losses remain close to constant for all simulations, and the soiling losses are simplified to be fixed at 3% regardless of the configuration. An unlimited shed assumption is used in the simulations, imposing an equal shading condition for every row, neglecting the increased irradiance at the ends of the system. An advanced view factor model takes into account the effect of self-shading from the system on the ground critical for bifacial modules (Wittmer and Mermoud, 2018). No shade from terrain is applied in the simulations.

The simulations are performed for one Arctic and one Antarctic climate to represent both hemispheres. The chosen climates are Longyearbyen, Svalbard (78°13′N) and Syowa station, Queen Maud Land (69°00′S). Irradiance and climate data is from Meteonorm 7.2 with data series from 1981 to 1989 (Meteonorm., 2020), while monthly values for albedo is calculated from 4 years of irradiance measurements at local weather stations (JARE, 2021; UNIS, 2020). Table 2 shows the climatic data used in the energy yield simulations.

A comparison of simulated and measured results is made to investigate the validity of the simulation method. The base-case configuration with the system specifications described above is simulated and compared with measured results of a system with the same orientation

Table 2
Climate data used in the energy yield simulations.

Location	Longyearbyen, Svalbard (78° N)	Syowa station, Queen Maud Land (69° S)
Yearly Global Horizontal Irradiance [kWh/m^2]	637	1114
Average albedo with sun above horizon [%]	31	82
Highest monthly mean temperature [°C]	7.3	−0.6
Average wind velocity [m/s]	4.9	6.8

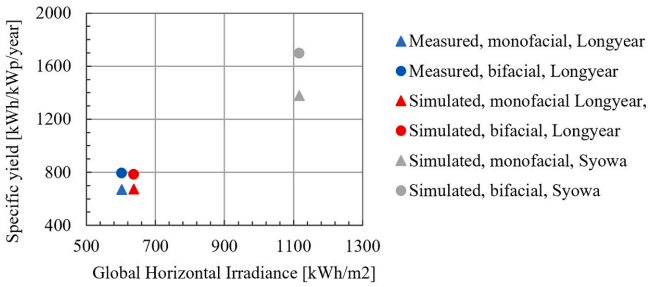

Fig. 4. Comparison of measured and simulated module yield in relation to GHI of a south-facing PV array with a 30° tilt.

and tilt in Longyearbyen (Frimannslund et al., 2021). In the Syowa climate, data of measured yield is not available for comparison. Fig. 4 shows the simulated and measured specific yield plotted against the Global Horizontal Irradiance (GHI).

It is apparent that the simulated and measured yield in Longyearbyen exhibit small discrepancies of <1.3% for both bifacial and monofacial modules. However, the GHI in the measurements are lower than in the simulations, signifying an underestimation of the simulated yield. The measurements have a lower annual GHI due to being performed in a year with below average GHI, while the simulations use average annual irradiance from the Meteonorm database. The underestimation of the simulated yield can arise from several factors which can be divided into differences in simulation conditions and inaccuracies in the estimation of yield itself. Regarding the simulation conditions, the simulated and measured setup does not use the same module and inverter. The difference in inverter choice is likely to contribute to the underestimation as the simulations use a string inverter opposed to the micro-inverter used in the measurements. The shading conditions are actually more favourable in the simulations (having no shading from terrain) and does not contribute to the underestimation of simulated yield. Apart from differences in simulation conditions, the uncertainties may also partly arise from inaccuracies in the estimation of yield itself. Performance of PV systems at high latitudes is little researched and the models commonly used to estimate yield may be less accurate in such climates. The focus in this study is nevertheless on the sensitivity of a PV system to the design parameters which will be dominated by the Plane-of-Array (POA) irradiance received by the panels. The determination of POA-irradiance is estimated through transposition models which modern simulation software capture with high accuracy (Yang, 2016).

Fig. 3 also shows that the simulated yield in the Syowa climate is significantly higher than in Longyearbyen. This is mainly due to a higher annual average irradiance, but the effect of lower temperatures also contributes to increased power output of the PV system. The high albedo in Queen Maud Land enhances the performance of bifacial modules which provides a bifacial gain of 23% compared to 16% in Longyearbyen. The two climates exhibit different characteristics which can influence the sensitivity to a parameter adjustment.

3. Results

With the methodology described in section 2, the effect of parameter adjustments is investigated on snow accumulation conditions (3.1) and the energy yield (3.2). After the snowdrift conditions and energy yield are investigated individually, section 3.3 compares the sensitivity to both snowdrift accumulation and energy yield for each parameter to compare the effect of a design adjustment.

3.1. CFD simulations

3.1.1. Wind direction

The effect of wind direction is investigated with 3D simulations of the base-case geometry as defined in Table 1. The wind direction is varied between 0 and 180° where 0° is facing the front of the panels. The investigated area is defined by a circle exceeding the corners of the system by 5 m. Fig. 5a) illustrates the friction velocity normalized to the undisturbed upwind friction velocity in the investigated area while Fig. 5b) quantifies the friction velocity in relation to the cumulative area within the circle.

Fig. 5a) shows that the PV system differentiates the friction velocity compared to the undisturbed flow, creating zones with friction velocity higher than the undisturbed upwind friction velocity (u^*/u^* upwind >1) prone to erosion and zones with friction velocity below the undisturbed friction velocity (u^*/u^* upwind <1) prone to accumulation. A wind direction perpendicular to the rows produce the largest are with low values of friction velocity, illustrated in Fig. 5b) where the approximately 50% of the area being below an u^*/u^* upwind = 0.9 for a wind direction directly facing the front or back of the panels. An incremental change of the wind direction closer to parallel provide an increasingly smaller area with low friction velocity. The most favourable wind direction is parallel, where only 2% of the area is below u^*/u^* upwind = 0.9.

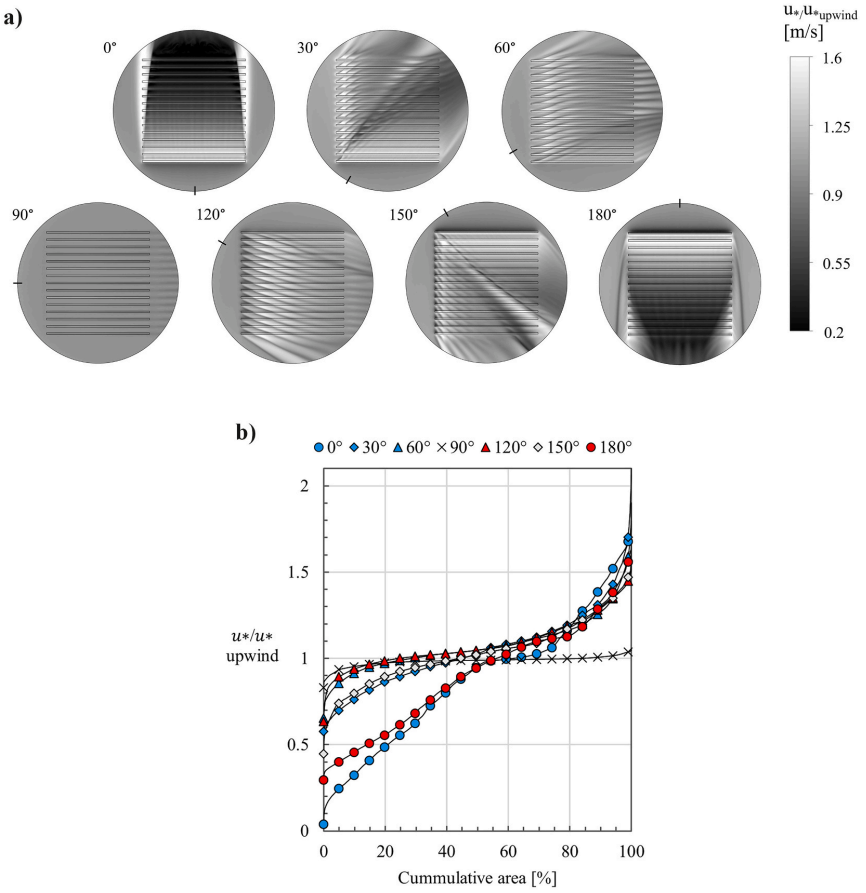

Fig. 5. a) The distribution of friction velocity normalized to the undisturbed upwind friction velocity b) Friction velocity normalized to the undisturbed friction velocity quantified in relation to the cumulative area within the circle.

It is evident from Fig. 5a) that the wind direction in relation to the panel inclination influence where in the plant the accumulation zones occur. For a wind direction facing the back of the rows, low friction velocity occurs windward to the system. This likely arises from the blockage of the fluid flow before being pushed under the panel, creating a windward recirculation zone. This can be critical as windward accumulation can reduce the effective gap-to-ground and change the flow field downwind which may have an adverse effect on the friction velocity throughout the remainder of the PV system. A wind direction facing the front of the panels provide slightly lower friction velocity although a similar trend exists when the incident angle of the wind remains the same (0 and 180, 30 and 150, 60 and 120), Overall, adjusting the azimuth of the plant to achieve a wind direction close to parallel to the rows can significantly reduce the area with low values of friction velocity and reduce the risk of snowdrift accumulation.

3.1.2. Gap-to-ground, tilt, pitch and scale

The effect of gap-to-ground, tilt, pitch and system scale is investigated with 2D-simulations of the base-case with a front-facing wind direction representing the worst-case scenario. The results are illustrated in Fig. 6.

The tendency for all the simulations in Fig. 6 is a small decrease in friction velocity prior to the first PV row, followed by a significant leap as the fluid flow passes the first row, and a subsequent row-wise decrease throughout the system. Leeward of the rows, a dent in the friction velocity occurs for most cases, with varying distinctiveness and location. The simulated configurations are susceptible to both windward, leeward and system accumulation depending on the configuration.

Increasing the gap-to-ground (Fig. 6a) has a stabilizing effect on the friction velocity as it partly cancels out the low and high points and is considered favourable to reduce the accumulation. This effect is evident windward, leeward and throughout the plant. Increasing the gap-to-ground also seems to displace the leeward low-point of friction velocity further downwind and decreases the distinctiveness of the low point.

The tilt of the rows (shown in Fig. 6b) has little effect on the row-wise development of the friction velocity but has a strong influence on the leeward and windward accumulation. Increasing the panel tilt creates a more distinctive low point both windward and leeward to the system. A panel tilt of 30° and above exhibit large variations in friction velocity passing the first row. This is likely to occur due to more wind being pushed beneath the panel at higher tilts. Thus, it seems that increasing the tilt differentiates the wind speed in the system, creating distinct accumulation and erosion zones. The tilt of 10° stands out from the rest of the simulations with small variations throughout the system with little leeward and windward reduction in friction velocity. The results indicate that a low tilt is favourable to maintain a stable friction velocity and reduce the likelihood of accumulation windward and leeward to the system.

A reduced row pitch (Fig. 6c) increases the friction velocity throughout the system and can be favourable to reduce the risk of snowdrift accumulation. Increasing the pitch seems to increase the row-wise amplitude of the friction velocity and reducing the leeward friction velocity low point. The effect of pitch is connected to studies of pitch on panel wind forces and further discussed in section 4.

Increasing the scale of the system (Fig. 6d) increases the friction velocity and can be favourable to reduce the accumulation in solar power plants. The friction velocity exhibits a similar pattern of development independent of the scale, with slightly higher values for the larger scales, although discrepancies arise in the leeward zone. The reasons for the influence of scale and discrepancies between the simulations are discussed in section 4.

3.1.3. Quantified friction velocity sensitivity

The sensitivity of friction velocity to all the investigated parameters is quantified and compared to indicate the efficiency of a parameter

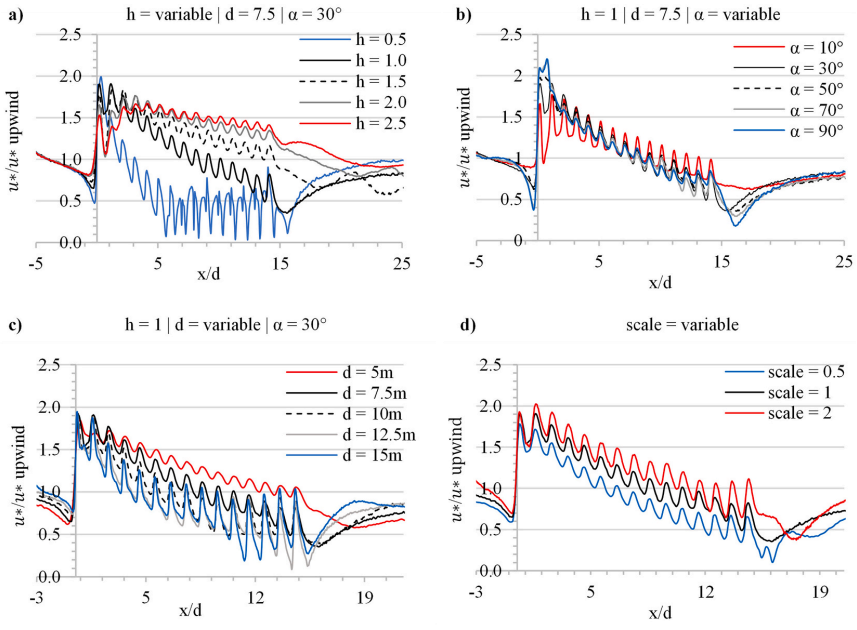

Fig. 6. Normalized friction velocity of the base-case geometry with varying: a) gap-to-ground b) tilt c) pitch and d) scale. Each peak in friction velocity is from one row (fifteen total). The x-axis is normalized to the pitch (d).

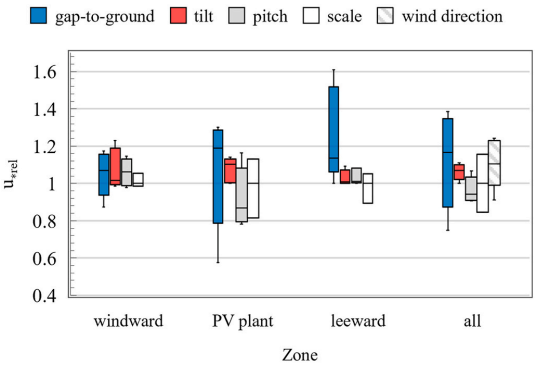

Fig. 7. Quantified sensitivity of friction velocity to each parameter. The line cap marks the endpoints of the sensitivity, while the bar represents the 2nd and 3rd quartiles.

adjustment. A dimensionless factor u_{*rel} is used to compare parameters and is defined in Eq. 2:

$$u_{*rel} = \frac{\overline{u}_{*(parameter)}}{\overline{u}_{*(base-case)}} \tag{2}$$

Where $\overline{u}_{*(parameter)}$ is the average friction velocity of the investigated parameter and $\overline{u}_{*(base-case)}$ is the average friction velocity of the base-case. The parameters are compared with the performance base-case with the dimensions the parameter is investigated in (2D parameters are compared with the 2D performance of the base-case and 3D parameters are compared with the 3D performance of the base-case). For the parameters simulated in 2D u_{*rel} is calculated in four different zones: windward to the PV plant, through the PV plant, leeward to the PV plant, and all areas as one. The windward zone is defined by an upwind distance of 10 m from the first PV row, while the leeward zone is defined by a downwind distance of 80 m from the last PV row. The PV plant zone is the distance from the first to the last PV array and varies in size due to that the pitch is variable for some simulations. For the wind direction/azimuth parameter, u_{*rel} is calculated for the circular zone defined in section 3.1.1. Fig. 7 shows u_{*rel} for all five investigated parameters.

When analyzing Fig. 7, it should be noted that u_{*rel} is a measure of the average friction velocity and that zones with both high and low values can cancel each other out, providing little effect on u_{*rel} although it in reality might be strongly susceptible to local accumulation. Fig. 5 should thus be analyzed in relation to Fig. 4 to reveal potential accumulation zones not captured solely by u_{*rel}. Nonetheless, u_{*rel} indicates the sensitivity of a parameter by the span of u_{*rel}, i.e. the distance from the highest to lowest registered value. The parameters exhibit a strongly variable sensitivity and also a large variation from zone to zone. If the parameters are ranked by the sensitivity (i.e. (the span of value u_{*rel}) in the zone category "all", the most sensitive parameters are 1. gap-to-ground ($u_{*rel\ span} = 0.64$), 2. wind direction ($u_{*rel\ span} = 0.33$), 3. scale ($u_{*rel\ span} = 0.31$), 4. pitch ($u_{*rel\ span} = 0.15$) and 5. tilt ($u_{*rel\ span} = 0.11$). If the parameters are ranked by the highest value of u_{*rel}, indicating how much the average friction velocity of the base-case can be increased by the parameter adjustment, the same ranking is achieved except for tilt being ranked higher than pitch.

The parameters exhibit a variable sensitivity to the different zones. All parameters show a significant impact in the windward and PV plant zone, while the leeward zone is less sensitive except for gap-to-ground adjustments. It should be noted that the windward zone can be critical as any snowdrifts developing here may influence the flow field in the downwind areas. Any significant low points here, which occurs for high inclination or low gap-to-ground configurations as shown Fig. 6a) and b) (u^*/u^* upwind $\approx$ 0.5) can potentially propagate the downwind accumulation and be critical for the snowdrift resilience of the plant.

3.2. Energy yield simulations

3.2.1. Individual parameter simulations

The influence of azimuth, tilt, gap-to-ground and pitch on energy yield is simulated in the Longyearbyen and Syowa climate. The scale parameter is also simulated but shows a negligible effect on the energy yield and is excluded from the results. As with the study of friction velocity, the base-case geometry is subjected to an incremental change to indicate the parameter effect on the energy yield. The results are normalized to the base-case specific yield, resulting in a dimensionless factor called SY_{rel} (relative specific yield), defined in Eq. 3:

$$SY_{rel} = \frac{SY_{(parameter)}}{SY_{(base-case)}} \tag{3}$$

Where $SY_{(parameter)}$ is the specific yield of the investigated parameter and $SY_{(base-case)}$ is the specific yield of the base case given in Fig. 4. The results of the energy yield simulations are illustrated in Fig. 8.

When analyzing the results in Fig. 8, it should be kept in mind that all the parameter adjustments are performed individually, which is uncommon in solar power plant design where parameters are adjusted interdependently to reduce the adverse effect of interrow shading. Coupling parameter adjustments can thus improve losses exhibited in the simulations arising from interrow shading. However, the isolated parameter adjustment is performed to provide a consistent method of evaluating the sensitivity. The following paragraphs elaborate on results from each parameter and the consequence of isolating the parameter adjustment.

The response of the specific yield to a parameter adjustment is dictated by the type of loss mechanism. Azimuth adjustments change the normal vector of the panel surface, determinative for the irradiance received by the panel during the course of a year. This has a strong influence on the yield, and any deviation from true south on the northern hemisphere or true north on the southern hemisphere will have a detrimental effect on the yield. This effect can somewhat be compensated by optimizing the tilt for the azimuth, which is not performed here.

Tilt adjustments exhibit a large influence on the yield. As with the azimuth, changing the normal vector of the plane strongly influences the yield. The effect of tilt as shown in Fig. 8b) is influenced by the pitch not being adjusted for increasing tilts and the resulting effect of interrow shading. An adaption of pitch with tilt would produce a more pronounced effect of increasing the tilt. For both tilt and azimuth adjustments, angle-of-incidence loss is a phenomenon affecting the results in addition to the actual irradiance received by a solar panel.

An adjustment of the gap-to-ground influence the ground shading conditions and the yield of bifacial modules. The result in Fig. 8c) shows that increasing the gap-to-ground increase the yield of bifacial modules, in conjunction which previous studies on bifacial performance (Yusufoglu et al., 2015). The effect is larger in the Syowa climate where the albedo is higher. Monofacial modules are unaffected by gap-to-ground adjustments.

The pitch influences the shading conditions internally in the solar power plant. A reduced pitch increases the interrow shading experienced at low solar altitudes. The effect is small in magnitude, but larger for bifacial panels where pitch adjustments also effect the power produced from the backside of the modules.

Variations in the parameter response occur between the Longyearbyen and Syowa climate, arising from differences in the solar geometry (9°13′ latitude difference) and from climatic conditions such as ground albedo. Nonetheless, the effect of the parameter adjustments on the specific yield exhibits a similar trend in both climates.

3.2.2. Quantified specific yield sensitivity

The sensitivity of the specific yield to each parameter is quantified and presented in Fig. 9.

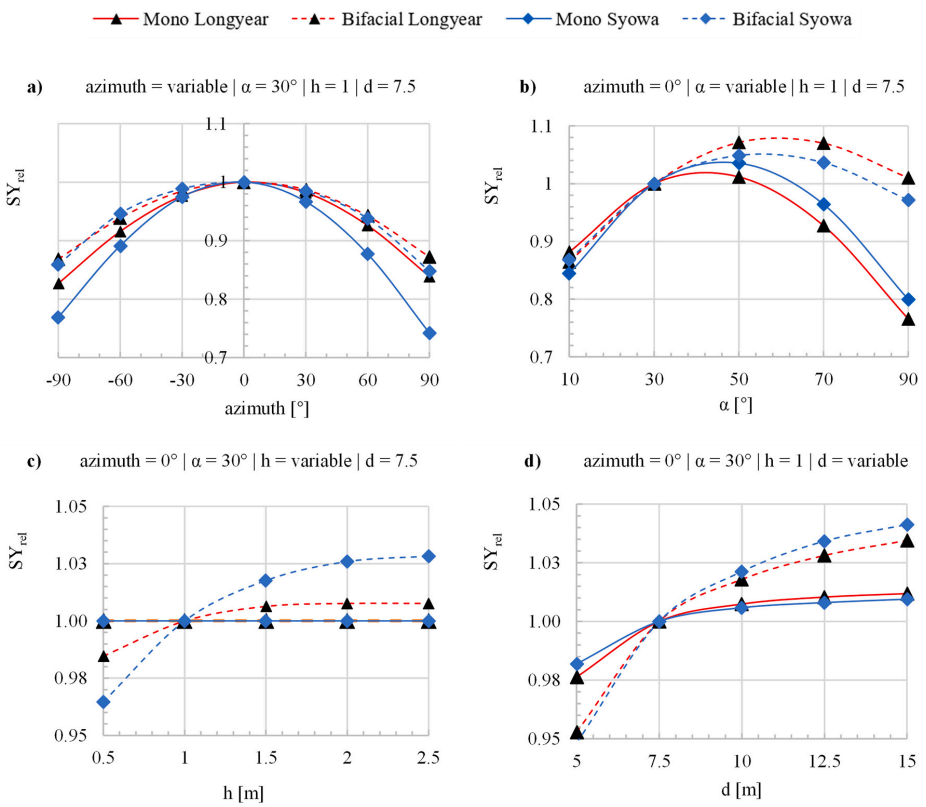

Fig. 8. Normalized specific yield (SY) with varying a) azimuth, b) tilt, c) gap-to-ground and d) pitch.

Again, the span of SY_{rel} indicates the sensitivity of the parameter. Monofacial modules are more sensitive to azimuth and tilt adjustments than bifacial, but bifacial modules are more sensitive to parameters effecting ground shading conditions such as the gap-to-ground and pitch. Ranked by the span of SY_{rel}, the most sensitive parameters are 1. azimuth,2. tilt, 3.pitch 0.4.gap-to-ground and 5.scale. The parameter adjustments mostly provide an $SY_{rel} < 1$, indicating that most adjustments have a negative effect on the specific yield, which is expected as the system is designed with established solar power plant principles optimizing solar power production. Some adjustments show little significance on the yield, namely gap-to-ground and scale adjustment.

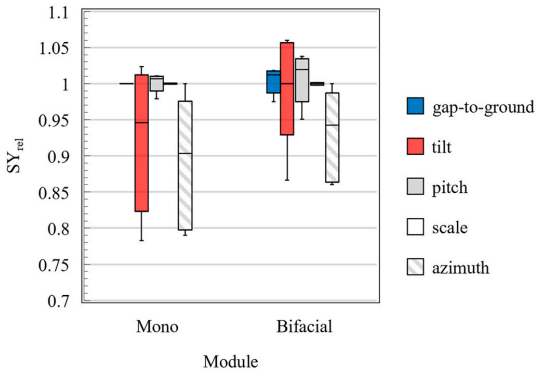

Fig. 9. Specific yield sensitivity to each parameter. The sensitivity is calculated as the average of the response of the Longyearbyen and Syowa parameters. The line cap marks the endpoints of the sensitivity, while the bar represents the 2nd and 3rd quartiles.

3.3. Friction velocity and specific yield sensitivity comparison

The sensitivity of the friction velocity and specific yield to the parameter adjustments are quantified and compared to indicate the consequence of a design adaption. Fig. 10 compiles the results from the prior presented sensitivity of friction velocity (Fig. 7) and energy yield (Fig. 9) to a plot categorized by parameters.

A value above 1 for u_{*rel} or SY_{rel} signifies an improvement in accumulation conditions or plant yield. If the response of a parameter adjustment is positive for both parameters (indicated by the arrow pointing up), then an adjustment of the base-case design is favourable. Fig. 8 shows that increasing the gap-to-ground and scale can significantly reduce the risk of snowdrift accumulation with an insignificant or positive response to the energy yield. Other design adjustments provide a conflicting response between the snowdrift accumulation conditions and the energy yield. This means that if the parameter is adjusted to reduce the risk of snowdrift accumulation, it is for a trade-off in energy yield. For pitch and tilt adjustments, this occurs for the base-case as a reduction in tilt and pitch has a positive influence on the friction velocity and a negative influence on the energy yield. Azimuth adjustments are

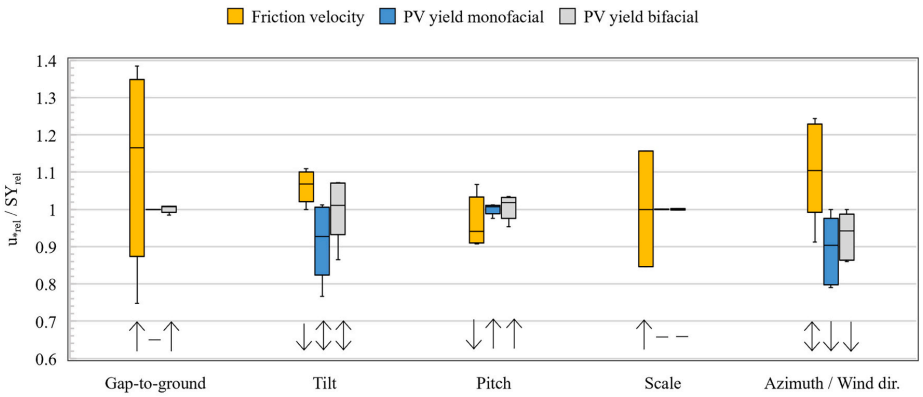

Fig. 10. Comparison of parameter influence on friction velocity and specific yield. The arrows signify whether an increase in the parameter of the base-case produce a positive or negative response to u_{*rel} or SY_{rel}. Two-headed arrows produce an ambiguous response while a dash signifies an insignificant response.

ambiguous for the accumulation conditions as this depends on the prevailing wind direction of the site. If the azimuth of the PV system is south-facing and the prevailing wind-direction is also from the south, shifting the azimuth produces a conflicting response (improving snowdrift conditions and decreasing yield), while if the prevailing wind direction is from the east or west, no adjustments should be made. The effect of azimuth adjustments thus depends on the local wind environment and is shown to have a strong influence on both the friction velocity and the specific yield.

4. Discussion

The results of the parameter influence on snowdrift accumulation can be connected to snow fence theory. As previously mentioned, snowdrifts produced from rows of solar panels exhibit a similarity with snowdrifts produced by snow fences (Frimannslund et al., 2021). This indicates that snow fence theory can be applicable to single PV rows. However, snow fence design theory concerns the snow fence influence on the snowdrift accumulation, while here the friction velocity is investigated. If the notion that the friction velocity is correlated to the snow retainment of a snow fence is assumed, as is supported by the comparison in Fig. 3, the simulated results agree well with the findings from snow fence theory. The parameters of gap-to-ground (referred to as bottom gap in snow fence theory), tilt (inclination), and azimuth in relation to the prevailing wind direction (attack angle) is in conjunction with the findings from Tabler (2003).

Increasing the scale of the system is shown to generally increase the friction velocity as presented in Fig. 6d). A well-known feature of dimensional analysis, such as CFD-simulations, is that scale-independent results can be produced if the geometric, dynamic and kinematic similarity criteria are met (Langhaar, 1951). Here, only a geometrical scaling is performed, while the kinematic and dynamic similarity criteria remain unchanged. This means that properties such as surface roughness and wind velocity remain unscaled for all the simulations, which is representative for a real case where only the geometry of the solar power plant is scaled. A study from Tabler (1980) shows that scaled models can produce snowdrifts similar to full-size models if the wind velocity and the surface roughness in the scaled measurements are low. Such conditions occur in short time intervals, but for extended measurements variations in wind velocity and surface roughness have an increased likelihood of producing snowdrifts which differ in shape and size from models of different scale. It is believed that the scaling of geometry without scaling the kinematic and dynamic properties is the reason for the variation in friction velocity between the scaled simulations and that an advantage can be gained from increasing the scale of solar power plants with regards to avoiding snowdrift accumulation.

The results of the influence of pitch on the friction velocity is not easily connected to snow fence theory due to large differences in distance between rows of solar panels and snow fences. However, a numerical study on the wind loading of solar panels from Shademan et al. (2014) provide a reference for comparison. Here it is shown that reducing the pitch diminishes the wind loading on the panels due to a sheltering effect from the upwind panel (Shademan et al., 2014). A small pitch reduces vertical exchange of fluid between the rows, causing low wind speed and wind loading on the panels behind the first row. In this study, the friction velocity remains stable for a small pitch. This phenomenon is believed to arise from little fluid interaction between the rows, resulting in stable wind speeds under and above the panels.

An important topic of discussion is if the uncovered parameter sensitivity is independent of the simulation conditions, i.e. the configuration of the base-case and simulation input such as wind velocity and wind direction for the CFD-simulations or climate and system specifications for the energy yield simulations. It is obvious that changing the simulation conditions will influence the outcome of the simulation itself, but the effect it has on sensitivity is more uncertain. Here, the sensitivity of a parameter is calculated as the response of the adjusted parameter normalized to the response of the base-case, as given by Eq. 2 and 3. Thus, how the simulation conditions influence the sensitivity of a parameter implies a larger or smaller response of an adjustment in relation to the base-case, which remains difficult to predict without further investigation. The conditions which may influence the sensitivity of the snow accumulation conditions can be the configuration of the base-case, the wind velocity and the wind direction, while the conditions which can influence the energy yield are the configuration of the base-case, the climatic conditions and the specifications of the system. Thus, the magnitude of sensitivity presented in in this study has an inherent uncertainty related to it as it is only based on one solar power plant configuration represented by the base-case and as the conditions both for the CFD and energy yield simulations remain fixed. The results are reassured by the conjunction in the response of the parameters (i.e. increasing or decreasing effect on the friction velocity or energy yield) with previous studies as elaborated on in the previous paragraphs. Further research on the topic will contribute to the certainty of the parameter sensitivity.

The following paragraphs concerns the implication of the results and future work. The findings on the parameter influence on friction velocity show that all the investigate parameters can be adjusted to increase the friction velocity and reduce the risk of snow accumulation in solar

power plants. Two parameter adjustments reduce the risk of snowdrift accumulation and have an insignificant or positive influence on the energy yield, namely increasing the gap-to-ground and the system scale as shown in Fig. 10. Thus, the results suggest that adjusting these two parameter adjustments are favourable to adapt solar power plants to snowdrift climates. However, this implication is limited by the framework of the study which only consider the two performance criteria of snowdrift accumulation and energy yield. An adverse consequence of increasing the gap-to-ground and the system scale is that the total height of each row will increase significantly, which is likely to increase the wind loading on the PV rows as well as prohibit the accessibility for plant maintenance. Increasing the gap-to-ground and system scale thus have implications for the design of the plant, without the scope of this study, which must be accounted for. The three out of five remaining parameters (tilt, pitch and azimuth) can be adjusted to reduce the risk of snowdrift accumulation but will result in a trade-off in energy yield. However, as increasing the gap-to-ground and scale has it disadvantages, performing adjustments which also influence the yield might be favourable in certain climatic conditions. For example, azimuth adjustments are shown to have a strong influence on the accumulation conditions if the rows are parallel to the wind direction. For climates with one dominant prevailing wind direction, typical for valleys, adjusting the azimuth can significantly reduce the risk of snowdrift accumulation. In some cases, this may be a preferred design adjustment compared to increasing the gap-to-ground, depending on the local conditions. Due to the dependency on local climatic conditions and as the required design adaptions to achieve a snowdrift resilient design likely depend on the size of the solar power plant, it is believed that the design adjustments should be determined for each specific design scenario. The optimal adaption of the plant is likely to differ from case to case as the wind and snow environment differs, and the choice of system will differ, both in size and in the choice of technology, i.e. the use of mono- or bifacial solar modules.

The necessary design adjustments which are required to achieve a snowdrift resilient design are comprehensive when only considering adjusting one parameter adjustment at the time as performed in this study but combining multiple parameter adjustments may lessen the magnitude of adjustments and may provide a design more similar to modern solar power plants. Future work on the adaption of solar power plants to Polar climates should include simultaneous adjustments of multiple parameters in realistic climatic conditions to investigate the required design adjustments to achieve a snowdrift resilient plant. The findings from this study provide a background for the effectiveness of adjusting the parameters to increasing the friction velocity in the windward, PV plant and leeward zones of the plant, and what can be the expected reduction in yield from the respective parameter adjustment.

An alternative solution to achieve snowdrift resilient solar power plants is through the implementation of solar tracking systems enabling a variable tilt. As shown in Fig. 6b), no significant low points in friction velocity occur for the lowest investigated tilt of 10°. If the solar power plant can have a variable tilt, the panels can be put in a horizontal position during snow transport events. At high latitudes, the wintertime irradiance is low in magnitude and the losses associated with having horizontal panels can be of little significance. Additionally, tracking systems increase the specific yield compared to fixed tilt systems, depending on the type of tracking and irradiance conditions (Wittmer and Mermoud, 2018). However, solar tracking systems use actuators and have several moving parts whose mechanical reliability may be compromised by the environmental stresses of the Polar climate. PV plants with solar tracking may thus offer increased snowdrift resiliency while maintaining a high yield but presupposes mechanical resiliency to the climatic effects during the lifetime of the system.

5. Conclusions

The results from the numerical simulations show that sensitivity of friction velocity and specific yield to the solar power plant design parameters is highly variable in magnitude and for the friction velocity it is also shown to vary in different zones (windward, PV plant and leeward). Defining the sensitivity as the difference between the highest and lowest response of the simulated parameter adjustments normalized the response of the base-case provide a parameter sensitivity between 0.11 and 0.64 for the friction velocity, and between 0 and 0.24 for the specific yield. The response of each parameter can be summarized as the following:

- Increasing the gap-to-ground significantly increase the friction velocity and the effect on energy yield is insignificant for monofacial modules and positive for bifacial modules.
- Reducing the panel tilt increases the friction velocity in the windward and leeward zone and has an adverse effect on the specific yield.
- Reducing the pitch increases the friction velocity, but reduces yield as shading between rows increases.
- Increasing the scale of the system (a proportional scaling of all geometric properties) increases the friction velocity and has in insignificant influence on the specific yield
- Adjusting the azimuth to achieve a prevailing wind direction closer to parallel to the rows significantly increase the friction velocity but will reduce the yield if the azimuth deviates from true south on the northern hemisphere or north on the southern hemisphere.

When comparing the response of the parameters, it is revealed that only two parameter adjustments which have a positive influence on the accumulation conditions have a positive or insignificant influence on the energy yield, namely the gap-to-ground and the scale. However, an increase of these parameters will increase the total height of each row which increase the wind loading and the accessibility for plant maintenance. An adjustment of tilt, pitch and azimuth can be performed but will result in a trade-off in energy yield with variable magnitude depending on the adjustment. The findings from this study are in conjunction with previous studies but the quantified sensitivity of the parameters depends on the simulation conditions and should be further researched to strengthen the validity of the findings. As the accumulation conditions will depend on the local climatic conditions and PV system characteristics such as system size, it is beneficial to perform the design adjustments to the specific design scenario. Performing adjustments of multiple parameters is likely to lessen the extremity of the required design adjustments to achieve a snowdrift resilient design. This study quantifies the effectiveness of adjusting the different parameters to increase the friction velocity and reduce the risk of snowdrift accumulation in the plant, as well as the consequences this has for the yield of the plant.

CRediT authorship contribution statement

Iver Frimannslund: Conceptualization, Methodology, Writing – original draft, Writing – review & editing. **Thomas Thiis:** Conceptualization, Supervision, Resources. **Almerindo D. Ferreira:** Validation. **Bjørn Thorud:** Supervision.

Declaration of Competing Interest

The authors declare that they have no known competing financial interests or personal relationships that could have appeared to influence the work reported in this paper.

References

Andenæs, E., Jelle, B., Ramlo, K., Kolås, T., Selj, J., Foss, S., 2018. The influence of snow and ice coverage on the energy generation from photovoltaic solar cells. Sol. Energy 159, 318–328. https://doi.org/10.1016/j.solener.2017.10.078.

Bintanja, R., Van Den Broeke, M.R., 1995. Momentum and scalar transfer coefficients over aerodynamically smooth antarctic surfaces. Bound.-Layer Meteorol. 74 (1), 89–111. https://doi.org/10.1007/BF00715712.
Brito, P., Ferreira, A., Thiis, T., Sousa, A., 2020. Prediction of erosion intermittency using Large Eddy simulation. Geomorphology 364, 107179. https://doi.org/10.1016/j.geomorph.2020.107179.
Brooks, A., Gamble, S., Dale, J., Gibbons, M., 2014. Determining snow loads on buildings with solar arrays. In: International Structural Specialty Conference, Halifax, NS.
Dou, Y., Zuo, G., Chang, X., Chen, Y., 2019. A study of a standalone renewable energy system of the Chinese Zhongshan Station in Antarctica. Appl. Sci. 9, 1968. https://doi.org/10.3390/app9101968.
Ferreira, A., Thiis, T., Freire, A., N. & M. C. Ferreira, A., 2019. A wind tunnel and numerical study on the surface friction distribution on a flat roof with solar panels. Environ. Fluid Mech. 19 https://doi.org/10.1007/s10652-018-9641-5.
Frimannslund, I., Thiis, T., Aalberg, A., Thorud, B., 2021. Polar solar power plants – investigating the potential and the design challenges. Sol. Energy 224, 35–42. https://doi.org/10.1016/j.solener.2021.05.069.
Gray, D.M., Male, D.H., 1981. Handbook of Snow : Principles, Processes, Management & Use. Pergamon Press, Toronto; New York.
Irwin, H.P.A.H., 1981. A simple omnidirectional sensor for wind-tunnel studies of pedestrian-level winds. J. Wind Eng. Ind. Aerodyn. 7 (3), 219–239. https://doi.org/10.1016/0167-6105(81)90051-9.
JARE, 2021. Antarctic Meteorological Data. Available at: https://www.data.jma.go.jp/antarctic/datareport/03_sfc_rad/sfc_rad_e.html (accessed: 01.03.21).
Jie, Z., Huang, N., 2009. Simulation of snow drift and the effects of snow particles on wind. Model. Simul. Eng. https://doi.org/10.1155/2008/408075.
Kaldellis, J.K., Kapsali, M., 2011. Simulating the dust effect on the energy performance of photovoltaic generators based on experimental measurements. Energy 36 (8), 5154–5161. https://doi.org/10.1016/j.energy.2011.06.018.
Langhaar, H.L., 1951. Dimensional Analysis and Theory of Models. Wiley, New York.
Lim, H.C., Thomas, T.G., Castro, I.P., 2009. Flow around a cube in a turbulent boundary layer: LES and experiment. J. Wind Eng. Ind. Aerodyn. 97 (2), 96–109. https://doi.org/10.1016/j.jweia.2009.01.001.
Mellor, M., 1965. Cold Regions Science and Engineering Part III, Section A3c. Hanover, New Hampshire.
Merlet, S., Thiis, T., Thorud, B., Olsen, E., Nyhus, J., 2016. Challenges of PV Generation in Polar Regions. Case Study: the Norwegian Research Station "Troll" in Antarctica. In: 32nd European Photovoltaic Solar Energy Conference and Exhibition.
Meteonorm., 2020. Features - Data sources. Available at: https://meteonorm.com/en/meteonorm-features (accessed: 18.10.21).
Obara, S.Y., Morizane, Y., Morel, J., 2013. A study of small-scale energy networks of the Japanese Syowa Base in Antarctica by distributed engine generators. Appl. Energy 111, 113–128. https://doi.org/10.1016/j.apenergy.2013.04.039.
Pawluk, R., Chen, Y., She, Y., 2019. Photovoltaic electricity generation loss due to snow – a literature review on influence factors, estimation, and mitigation. Renew. Sust. Energ. Rev. 107, 171–182. https://doi.org/10.1016/j.rser.2018.12.031.
PVsyst SA, 2020. PVsyst. Route du Bois-de-Bay 107, Satigny, Switzerland.
Sánchez-Carbajal, S., Rodrigo, P.M., 2019. Optimum array spacing in grid-connected photovoltaic systems considering technical and economic factors. Int. J. Photoenergy 2019, 1486749. https://doi.org/10.1155/2019/1486749.
Schmidt, R., 1980. Threshold wind-speeds and elastic impact in snow transport. J. Glaciol. 26, 453–467.
Shademan, M., Barron, R., Balachandar, R., Hangan, H., 2014. Numerical simulation of wind loading on ground-mounted solar panels at different flow configuration. Can. J. Civ. Eng. https://doi.org/10.1139/cjce-2013-0537.
Tabler, R.D., 1980. Self-similarity of wind profiles in blowing snow allows outdoor modeling. J. Glaciol. 26 (94), 421–434. https://doi.org/10.3189/S0022143000010947.
Tabler, R.D., 2003. Controlling Blowing and Drifting Snow with Snow Fences and Road Design. Niwot, Colorado, p. 345.
Thiis, T., Ferreira, A., Molnar, M., Erichsen, A., 2015. Characterisation of shear stress distribution on a flat roof with solar collectors. Czasopismo techniczne.
Tian Shen, L., Pravettoni, M., Deline, C., Stein, J., Kopecek, R., Singh, J.P., Luo, W., Wang, Y., Aberle, A., Khoo, Y.S., 2019. A review of crystalline silicon bifacial photovoltaic performance characterisation and simulation. Energy Environ. Sci. 12 https://doi.org/10.1039/C8EE02184H.
Tin, T., Sovacool, B.K., Blake, D., Magill, P., El Naggar, S., Lidstrom, S., Ishizawa, K., Berte, J., 2010. Energy efficiency and renewable energy under extreme conditions: case studies from Antarctica. Renew. Energy 35 (8), 1715–1723. https://doi.org/10.1016/j.renene.2009.10.020.
Tominaga, Y., Mochida, A., Yoshie, R., Kataoka, H., Nozu, T., Yoshikawa, M., Shirasawa, T., 2008. AIJ guidelines for practical applications of CFD to pedestrian wind environment around buildings. J. Wind Eng. Ind. Aerodyn. 96 (10), 1749–1761. https://doi.org/10.1016/j.jweia.2008.02.058.
UNIS, 2020. UNIS Weather stations and CTD stations. Available at: https://www.unis.no/resources/weather-stations/ (accessed: 10.11.2019).
Urraca, R.H., Thomas, Lindfors, V. Anders, Riihelä, Aku, Martinez-de-Pison, Javier, Francisco, Sanz-Garcia, Andres, 2018. Quantifying the amplified bias of PV system simulations due to uncertainties in solar radiation estimates. Sol. Energy 176, 663–677.
VDMA, 2020. International Technology Roadmap for Photovoltaic, Results 2019.
Wittmer, B., Mermoud, A., 2018. Yield Simulations for Horizontal Axis Trackers with Bifacial PV Modules in PVsyst. In: 35th European Photovoltaic Solar Energy Conference and Exhibition.
Yang, D., 2016. Solar radiation on inclined surfaces: Corrections and benchmarks. Sol. Energy 136, 288–302. https://doi.org/10.1016/j.solener.2016.06.062.
Yusufoglu, U., Pletzer, T., Koduvelikulathu, L., Comparotto, C., Kopecek, R., Kurz, H., 2015. Analysis of the Annual Performance of Bifacial Modules and Optimization Methods. IEEE J. Photovoltaics 5, 320–328. https://doi.org/10.1109/JPHOTOV.2014.2364406.

Paper III

Reliability of building roofs with photovoltaic systems with active snow mitigation

Frimannslund, I., Thiis, T., Kohler, J. & Aalberg, A.

Manuscript in preparation.

Reliability of building roofs with photovoltaic systems with active snow mitigation

Iver Frimannslund[a,*], Thomas Thiis[a], Jochen Köhler[b], Arne Aalberg[b]

[a]*Norwegian University of Life Sciences, Department of Building- and Environmental Technology, NO-1432 Ås, Norway*
[b]*Norwegian University of Science and Technology, Department of Structural Engineering, NO-7034 Trondheim, Norway*

**Corresponding author*

Abstract: The added load from a photovoltaic (PV) system often prevents installation of such systems on existing building roofs. A new use of the PV technology allows for an active mitigation of the roof snow load to utilize the roof area of existing under-designed structures for PV power production. To investigate how PV snow mitigation systems influence the structural reliability of building roofs, a limit-state-function is developed where the snow load is reduced dependent on the function of the system. The limit state function is applied to a roof structure with variable snow load and structural strength to indicate the influence on the structural reliability. Here we show that the influence of the added load of PV systems is small for roofs designed for significant snow loads, whereas the use of active snow mitigation can have a strong positive effect depending on the function of the mitigation system. A sensitivity analysis of the snow mitigation variables shows that the uncertainty in successfully reducing the load gives the highest impact on the structural reliability. The threshold for when melting is initiated as well as the coverage of PV panels on the roof can be adjusted within a range with insignificant effect on the reliability, indicating that less energy can be used to achieve the target reliability. The results from this study can be used by standardization organizations to develop provisions for the use snow mitigation systems, contributing to increasing the deployment of PV systems on existing structures with a positive impact on the structural safety.

Keywords: structural reliability, photovoltaic systems, snow mitigation, sensitivity analysis, climate robustness

1. Introduction

In the development of structural design standards significant efforts are made to give provisions which yield a structural reliability in accordance with the target reliability criteria. The measures to tune the structural reliability include either a calibration of partial factors (Croce et al., 2021; Ghosn et al., 2016) or adjusting the environmental loads used in the design (Liel et al., 2017). The current standards contribute to adequate safety level in new structures, but for existing structures the structural reliability is governed by the design standards at the time the structure was designed and possible changes in the environmental loads. A historic development in the characteristic snow loads used in the design result in many existing buildings being design for a lower snow load than current requirements prescribe (Meløysund et al., 2006). This has resulted in a limited possibility of installing photovoltaic (PV) power system on existing building roofs. PV systems are often ballasted to secure for wind loads and impose a load of 0.1-0.5 kN/m^2 on the building roof. The added weight and the reduced accessibility for manual snow removal impacts the structural safety adversely and therefore limits the installation of PV systems on existing structures. Insufficient structural capacity is commonly not considered in studies estimating the available rooftop area for PV power production (Melius et al., 2013). Thus, existing estimates of rooftop PV potential may be significantly overestimated.

To compensate for the increased roof dead load PV systems impose, a function of heating the modules to melt roof snow loads have been developed. Several solutions exist for achieving this result (Pawluk et al., 2019), where one of the more convenient methods is to apply electric power to the modules (referred to as “forward bias” in PV terminology) which generate heat due to the electrical resistance in the cells. Other methods involve transferring heat from a circulating liquid medium from a closed loop to the back of the modules or using heating by electrical resistive wires embedded in the layers of the PV module (Anadol, 2020). For flat roofs, the snowpack is melted bottom-up and relies on modules with a low tilt so that the snow does not slide off the module and onto the roof. This is a common configuration for industrial roof-mounted PV systems as a high utilization of the roof surface is achieved. PV snow mitigation systems measure the snow load with load sensors mounted on the support of

individual PV modules and melting is initiated when the snow load exceeds a predefined threshold. An example of the layout of a photovoltaic snow mitigation system on an industrial building roof is shown in Figure 1.

Figure 1. A photovoltaic snow mitigation system installed at a warehouse in Oslo, Norway. The modules have a low angle tilt and face each other. Between the modules are heated gutters to transport meltwater off the roof. The system is designed by Innos AS (Innos, 2022).

The influence of PV snow mitigation systems on the structural reliability of building roofs depends the function of the system. If the system is not successful in reducing the snow load in a heavy snow load scenario, the total load on the roof is increased due to the weight of the PV system. There are several factors which may prevent sufficient load reduction. Melting may not be initiated due to technical malfunction, hardware failure or power outages. Additionally, climatic phenomena such as refreezing of the meltwater and water saturation of the snow can prevent the meltwater from being transported off the roof (Frimannslund & Thiis, 2019). The uncertain function of the snow mitigation system is suitable for implementation in probabilistic structural reliability analysis to indicate the impact on structural safety. PV snow mitigation systems have been analyzed by several (Aarseth et al., 2018; Rahmatmand et al., 2018; Yan et al., 2020), but not with regards to structural safety to the knowledge of the authors. However, Diamantidis et al. (2018) investigated the use of snow mitigation measures to achieve a desired safety risk for a structure under-designed with respect to snow load. The authors quantified the uncertainty and costs of different monitoring methods for determining the roof snow load which was then used to support decision making for snow removal. Their findings were then related to Structural Health Monitoring (SHM) standards to address areas for improvement in future standards.

This study aims to show how the PV snow mitigation systems influence the structural reliability of existing under-designed building roofs. The use of active snow mitigation with PV systems can increase the deployment of PV systems on existing structures, but it is important that such systems are implemented in such a way that a satisfying structural safety is achieved. Additionally, melting snow is energy consuming, and a cost optimized operation requires information on the influence of snow removal on both the structural reliability and the amounts of snow removed from the roof. The method in this study is focused on PV snow mitigation systems, but can be applied to other mitigation methods as well (Mensah & Choi, 2015).

2. Method

To study the present problem, limit state functions for the component reliability of a simply supported beam are developed to represent the load conditions occurring on a roof with a PV snow mitigation system. To isolate the influence of the added load from the PV system from the mitigation function itself, different load scenarios of roofs with and without the PV system load and snow mitigation function are investigated. The function of the snow

mitigation is modelled with several variables which influence on the structural reliability are investigated in a sensitivity analysis. The influence on the snow load reduction quantity and frequency is also investigated. The study is limited to low-tilt PV systems installed on flat roofs with a where snow is retained on the modules during melting.

2.1 Limit state functions

Three limit state functions (LSF) are formulated to represent three different load scenarios: (1) roof without a PV system (2) roof with a PV system without snow mitigation (3) roof with a PV system with snow mitigation. The limit state functions are for the plastic bending moment capacity of a uniformly loaded, simply supported steel beam.

$$Z(X) = \theta_R W_{pl} f_y - \frac{\theta_E L^2}{8} [\gamma_{steel} A_s + gb + \mu_i bS] \quad (1)$$

$$Z(X) = \theta_R W_{pl} f_y - \frac{\theta_E L^2}{8} [\gamma_{steel} A_s + gb + g_{PV} b + \mu_i bS] \quad (2)$$

$$Z(X) = \theta_R W_{pl} f_y - \frac{\theta_E L^2}{8} [\gamma_{steel} A_s + gb + g_{PV} b + \mu_i bS^*] \quad (3)$$

LSF 1 represents the capacity of a beam subjected to dead loads (the self-weight of the beam and the self-weight of the roof) and to the variable action of snow load. LSF 2 additionally includes the self-weight from the PV system, while LSF 3 includes a reduction of the snow load dependent on the function of the system. Table 1 list the variables in LSF 1-3. The limit state functions are solved using the Monte Carlo method in Matlab (MATLAB, 2021)

Table 1. Limit state function variables. CoV denotes the Coefficient of Variation. DET signifies a deterministic variable.

Symbol	Input	Distribution	Mean	CoV	Char. value	Unit	Source
W_{pl}	Section modulus	DET	-	-		m^3	
γ_{steel}	Steel density	DET	77	-		kN/m^3	
L	Beam span	DET	12	-		m	
b	Beam spacing	DET	7	-		m	
A_s	Beam cross-section area	DET	-	-		m	
f_y	Yield strength	LogNormal	0.283	0.05	μ*0.83	kN/m^2	(CEN, 2022)
g	Permanent load	Normal	1	0.1	1	kN/m^2	(CEN, 2022)
g_{PV}	Weight of PV	Normal	0.2	0.05	-	kN/m^2	
μ_i	Shape coefficient	LogNormal	0.66	0.16	0.8	-	(CEN, 2021)
S	Snow load (1-year)	Gumbel	Variable	0.51	μ*2.1	kN/m^2	(CEN, 2022)
S^*	Snow load w. mitigation	*	Variable	-	-	kN/m^2	
θ_R	Resistance unc.	LogNormal	1.15	0.055	-	-	(CEN, 2022)
θ_E	Permanent load unc.	LogNormal	1	0.05	-	-	(CEN, 2022)

*The distribution of S^* is the product of other variables. See section 2.2 for details.

The beam material, length and load span are fixed for all simulations. The limited amount of investigated structural properties and load conditions limits the applicability to different types of structures but is suitable for the aim of the study which is to identify the general influence of PV snow mitigation systems on the reliability.

The snow load distribution is for annual maximum values, making the target reliability index $\beta = 4.7$ for buildings in Reliability Class 2 in the Eurocodes (CEN, 2002). This class encompass residential buildings, offices, and public buildings where consequences of failure are medium. The uncertainty in the snow load is included through the shape coefficient (μ_i), accounting for both uncertainties in the spatial occurrence of the load and its conversion to the roof. This is in accordance with the methodology used in the development of the second generation of the Eurocodes (CEN, 2021). The snow load S is thus the expected snow load, excluding all uncertainties.

Previous studies have shown that the presence of a PV system can influence the shape coefficient for roof snow loads, but that it is highly dependent on the configuration of the system (Thiis et al., 2015). Systems with PV modules that extend high above the roof surface are likely to prevent wind erosion of snow from the roof which can increase the shape coefficient (Ferreira et al., 2019; Grammou et al., 2019). In the draft for the new version of Eurocode 1991-1-3 snow load design standard (prEN-1991-1-3), the shape coefficient remains unchanged if the maximum snow depth is larger than the 0.8 * the total height of the PV structure. This study investigates low tilt systems installed closed to the roof surface and it is assumed that the shape coefficient is the same as for a flat roof. PV systems may also influence the thermal coefficient of the roof, but research on this is scarce and it is assumed that it remains the same as for roofs without a PV system, in accordance with what is proposed by O'Rourke and Isyumov (2016).

2.2. Snow mitigation modelling

For the modelling of the influence of active snow mitigation in LSF 3, a snow load which is influenced by mitigation is applied (S*). This is a censored variable, defined as the snow load S reduced according to the function of the system as given by Equation 4:

$$S^* = S - S_{PV}\theta_{PV}\alpha \tag{4}$$

where S_{pv} is the intended snow load reduction, θ_{PV} is the load reduction uncertainty and α is the melting area coefficient. The reduction is only performed for roof snow loads exceeding a melting limit, S_{lim}. The distributions of the snow load mitigation variables are given Table 2 and elaborated on the following sections. Nominal values are set for the snow mitigation variables, but they are later investigated in a sensitivity analysis.

Table 2. PV snow mitigation variables.

Symbol	Input	Distribution	Default mean	CoV	Unit	Definition
S_{lim}	Melting limit	Det.	Eq. 5	-		Section 2.2.1
S_{PV}	Intended snow load red.	Censored	Eq. 6	-	kN/m^2	Section 2.2.2
θ_{PV}	Reduction unc.	Bernoulli	0.95	-	-	Section 2.2.3
α	Melting area coef.	Normal	0.8	0.03	-	Section 2.2.4

2.2.1 Melting limit

Snow load mitigation systems are operated to ensure that the snow load does not exceed a threshold. The melting limit variable defines for which load melting is initiated. In this study we focus on structures designed for a lower snow load than current requirements prescribe and define the melting limit (S_{lim}) as the following:

$$S_{lim} = S_{design} - g_{PV-mean} \quad (5)$$

where S_{design} is the design snow load used to dimension the structure at the time of the original design and construction (further elaborated in section 2.3) and $g_{PV\text{-}mean}$is the mean self-weight of the PV system, here set to 0.2 kN/m^2. The melting limit is later quantified by its ratio to the value given by Equation 5 in percentage (100% being the exact value given by Equation 5).

2.2.2 Intended snow load reduction

The intended snow load reduction, S_{PV}, is modelled to reduce snow loads exceeding the threshold limit to the exact value of the threshold with certainty. S_{PV}, is defined conditional on the value of the roof snow load and is achieved with an if-statement as given by Equation 6:

$$\begin{array}{ll} \text{If} & S * \mu_i > S_{lim} \\ \text{Then} & S_{PV} = S * \mu_i - S_{lim} \\ \text{Else} & S_{PV} = 0 \end{array} \quad (6)$$

The equation states that for a realized roof snow load exceeding the threshold, the snow load is reduced by the magnitude of exceedance over the threshold. A one-to-one correlation of S_{PV} and $S^*\mu_i$ ensures a load reduction to the exact limit.

2.2.3 Reduction uncertainty

The reduction uncertainty variable (θ_{PV}) accounts for uncertainties in the load being successfully reduced to the threshold. This includes power outages during mitigation, potential PV system component malfunctions and climatic effects such as refreezing of meltwater. Too little knowledge on the function of PV snow mitigation systems exists for approximating the distribution and potential correlations of this variable. In this study, it is implemented as a Bernoulli distribution, being realized as either 0 or 1 according to a defined probability. This means that the intended load reduction S_{PV} is either completely successful or not successful at all. An underlying assumption with this modelling approach is that there is no redundancy in removing the snow. This is suitable for PV snow mitigation systems where the panels hinder manual snow removal. The default probability for successful snow load reduction ($\theta_{PV} = 1$) is set to 95%.

2.2.4 Area coefficient

The melting area coefficient (α) accounts for that the PV system does not cover the entire roof. As the area effective are which the snow load is reduced depends on the snow coverage on the roof, it is represented as an uncertain variable. It is set to have a normal distribution with a mean based on the PV system in Figure 1, giving a mean of 0.8 (i.e., 80% of the roof covered with solar panels). The CoV is set to 0.03.

According to the limit state functions, the load is reduced uniformly at the beam. This is a simplification as the load only is reduced on the surface of the PV panels, while the snow load in the areas between the panels remain unchanged. However, as the gaps between the panels are evenly spaced over small distances (module width is 1.0 m) and the snow load is never completely mitigated from the panel, the simplification of uniform load may be of small influence. However, for low area coefficients where uneven load distributions occur, the modelling method is less accurate.

2.3 Beam capacity

The limit state functions require input of the bending moment resistance of a simply supported beam. This study focus on roofs designed for lower snow loads than current prescribed by current standards. To represent such

structures, the capacity of the beam is determined in accordance with Eurocode 1991-1-1 for steel design, but with a lower characteristic snow load than the 50-year return period load. The snow load used in the design (S_{design}) is set to be a defined fraction of the snow load 50-year return period snow load of S that is applied in the Monte Carlo simulations. The relationship between the snow load in the design and the 50-year snow load of the snow load distribution is here referred to as the under-design ratio (ω) and is illustrated in Figure 2.

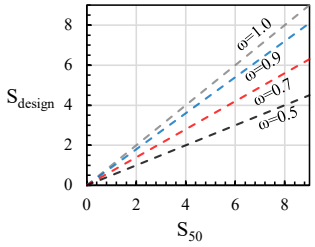

Figure 2. The capacity ratio (ω) defines the relationship between the 50-year return period snow load (S_{50}) and the snow load used to determine the load carrying capacity of the beam (S_{design}).

In the study ω is varied between 0.5-1 and the snow load is varied to yield an expected 50-year return period load between 0.5-9 kN/m^2. The capacity ratio concept can also be related to designing for different return-period snow loads which has been done by several previous and existing national standards for structural design (Croce et al., 2019). For a snow load with a Gumbel distribution, an ω = 0.9 is the equivalent of a snow load with a 25-year return period, ω = 0.7 equals an 8.3-year return period and ω = 0.5 equals a 3.3-year return period.

The partial factors used in the design are 1.2 for permanent actions (γ_G) and 1.5 for variable actions (γ_Q) and a material factor for structural steel of 1.05 (γ_m), corresponding to a Reliability Class 2 building in the Eurocodes (CEN, 2002). The permanent load is kept fixed at 1 kN/m^2 in all simulations while the snow load is varied incrementally between 0.5-9 kN/m^2. This yields a variable relationship between the permanent load and the snow load known to influence the reliability of structures due to environmental loads commonly having higher CoV than permanent loads (Vitali et al., 2019). The weight from the PV system is not included in the design and is applied as an additional load in the Monte Carlo simulations to represent the case of installing a PV system on an existing structure.

3. Results

3.1 Scenario reliability

The reliability index (β) for the three different scenarios in LSF 1-3 are shown in Figure 3, while Figure 4 shows the difference in reliability (Δβ) between the scenarios. The figures contribute to the understanding of two important effects: how the PV systems weight and active snow mitigation influence the structural reliability and how this varies for structures with different load and capacity characteristics.

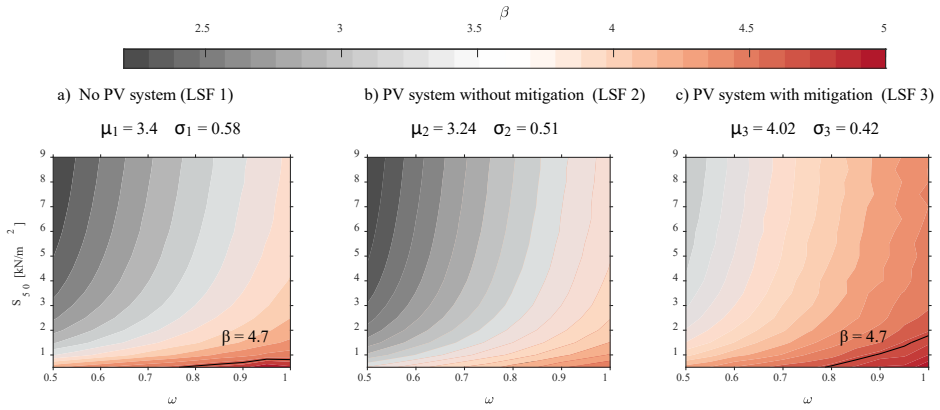

Figure 3. Reliability index (β) with varying snow load (S_{50}) and capacity ratio (ω) for: a) a building without a PV system, b) a building with a PV system without snow mitigation and c) a building with a PV system with snow mitigation (given fixed snow load mitigation variables: $\theta_{pv} = 0.95$ and α=0.8 and S_{lim}=100%). The mean (μ) and standard deviation (σ) reliability for all variations of S_{50} and ω is given for each figure.

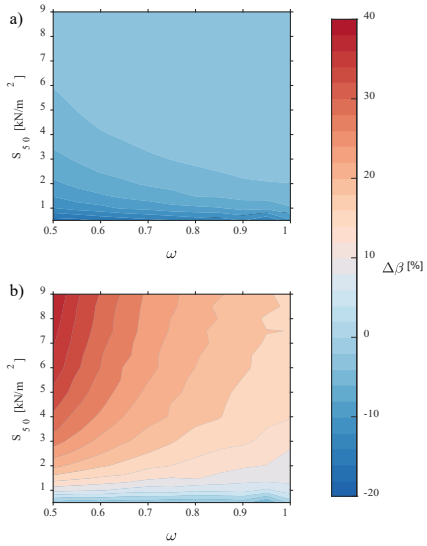

Figure 4. Difference in reliability (Δβ) between a) a structure with and without a PV system (LSF 1 - LSF 2) and b) a structure without a PV system and a structure with a PV system with snow mitigation (LSF 1 - LSF 3), given fixed snow load reduction variables ($\theta_{pv} = 0.95$ and α=0.8 and S_{lim}=100%).

The general trend in Figure 3 is a decrease in reliability with decreasing capacity ratio (ω) and with increasing snow loads (S_{50}). For a building without a PV system in Figure 3a, the target level reliability (β = 4.7) is only achieved for structures with S < 1 and ω > 0.75. The decrease in reliability with increasing snow load is in

conjunction with other studies indicating that the partial factor for variable actions in the Eurocodes are too low (Köhler et al., 2019).

The influence of the added weight of a PV system has an adverse impact on the reliability on all the investigate load and capacity conditions but is most significantly for structures designed for lower snow loads as shown in Figure 4a. The average decrease in reliability is 4.7%, but ranges between 1-17% depending on the snow load and capacity ratio. That structures with lower snow loads are more influenced by the weight of the PV system is due to the self-weight of the PV system making up a larger part of the total load. However, it is for structures with low snow loads that the reliability is the highest to begin with, making the decrease in reliability less severe.

The influence of active snow mitigation has a stronger positive impact than the negative influence of the weight increase. The average increase in reliability is 18.2%, ranging between 0-40% depending on the snow load and capacity ratio. The impact of active snow mitigation is most significant for structures which have high snow loads and low capacity ratio as shown in Figure 4b. For structures with a low snow load, the impact is close to neutral, where the active mitigation of snow merely compensates for the weight of the system.

However, the result in this section is made with a fixed performance of the snow mitigation system which the reliability can be sensitive to. The next section investigates the influence of the snow mitigation variables.

3.2 Sensitivity analysis of the reliability to the snow mitigation variables

The modelling of the snow mitigation involves three important variables which can influence the structural reliability: the load reduction uncertainty (θ_{pv}), the melting threshold (S_{lim}) and the melting area coefficient (α). In this section the sensitivity of the reliability to the snow mitigation variables is analyzed by varying a single variable while the others are held constant. The results presented in Figure 5.

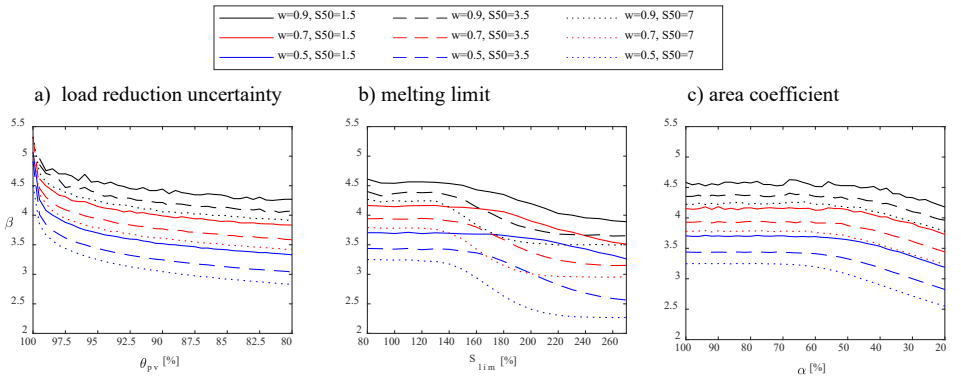

Figure 5. Sensitivity of the reliability index (β) to: a) the probability of successful load reduction (θ_{pv}), b) melting limit (S_{lim}) and c) melting area coefficient (α). S_{lim} is normalized to the default melting limit given by Eq.5, meaning that S_{lim} = 100% equals melting at the load which the roof was designed for. α =100% means that the whole roof is covered with solar panels. The variables which are not varied are held constant (θ_{pv} = 0.95, S_{lim}=100%, α=0.8).

The sensitivity to the load reduction uncertainty (Figure 5a) shows a logarithmic increase in reliability as θ_{pv} increases towards 100% for all the simulated variants. The high reliability achieved for θ_{pv}=100 is expected as this means that the snow load never exceeds the threshold limit. High reliability levels can thus be achieved for all types of structures if the success rate is high. The uncertainty of load reduction depends on factors which are difficult to control and a high success rate cannot be guaranteed, but will be influenced by factors such as system design and operation. To achieve a target reliability of β = 4.7, the success rate of the system must be above 99% for 8/9 of the simulated cases.

The influence of the melting threshold (S_{lim}) is shown in Figure 5b. The reliability is quite constant for a range of S_{lim} (between 120-140% dependent on the case) and subsequently decreases with increasing S_{lim}. The reliability stagnates at a high level where the melting limit is larger than the snow load and no snow is mitigated from the roof. The plateau occurs due to the partial factor used for variable actions, resulting in a structural capacity capable of withstanding loads higher than the characteristic snow load applied in the design. The presence of the plateau indicates that if the snow load on the roof is known, melting at a snow load limit higher load than roof's design capacity gives an insignificant chance for structural failure in a certain range. Thus, the operation of PV snow mitigation systems can be adjusted to reduce the amounts of mitigated snow, with insignificant influence on the reliability. That the decrease in reliability occur at different melting limits is due to the increased impact of the PV load for structures designed for lower snow loads. By normalizing the melting threshold to the snow load used in the design (S_{design} from Eq. 5) without subtracting the PV load, the plateau in the obtained reliability ends at 120% for all the simulated cases.

The influence of melting area coefficient (α) on the roof in Figure 5c is similar to the influence of the melting limit. There is a plateau with constant reliability for α < 50-70% (depending on the snow load and capacity ratio), and a decrease in reliability for α exceeding this limit. This indicates that as long as the snow load is reduced uniformly on the load area of the beam and if it is initiated at the melting limit equal to the design load capacity, the area of solar panels on the roof can be reduced to 50-70% without significantly influencing the reliability.

3.3 Snow load mitigation frequency and quantity

The frequency and quantity of mitigated snow is important for the energy use and competitiveness of PV snow mitigation systems. Figure 6 shows the obtained snow load mitigation frequency and quantity for varying snow load and capacity ratio.

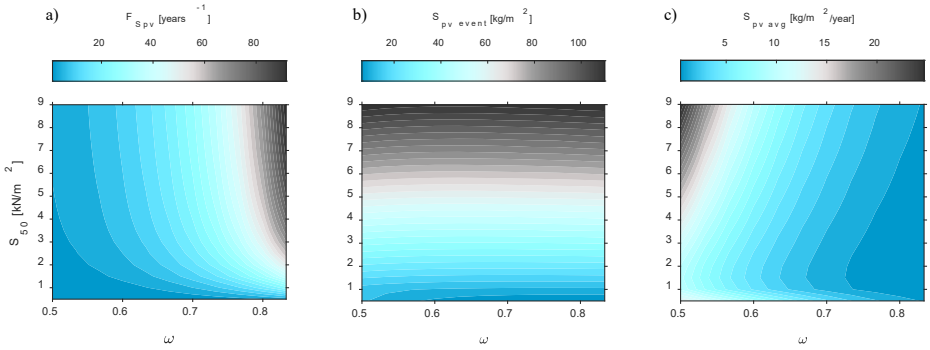

Figure 6. Snow load reduction variables for varying snow load (S_{50}) and capacity ratio (ω) showing a) average reduction frequency (F_{Spv}) given in years, b) average reduction amount per event ($S_{pv\ event}$) given in kg/m^2, and c) average annual reduction quantity ($S_{pv\ avg}$) in kg/m^2/year. The snow mitigation variables are fixed (θ_{pv} = 0.95, S_{lim}=100%, α=0.8).

The average reduction frequency in Fig. 6a shows that melting only occurs with 1-95 years intervals. Decreasing the capacity ratio and decreasing the snow load results in more frequent mitigation of snow. The influence of snow load on the reduction frequency is due to the self-weight of the PV system making up a relatively larger part of the total load imposed on the roof, resulting in a relatively lower melting limit and thus more frequent snow mitigation. As the snow load reduction uncertainty θ_{pv} is constant for each reduction event, scenarios with more frequent snow load reduction will also experience a higher number of unsuccessful reductions where the snow load exceeds the threshold limit. Thus, the frequency of snow load mitigation as modelled here also impacts the results on the reliability in the previous sections.

The average reduction amount per event ($S_{pv\ event}$) in Fig. 6b varies between 6-113 kg/m^2 and is mainly a function of the snow load. The limited influence from the capacity ratio is due to ($S_{pv\ event}$) being the *average* reduction amount. Of course, more snow is removed per event for a structure with lower capacity for a realized snow load of high magnitude, but structures with lower capacity experience more frequent snow load mitigation (due to the shape of the snow load distribution), reducing the average snow load reduction amount per event.

The average annual reduction quantity ($S_{pv\ avg}$) in Fig. 6c is influenced both by how often snow is mitigated from the roof (Fig. 6a) and how much snow is mitigated per event (Fig. 6b). An exponential increase in reduction quantity with increasing snow load and decreasing capacity ratio is evident. The differences in load reduction amounts are large, indicating that far less energy is required to operate PV snow mitigation systems for structures with high capacity ratios and low snow loads.

3.4 Reliability and reduction quantity comparison

The optimal performance of a snow mitigation system is achieved by balancing the mitigation amounts with the impact on the reliability. Figure 7 shows the reliability and reduction quantity as a function of the melting threshold and the area coefficient.

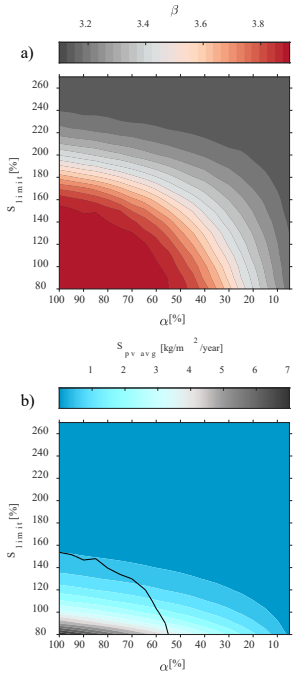

Figure 7. Influence of the melting threshold (S_{lim}) and the melting area coefficient (α) for a structure with S_{50} = 3 kN/m^2 and ω=0.7 on: a) the reliability index (β) and b) the annual average reduction quantity ($S_{pv\ avg}$). The black line in Fig. b) shows the contour of β = 3.8. The reduction uncertainty is fixed at θ_{pv} = 0.95

Figure 7a shows that the reliability is constant for low values of S_{lim} and high values of α. However, for the same combinations of S_{lim} and α, the reduction quantity varies significantly. A black line in Figure 7b shows for which combinations the constant values of reliability occur, indicating that the S_{lim} and α can be adjusted within this range with insignificant effect on the reliability. It is evident that it less snow is melted by increasing the melting

limit rather than reducing the coverage of solar panels on the roof. The impact is large; if the melting limit is increased from 100% to 130% for a system with an area coefficient of 80%, the reduction quantity is reduced by 68% while the reliability decreases with 0.15%

4. Discussion

The discussion section encompasses the modelling approach and its representability of the actual system, as well as the implications of the results and future work.

4.1 The modelling approach

As the modelling of snow mitigation is time-invariant, the physical interpretation of the load reduction uncertainty parameter is somewhat abstract. During a winter, several snow load mitigations event may be necessary to keep the load below the melting limit. However, the load reduction uncertainty variable only gives a successful or unsuccessful reduction of the realized snow load to the threshold, without considering how many mitigation events this may comprise. Thus, the snow load reduction uncertainty is not the probability of load reduction each time the system is used but rather total probability of the snow being reduced from to the threshold limit. To correlate the load reduction uncertainty from this study to a physical representable quantity, time-variant probability methods can be applied.

The model is developed to represent snow load reduction on roofs but does not accurately represent all physical phenomena which can influence the reliability. The assumption of a uniform load reduction neglects how insufficient drainage of meltwater can contribute to increased local loads (Frimannslund & Thiis, 2019). Ideally, the potential of increased loads from poor functioning systems should be considered in the reliability analysis. This can easily be implemented in the presented framework where what is here referred to as the area coefficient can be given negative values to give increased loads (which then could be termed a distribution coefficient). The challenge is to quantify the probability of such events as they may occur rarely (Chan & Kroese, 2011).

The model can also be improved to better consider the influence of a PV system on the shape coefficient and the thermal coefficient. Existing building under-designed with respect to snow load may also have poor roof insulation which contribute to increased melting of the roof snow load. Having elevated PV panels on the roof surface can significantly reduce the amounts of passive heat transferred to the snowpack, giving increased snow loads. This phenomenon can contribute to an under-estimation of the results in this study showing the influence of installing PV systems on existing roofs on the structural reliability. With more knowledge on this topic, it should be included in future studies.

In this study, a simplification is made by neglecting the uncertainty of the measurement method and regarding the roof snow load as known. (Diamantidis et al., 2018) demonstrated how the uncertainty of different monitoring methods for the roof snow load influenced the required frequency of snow removal to achieve a defined target reliability. The authors showed that larger roof snow loads can be tolerated for decreasing uncertainty in the monitoring method. The uncertainty of the measurement method with load sensors on the PV modules should ideally be considered with the present study, and would contribute to melting at an earlier limit as there is inherent uncertainty in the estimation of the roof snow load.

4.2 Implications of the results

In this study, it is demonstrated how the reliability of structures with different capacity and load characteristics are influenced by the PV snow mitigation system. The impact is largest for structures which have a low capacity ratio and high snow loads, exhibiting the lowest reliability prior to the PV installation. A consequence of this is that structures characterized by a lower reliability require better functioning systems to achieve the target reliability. Previous research on the performance of PV snow mitigation system indicate that has a higher probability of succeeding in climates experiencing abrupt snow loads rather than climates with long and cold winters (Frimannslund & Thiis, 2019). With the climatic performance of the system in mind, a positive impact on the

structural reliability is more likely achieved in warmer climates with lower snow loads. The inclusion of the influence of climate on the reduction uncertainty should be considered in future work on this.

The results from this study also have implications for the design and operation of PV snow mitigation systems. Both the reduction uncertainty, the melting limit and the area coefficient are variables which are influenced by the design and operation of the PV snow mitigation system. The high system success rate can be achieved with reliable electrical system components, a mechanical design efficient in transporting meltwater off the roof, and an operation considering the climatic conditions. The melting limit is set by the system operators and is demonstrated here that can be adjusted to reduce the snow load reduction amounts with an insignificant effect on the structural reliability. A similar mechanism occur for the area coefficient, but with less impact, and is perhaps less relevant as a high utilization of the roof surface often is desired for roof mounted PV systems. Based on the sensitivity analysis of the snow mitigation function, the system design and operation can be adjusted to achieve a favourable impact on the reliability on snow load reduction amounts.

The value of estimating the snow load with load censors on the PV modules can also be utilized on traditional PV systems without the mitigation function, where the safety measure of a roof snow load exceeding the threshold could be evacuation of the occupants in the building (instead of snow removal). This may be a sufficient measure for buildings where temporary stop in the occupant activity is not critical or for buildings with low probability of exceeding the threshold. Measuring the load with load cells on the mount of the PV modules have small costs compared to implementing the active snow mitigation function to a PV system.

The findings of the study can be of value for standardization organizations. The PV snow mitigation system is an innovation which serves to increase the deployment of PV systems on existing structures. Having provisions in structural design standards for how snow mitigation system is implemented can reduce the resources used to document and evaluate the use of such systems. A structural design standard which addresses the use of snow mitigation systems is the international snow load standard ISO4355 in its Annex F "*Snow loads on roofs with snow control*" (ISO, 2013). Here, provisions are given for reducing the roof snow load used in the design if a reduction of the snow load during a reference period can be guaranteed. The provisions may not be intended for PV snow mitigation systems but can be argued to be valid for this type of system. However, ISO4355 lacks in addressing limitations in the applicability to different structures, how the system must function, and no distinction is made between systems with and without redundancy. This is problematic as the use of snow mitigation systems as analyzed here depicts a highly variable reliability depending on the characteristics of the structure and the function of the mitigation system. To ensure a satisfying impact on the structural safety, the standard should consider the above mentioned (applicability to different structures, requirements for system function, redundancy). The topic of structural safety and snow mitigation is closely related to SHM which could be an inspiration for the development of such provisions.

5. Conclusion

To investigate the influence of PV snow mitigation systems on the structural reliability, a probabilistic modelling approach is developed with a limit-state-function including a reduction of the snow load depending on the function of the system. The model is applied to a steel beam with varying snow load and capacity ratio. The results show that the increase in load from the self-weight of the PV system itself (without snow mitigation) has a negative influence on the reliability which is larger for structures designed for low snow loads. The snow mitigation function can have a strong positive impact on the structural reliability depending on the function of the system. Increasing the probability of successful load reduction gives a logarithmic increase in reliability, indicating the importance of reliable snow mitigation systems. The sensitivity of melting threshold and roof area coefficient is shown to have little influence on the structural reliability within a defined range of adjustment. The margin can be utilized to reduce the snow mitigation quantity and the resulting energy consumption of the system. There is a potential for improving the present model to better represent the physical phenomenon occurring on roofs with PV snow mitigation systems which should be incorporated in future studies to increase the accuracy of the findings. The results from this study

can be used by standardization organizations to develop provisions for the use snow mitigation systems, contributing to increasing the deployment of PV systems on existing structures with a positive impact on the structural safety.

References

Aarseth, B. B., Øgaard, M. B., Zhu, J., Strömberg, T., Tsanakas, J. A., Selj, J. H. & Marstein, E. S. (2018, 26 September 2018). Mitigating Snow on Rooftop PV Systems for Higher Energy Yield and Safer Roofs. *EU PVSEC 2018: 35th European Photovoltaic Solar Energy Conference and Exhibition*, Brusells.

Anadol, M. A. (2020). Snow melting on photovoltaic module surface heated with transparent resistive wires embedded in polyvinyl butyral interlayer. *Solar Energy*, 212: 101-112. doi: https://doi.org/10.1016/j.solener.2020.10.073.

CEN. (2002). *Eurocode - Basis of Structural Design*. Annex B - Management of Structural Reliability for Construction Works.

CEN. (2021). *SC1.T6; Final Draft "Interdependence of climatic actions"; Background document "Probabilistic basis for determination of partial safety factors and load combination factors";*: 1-317.

CEN. (2022). *CEN/TC 250/SC 10/AHG "Reliability background" Report Draft version May 2022*.

Chan, J. & Kroese, D. (2011). Rare-event probability estimation with conditional Monte Carlo. *Annals of Operations Research*, 189: 43-61. doi: 10.1007/s10479-009-0539-y.

Croce, P., Formichi, P., Landi, F. & Marsili, F. (2019). Harmonized European ground snow load map: Analysis and comparison of national provisions. *Cold Regions Science and Technology*, 168: 102875. doi: https://doi.org/10.1016/j.coldregions.2019.102875.

Croce, P., Formichi, P. & Landi, F. (2021). Probabilistic Assessment of Roof Snow Load and the Calibration of Shape Coefficients in the Eurocodes. *Applied Sciences*, 11: 2984. doi: 10.3390/app11072984.

Diamantidis, D., Sykora, M. & Lenzi, D. (2018). Optimising Monitoring: Standards, Reliability Basis and Application to Assessment of Roof Snow Load Risks. *Structural Engineering International*, 28 (3): 269-279. doi: 10.1080/10168664.2018.1462131.

Ferreira, A., Thiis, T., A. Freire, N. & M. C. Ferreira, A. (2019). A wind tunnel and numerical study on the surface friction distribution on a flat roof with solar panels. *Environmental Fluid Mechanics*, 19. doi: 10.1007/s10652-018-9641-5.

Frimannslund, I. & Thiis, T. (2019). A feasibility study of photovoltaic snow mitigation systems for flat roofs. *Technical Transactions*: 81-96. doi: 10.4467/2353737XCT.19.073.10724.

Ghosn, M., Frangopol, D. M., McAllister, T. P., Shah, M., Diniz, S. M. C., Ellingwood, B. R., Manuel, L., Biondini, F., Catbas, N., Strauss, A., et al. (2016). Reliability-Based Performance Indicators for Structural Members. *Journal of Structural Engineering*, 142 (9): F4016002. doi: doi:10.1061/(ASCE)ST.1943-541X.0001546.

Grammou, N., Pertermann, I. & Puthli, R. (2019). Snow loads on flat roofs with elevated solar panel arrays. *Steel Construction*, 12 (4): 364-371. doi: https://doi.org/10.1002/stco.201900031.

Innos. (2022). *Innos AS*. Available at: www.innos.no (accessed: 18.01.2022).

ISO. (2013). *ISO 4355 Bases for design of structures, Determination of snow loads on roofs*: ISO. p. 42.

Köhler, J., Sørensen, D., John & Baravalle, M. (2019). Calibration of existing semi-probabilistic design codes. *13th International Conference on Applications of Statistics and Probability in Civil Engineering*, Seoul, South Korea.

Liel, A. B., DeBock, D. J., Harris, J. R., Ellingwood, B. R. & Torrents, J. M. (2017). Reliability-Based Design Snow Loads. II: Reliability Assessment and Mapping Procedures. *Journal of Structural Engineering*, 143 (7): 04017047. doi: doi:10.1061/(ASCE)ST.1943-541X.0001732.

MATLAB. (2021). MATLAB R2021a. Natick, Massachusetts: The Mathworks, Inc.

Melius, J., Margolis, R. & Ong, S. (2013). *Estimating Rooftop Suitability for PV: A Review of Methods, Patents, and Validation Techniques*. United States: Medium: ED; Size: 35 p. doi: 10.2172/1117057.

Meløysund, V., Lisø, K. R., Siem, J. & Apeland, K. (2006). Increased Snow Loads and Wind Actions on Existing Buildings: Reliability of the Norwegian Building Stock. *Journal of Structural Engineering*, 132 (11): 1813-1820. doi: doi:10.1061/(ASCE)0733-9445(2006)132:11(1813).

Mensah, K. & Choi, J. (2015). Review of technologies for snow melting systems. *Journal of Mechanical Science and Technology*, 29: 5507-5521. doi: 10.1007/s12206-015-1152-4.

O'Rourke, M. & Isyumov, N. (2016). *Snow Loads on Solar-Paneled Roofs*: American Society of Civil Engineers.

Pawluk, R., Chen, Y. & She, Y. (2019). Photovoltaic electricity generation loss due to snow – A literature review on influence factors, estimation, and mitigation. *Renewable and Sustainable Energy Reviews*, 107: 171-182. doi: 10.1016/j.rser.2018.12.031.

Rahmatmand, A., Harrison, S. J. & Oosthuizen, P. H. (2018). An experimental investigation of snow removal from photovoltaic solar panels by electrical heating. *Solar Energy*, 171: 811-826. doi: https://doi.org/10.1016/j.solener.2018.07.015.

Thiis, T., Ferreira, A., Molnar, M. & Erichsen, A. (2015). Characterisation of shear stress distribution on a flat roof with solar collectors. *Czasopismo techniczne*.

Vitali, N., Rózsás, Á. & Sýkora, M. (2019). Calibrating Partial Factors – Methodology, Input Data and Case Study of Steel Structures. *Periodica Polytechnica Civil Engineering*, 63. doi: 10.3311/PPci.12822.

Yan, C., Qu, M., Chen, Y. & Feng, M. (2020). Snow removal method for self-heating of photovoltaic panels and its feasibility study. *Solar Energy*, 206: 374-380. doi: https://doi.org/10.1016/j.solener.2020.04.064.

Paper IV

Energy demand and yield enhancement of photovoltaic snow mitigation systems

Frimannslund, I., Thiis, T., Skjøndal, V. & Marke, T.

Submitted manuscript.

Energy demand and yield enhancement for roof mounted photovoltaic snow mitigation systems

Iver Frimannslund[a,*], Thomas Thiis[a], Louise V. Skjøndal[a] and Thomas Marke[b]

[a]*Norwegian University of Life Sciences, Department of Building- and Environmental Technology, NO-1432 Ås, Norway*
[b]*University of Innsbruck, Institute of Geography, 6020 Innsbruck, Austria*

**Corresponding author*

Abstract:

The deployment of photovoltaic (PV) systems in the built environment is limited by lacking structural capacity of existing roofs. PV snow mitigation systems can overcome such limitations by reducing heavy snow loads through active snow melting, so that roof area previously indisposed for PV systems can be utilized. The competitiveness of such systems is influenced by how much energy is needed to melt the snow and how much the yield is increased by reducing the snow cover on the modules. This study aims to quantify the energy consumption and yield enhancement of PV snow mitigation systems using numerical simulations. With an adapted energy balance snow model simulating Snow Water Equivalent (SWE), the energy consumption from melting snow as well as the snow cover duration on the modules are estimated. The snow cover duration is then used as input in PV yield simulations to quantify the yield enhancement. Different types of snow load climates are investigated. The results show that the energy consumption is <11.8 kWh/m^2 and the yield enhancement <3 kWh/m^2 per year depending on the climate and the melting limit. Climates with low characteristic snow loads give the lowest energy consumption and the highest yield enhancement. For the investigated climate with the lowest snow load (50-year return period snow load = 0.7 kN/m^2) the enhancement is larger than the consumption giving a positive energy balance of 0.6 kWh/m^2. The relative influence on the energy production is +1% to -13% of the production of PV systems without active snow mitigation.

Keywords: photovoltaic systems, snow mitigation, energy demand, energy balance snow model, PV yield, existing structures

1. Introduction

Photovoltaic (PV) systems are increasing in popularity and are expected to do so in the future as well (VDMA, 2020). In the built environment, roof surfaces are attractive for the installation of PV systems due to often being unused, accessible for maintenance, and in proximity to the consumer. However, not all roofs are suitable for the installation of PV systems as the irradiance conditions can be suboptimal (Sailor et al., 2021) and the building roof may lack structural capacity.

One of the reasons some existing buildings lack structural capacity is due to being built at a time where the environmental loads used in the design of structures were lower than modern standards require. The characteristic snow load used in the design of buildings is commonly determined with the return period concept defining the load with a set probability of being exceeded. Modern design standards such as the Eurocode standard, ASCE and ISO use characteristic snow load with 50-year return period (YRP), equaling a 2% yearly probability of being exceeded. However, previous building codes have used lower return period loads in the design. Prior to the use of international standards, these loads were commonly determined on a national basis and large variations exist depending on the year the structural design was made. To summarize some return periods used for snow load in national building codes Croce et al. (2019) elaborate that a 30 YRP was used in the Canadian Building Code until 2005, while 25 YRP is currently used in Russia and 100 YRP in Japan. In Norway, a 5 YRP snow load was used before 1999 (Meløysund et al., 2006). If the current characteristic snow load is higher than what was used in the design of the building, building owners are often prevented from installing PV systems. The structural capacity of building roofs is not commonly considered in studies concerning the rooftop potential for PV systems (Melius et al., 2013), but is a known limitation for PV deployment in the built environment (Richards et al., 2011). Thus, existing estimates of rooftop PV potential may be significantly overestimated.

To increase PV deployment on existing building roofs which lack structural capacity, PV systems that melt snow by applying heat to the modules surface have been developed (Frimannslund & Thiis, 2019). Such systems are often referred to as *PV snow mitigation systems* or *self-heating PV systems*. PV snow mitigation systems which reduce snow loads are designed with a low angle tilt to retain the snow on the modules during melting. Such systems have been used in Norway since the 2016. Since then, PV snow mitigation systems have increased in popularity and are now being utilized by several PV manufacturers. The typical configuration of a PV snow mitigation system is shown in Figure 1.

Figure 1. A PV snow mitigation system installed on a warehouse in Oslo. The system is designed by Innos (Innos, 2022).

There are also PV snow mitigation systems that intend only to increase the yield by having higher tilts and sliding snow off the module surface have been developed (Yan et al., 2020) as reduced efficiency from snow covered modules is a challenge in cold climates (Jelle, 2013). PV snow mitigation systems which are designed for reducing snow loads monitor the snow load on the roof and trigger a heat flux when the load exceeds a defined threshold. Commonly only the peak loads are reduced and all the snow on the modules is not removed. However, reducing the peak loads potentially contribute to increased yield as the snow cover duration on the modules is shortened.

The profitability of PV snow mitigation systems compared to ordinary PV systems is influenced by how much energy is used to reduce the snow load as well as how much energy is gained from reducing the snow cover. Actively mitigating snow is likely to reduce the profitability compared to ordinary PV systems, but the advantage is that a higher share of the surfaces in the urban environment can be utilized for PV power production. Using energy to mitigate the snow loads can thus be considered a tradeoff to utilize the unused surfaces which without active snow mitigation would be indisposable for PV production. No previous studies have quantified the long-term influence of active snow mitigation with PV systems.

2. Method

In this study, we combine an energy balance snow model with PV yield simulations to quantify the energy consumption and power production of PV snow mitigation systems. The outline of the method is given in Figure 2. The energy balance snow model simulates the buildup of snow represented by the Snow Water Equivalent (SWE) using hourly meteorological data. The model is adapted so that SWE exceeding a threshold limit is subjected to a heat flux from the PV system. From this model, the energy required to melt the snow and the duration of snow cover

on the modules is calculated. PV yield simulations are used to determine the yield of PV systems with a configuration typical for the PV snow mitigation system. To quantify how the yield is enhanced by snow mitigation systems, the duration of the snow cover from the energy balance snow model is used as input to the PV yield simulation.

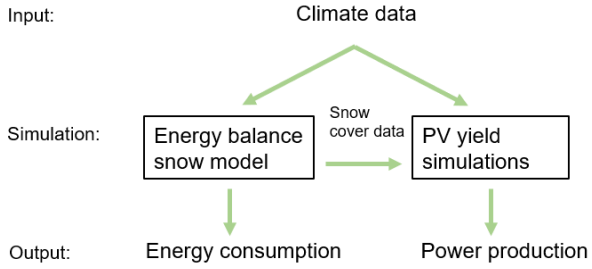

Figure 2. Outline of the method used in the study.

As both the power production and energy consumption of the system is dependent on climate, the simulation method is applied to four locations with different climatic conditions. The locations are chosen based on having different characteristic snow loads and irradiance conditions. An overview of the climate data for the chosen locations are shown in Table 1.

Table 1. Irradiance and snow load data for the four investigated locations. GHI is the Global Horizontal Irradiance obtained from Meteonorm (Meteonorm, 2020). S_{50} is the simulated characteristic 50-year return period snow load obtained according to the method described in 2.1.1.

Location	**Tromsø**	**Oslo**	**Munich**	**Davos**
Latitude	69.6° N	59.9° N	48.4° N	48.8° N
GHI (annual average) [kWh/m^2]	735	972	1198	1432
S_{50} [kN/m^2]	5.9	3.0	0.7	7.9

Tromsø is located high north and has a low Global Horizontal Irradiance (GHI) and a high snow load. Oslo is at a lower latitude and has a higher GHI than Tromsø and a lower characteristic snow load. Munich has relatively high irradiance and a low snow load, while Davos has high irradiance and a high snow load. The varying climatic conditions contribute to a better understanding of the system's energy production and demand for different locations. The following sections present the modelling approach in detail.

2.1 Energy balance snow model

2.1.1 The ESCIMO model

The energy balance snow model used in this study is a physically based point snow surface model called the Energy Snow Cover Balance Integrated Model (ESCIMO v.2) by Marke et al. (2016). Based on hourly climatic data, the energy and mass balance of the snowpack is calculated to yield the Snow Water Equivalent (SWE) (the amount of liquid water contained within the snowpack in mm). Hourly data from six climatic variables is required, including ambient temperature (K), relative humidity (%), wind speed (m/s), precipitation (mm/h), global horizontal irradiance (W/m2), and incoming longwave radiation (W/m2). The energy balance equations calculate the following heat fluxes for a single-layer snowpack: sensible heat, latent heat, advective heat, as well as the short- and longwave radiation balance. The model has recently been evaluated in different climatic and environmental settings with other energy balance snow models by Krinner et al. (2018) and has relatively high accuracy. The hourly temporal

resolution of the model is superior to many other existing snow models, but the snowpack is represented by a single layer in the model, meaning that the properties of the snowpack are considered to be homogeneous. This simplification influences the layered properties of the snow which influences heat transfer in the snowpack (Nuijten et al., 2016) and sublimation fluxes (Sexstone et al., 2016). Moreover, the model is describing the relevant processes at the point-scale, hence spatial differences in snow cover conditions are not accounted for by the model. Given the limited size and as a result rather homogeneous conditions on flat roofs, this model characteristic is assumed to have little effects on the results of this study.

As input to the model, the ERA5 reanalysis dataset is used (Hersbach, 2018). The database provides consistent climate data from 1979 to present in an hourly temporal resolution. Data from 1980-2021, equaling 41 complete winters is used as input to adequately capture the climatic variability at the study locations. The spatial resolution of the data is 0.25x0.25° corresponding to below 28x28 km depending on the latitude. As the grid often extends beyond the borders of the investigated location of interest (the city) and have a mean elevation often higher than this point of interest, the simulated SWE will not always accurately depict the local snow load climate of the cities, which can change significantly with local topography (Croce et al., 2018).

2.1.2 Model adaption for PV snow mitigation

In this study, the model is adapted to incorporate the heat flux transferred from the PV modules replacing a constant soil heat flux assumed to be 2 W/m2 in the standard model setup for natural settings. As mentioned in the introduction, the PV snow mitigation systems function by monitoring the snow load on the roof and applying heat to the modules when the snow load exceeds a threshold limit. The SWE the model estimates is analogous with the snow load in N/m^2. A condition is imposed that a melting heat flux from the PV panel is added to the snowpack when the snow load exceeds the threshold limit. The energy transferred to the snowpack is then calculated as the sum of hours with applied power as defined by Equation 1.

$$E_{cons} = \frac{\sum_i^T P_{PV}}{Y} \tag{1}$$

Where P_{PV} is the power per PV module area in W/m^2, T is the number of hours with applied power during the simulation, Y is the number of years in the simulation and E_{cons} is the total energy consumed per module area in Wh/m^2/year during the simulation. In this study, P_{PV} is set to 300 W/m^2 which is similar to what is used in existing PV snow mitigation systems. The model does not consider the erosion of snow from the roof (Liu et al., 2019) or passive heat loss from the building roof at the present time (Zhao et al., 2015).

2.1.3 PV snow mitigation model validation

To investigate the accuracy of the adapted energy balance snow model, a real snow melting event from a building with a PV snow mitigation system is simulated and compared with measured snow load data. The event occurred on a flat roof building in Porsgrunn, Norway. The building lacks structural capacity due to being designed for a lower snow load than given by current regulations. The building owners previously relied on manual snow removal after heavy snow fall, but decided to install a PV snow mitigation system in 2019. The PV system has an installed capacity of 1137 kWp and constitutes of 3670 modules. After installation, the maximum snow load limit was set to 80 kg/m^2. The roof snow load is monitored by 12 load cells connected to the PV mounting rack.

The investigated event is from a heavy snow fall that occurred on the 10th and 11th of March where the snow load increased from an average of 0 to 62.0 kg/m^2 with single sensors measuring as high as 77.6 kg/m^2. As the snow load was nearing the melting threshold and was still increasing, the operators decided to initiate melting at approximately 08:00 the morning of March 11th. Unfortunately, there is limited information on the timeline for applying power after 08:00 and if power was applied to the whole system at once or only parts.

To simulate the event, measured data from nearby weather stations is used as input in the energy snow balance model. The longwave radiation is estimated using a cloud-based radiation model for all sky conditions

(Liston & Elder, 2006). As the measured temperature on the PV modules is approximately 2°C lower than the temperature from the nearest weather station, the input temperature is applied a correction of -2°C. Melting is initiated at 08:00 with an applied power of 300 W/m^2 for the remainder of the simulation. The simulated and measured snow load is shown in Figure 3.

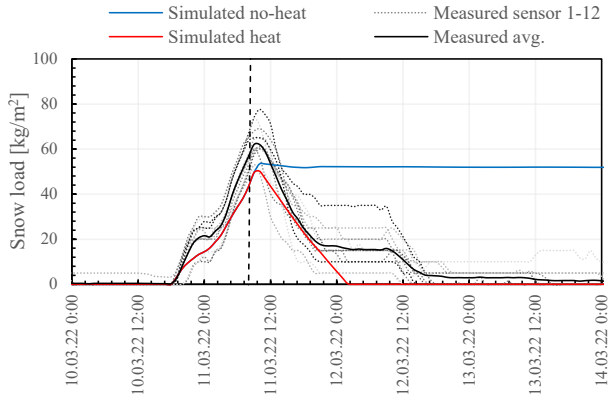

Figure 3. Measured and simulated snow load during a snow fall event in Porsgrunn, Norway. The vertical dashed line signifies when power was applied to the modules.

The simulated buildup of snow shows a good agreement with the measured snow load but builds up slightly slower and ends up 21.5% lower than the average peak load. When power is applied to the modules, the reduction of the snow load is delayed by approximately 2 hours both in the measurements and simulations. This likely occurs as energy is required to increase the temperature of the snowpack to 0°C (reducing the snowpack's cold content) before the energy induces melting of the snowpack and as it takes time for the water to drain. During melting, the snow load is reduced slightly slower than the measured load for an applied effect of 300 W/m^2. During the measurements, the snow load reduction ceases close to midnight on March 11th when the snow load is reduced to an acceptable level. On the morning of the 12th, melting is continued and most of the snow is melted. The simulations consistently apply power and do not capture these variations.

The comparison between measured and simulated snow load in the event indicates that both the buildup and melting of the snowpack are reproducible with the simulation method. However, the comparison is not sufficient to determine the energy efficiency of the system as data lacks for the timeline of applied power in the measurements.

2.1.4 Snow load melting thresholds

To generalize the method and make it applicable to different climates without case-specific knowledge of the structural capacity, the melting threshold defining when the PV heat flux is triggered is set using the return period concept as described in the introduction. To determine the return period snow loads, energy balance snow model simulations without any PV heat flux are performed for the four investigated locations. A distribution is fitted to the annual maximum snow loads of the dataset using the Akaike Information Criterion (Akaike, 2011). The return period loads are then obtained as the value with the desired probability of being exceeded. The distribution fit to the data for the four cities is shown in Figure 4 and the return period loads are shown in Table 2.

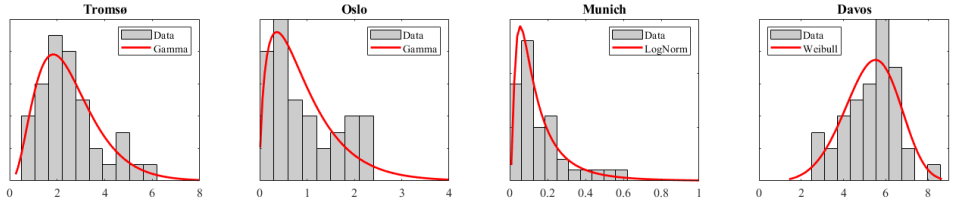

Figure 4. Histogram of maximum annual snow load in kN/m^2 with the best fitting distribution for the four investigated locations.

Table 2. Snow loads for a 50-, 30-, 20-, 10- and 5-year return period for the investigated locations in kN/m^2 as well as the Coefficient of Variation (COV) of the annual maximum loads.

Location	**Tromsø**	**Oslo**	**Munich**	**Davos**
Snow load distribution	Gamma	Gamma	Lognormal	Weibull
Return period snow loads				
S_{50}	5.9	3.0	0.7	7.9
S_{30}	5.4	2.7	0.6	7.5
S_{20}	5.0	2.4	0.5	7.3
S_{10}	4.3	1.9	0.4	6.9
S_5	3.5	1.4	0.2	6.4
$CoV_{annual\ max}$	0.54	0.77	0.85	0.24

Figure 4 shows that the simulated snow loads exhibit different characteristics for the different climates. For Munich, heavy snow loads occur infrequently and are best approximated by the lognormal distribution. In Tromsø and Oslo, the occurrence of heavy snow loads is more frequent and follows the gamma distribution best. In Davos, heavy snow loads occur frequently, best approximated with a Weibull distribution. The shape of the distributions influences the return periods snow loads given in Table 2. Distributions with longer tails (such as for Munich) contribute to a larger relative difference in the melting threshold compared to short tail distributions (such as for Davos).

As the PV system utilizes load capacity on the roof, the melting limit (S_{lim}) is the return period snow load subtracted by the self-weight of the PV system as defined in Equation 2:

$$S_{lim} = S_{return\ period} - g_{PV} \tag{2}$$

Where $S_{return\ period}$ is the return period load from Table 2 and g_{PV} is the self-weight of the PV system. PV systems commonly weigh between 0.1-0.5 kN/m^2, depending on mounting and roof ballast. Here g_{PV} is set to 0.2 kN/m^2, representing a system without heavy ballast. An example of how the melting limit influence the SWE for a single winter in Tromsø, Norway is shown in Figure 5.

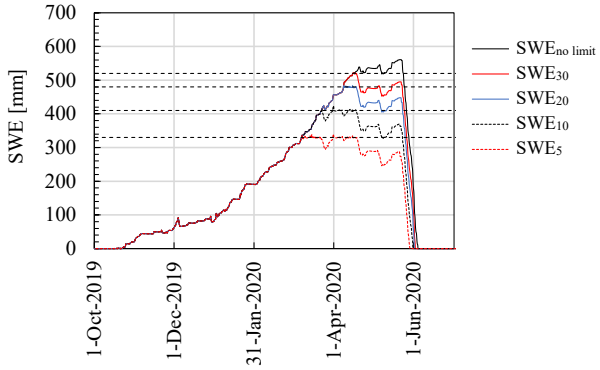

Figure 5. Single year simulation of SWE for different return period melting limits (subscript in legend) in Tromsø the winter of 2019-2020. The horizontal dashed lines signify the SWE threshold for when power is applied.

Here we see that the SWE is kept under the melting threshold. The snow cover duration is calculated as the number of hours with a snow cover larger than 2 mm SWE. This limit is chosen as light can be transmitted for snow covers of smaller magnitude than this, causing the module to produce power and passively shed snow (Pawluk et al., 2021).

2.2 PV yield simulations

To quantify the yield of PV snow mitigation systems, energy yield simulations are performed in PVsyst 7.2 (PVsyst SA, 2021). The system configuration and electrical design is set to be representable of typical PV snow mitigation systems with an east and west facing orientation with a module tilt of 10° as shown in Figure 1. A 100 kW string inverter is used with 21 strings and 19 modules per string on average. This yields a ratio between the nominal PV capacity and inverter power of approximately 1.25. The modules are the LR6-60PE 310M from Longi Solar and the inverter is the PVS-100-TL from FIMER. For climate and irradiance data, Meteonorm 8.0 is used. Meteonorm generates site specific data from ground stations and satellite data to generate hourly climate data. PV yield simulations are generally accurate with the largest uncertainty being the input irradiance (Urraca, 2018).

To account for the loss in power production due to snow covered modules (in this study referred to as *snow loss*), we use the snow cover duration from the energy balance snow model as input to PVsyst. The average monthly snow cover duration is calculated from the 41 years of simulated SWE and defined as monthly snow loss in PVsyst. Commonly, snow is cleared earlier from solar panels than a roof surface due to the module being tilted and having a low friction surface (Øgaard et al., 2021). However, PV snow mitigation systems are designed to retain the snow on the module surface and an assumption can be made that the snow duration on the modules is equal to the roof.

3 Results

The result section is divided into three sections. In section 3.1 the energy demand required to maintain the snow load below the threshold limit is presented, section 3.2 shows how the reduction of snow cover influences the power production and section 3.3 shows the net energy balance of PV snow mitigation systems.

3.1 Energy consumption

The yearly average energy consumption (E_{cons} as defined in equation 1) is shown in Figure 6a while Figure 6b shows the average annual snow load reduction amount (ΔS_{avg}). The energy amount used per kilo of mitigated snow is shown in Table 3.

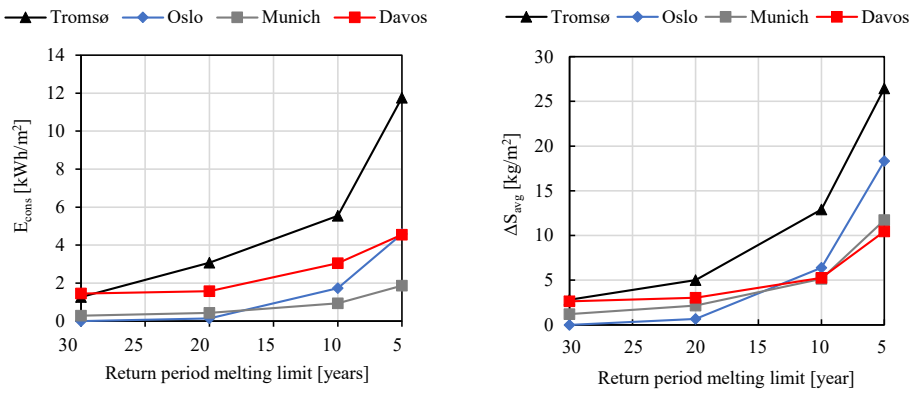

Figure 6. a) Average annual energy consumption (E_{cons}) and b) average annual snow load reduction amount (ΔS_{avg}) per year for a PV snow mitigation system with different return period melting limits.

Table 3. Average melting energy per kilogram of snow (E_{avg}) for the different locations.

Location	Tromsø	Oslo	Munich	Davos
E_{avg} [kWh/kg]	0.48	0.24	0.19	0.52

The amount of snow melted by the PV system (ΔS_{avg}) in Figure 6b shows an exponential increase with decreasing return period melting limits. Tromsø and Oslo exhibit an almost identical development in snow load reduction amount with a magnitude maximum ΔS_{avg} = 26.4 kg/m^2 and 18.3 kg/m^2 respectively. Munich and Davos have similar reduction amount (the maximum being ΔS_{avg} = 11.7 kg/m^2) and have a similar development with return period melting limits although they are characterized by very different snow load climates. This can be explained by ΔS_{avg} being dictated by the magnitude of the snow load as well as the shape of the distribution of the snow load. Higher magnitude snow loads contribute to more snow being removed from the roof and as well does the length of the distribution tail as longer tails result in a larger difference between the maximum snow loads and the melting limits. Although Davos has the highest snow loads, the short tail distributions reduce the snow load reduction amounts, contrary to Munich which has the lowest snow load with a long-tailed distribution. The result of this is that if normalizing the snow load reduction amount to the 50-year snow load, the longer tail distributions and high CoV's (such as Oslo and Munich) have a higher average snow load reduction amount than distributions with shorter tails with low CoV's (Such as Davos).

The melting energy per kilo of snow (E_{avg}) in Table 3 varies with climate. In general, higher snow load climates give a higher E_{avg}. This is influenced by snowfall and snow load reduction is more frequent in high snow load climates. The thermal mass of the snow results in more energy required to heat up the snow to reduce the snowpack's cold content before the energy is used to melt the snowpack as experienced in the validation case. Higher snow load climates commonly also have lower average temperatures which contribute to a larger amount of cold content in the snowpack. A high E_{avg} indicates a low efficiency of the active melting process. Variations in the climate-related efficiency contribute significantly to variations in the total energy consumption.

The average annual energy consumption (E_{cons}) in Fig. 6a is influenced by the snow load reduction amounts (as given in Figure 6b) and the efficiency of the system (Table 3). Tromsø has the highest snow load reduction amounts and a low melting efficiency giving the highest consumption (E_{cons} = 11.8 kWh/m^2). Davos has relatively stable snow load reduction amounts for the varying melting limits compared to the other climates but has the lowest efficiency. This results in stable and high energy consumption for all the melting limits in Davos (E_{cons} < 4.56

kWh/m^2). In Oslo, the snow load reduction amount increases strongly with melting limit and has the second highest consumption for the 5-year return period melting limit (E_{cons} = 4.59 kWh/m^2) although the efficiency is the second highest. Due to a poor distribution fit for high snow loads no melting occurs in Oslo for the 30-year return period melting. Munich has the lowest consumption for return period melting limits smaller than 20 years (E_{cons} < 1.87 kWh/m^2), due to having a small snow load reduction amount and high efficiency.

3.2 Influence of snow mitigation on power production

The energy yield of a PV system with a configuration as described in section 2.2 is simulated with snow losses obtained from the simulated snow cover duration from the energy balance snow model. The power production of a PV system without active melting is shown in Table 4, while Figure 7 shows the monthly snow loss.

Table 4. PV system power production for the four investigated locations. The yield is given by two measures which have a linear relationship. Specific yield (kWh/kWp/year) is commonly used in the PV discipline while E_{prod} (kWh/m^2/year) is in line with the units used in the rest of the study. The system design is described in section 2.2.

Location	Tromsø	Oslo	Munich	Davos
E_{prod} [kWh/m^2/year]	86	141	190	113
Specific yield [kWh/kWp/year]	456	751	1011	600

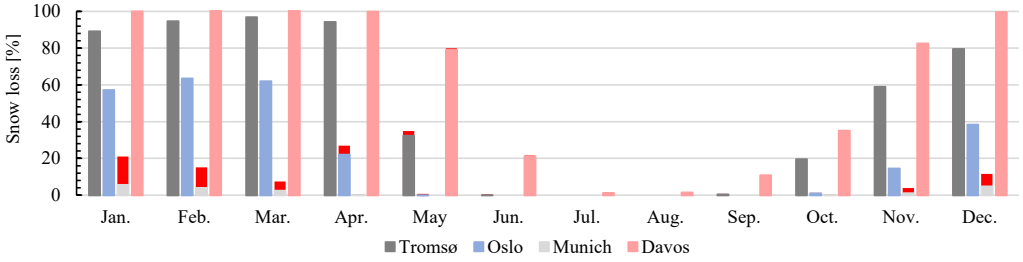

Figure 7. Monthly snow loss [%] obtained from the energy balance snow model. The difference in snow loss between the 5-year return period melting limit and no melting limit is illustrated by the red bars.

Figure 7 shows that the monthly snow loss varies significantly between the locations. Snow rich climates such as Tromsø and Davos have monthly snow losses of more than 80% for 5 months or more during the year. Oslo has more intermediate snow losses and is only above 50% for 3 months of the year. The snow losses in Munich are significantly smaller being less than 22% in the most snow rich month. The red bar shows the difference in snow losses between the 5-year return period melting limit and no melting limit. For Oslo, Tromsø, and Davos only small reductions in monthly snow losses occur in the spring months of April and May. Munich, however, which has a very low melting limit 5-year return period melting limit, experiences a more significant reduction in snow losses during all the winter months.

Table 4 shows that the production of the PV system (E_{prod}) shows an increase with decreasing latitude except for Davos. In high latitude climates, the irradiance is lower, and the snow losses are more significant. Davos has an abnormally low yield for its latitude and arises from the heavy snow losses for the largest parts of the year. The yield enhancement from the reduced snow cover duration is shown in Figure 8.

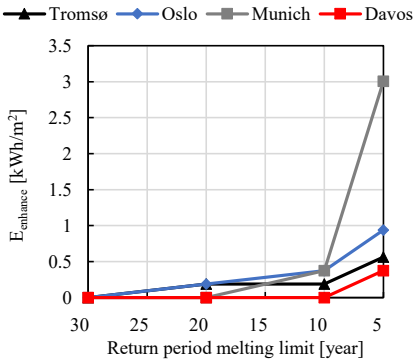

Figure 8. The yield enhancement ($E_{enhance}$) per year from the decrease in snow losses for different return period melting limits in relation to a PV system without snow mitigation (given in Table 3).

Here we see that the yield enhancement ($E_{enhance}$) is small for Oslo, Tromsø and Davos which show only minor difference in the monthly snow losses from snow melting ($E_{enhance}$ <1 kWh/m^2). The yield enhancement in Munich is low for the return period melting limit between 30-10 years but increase significantly for the 5-year return period melting limit ($E_{enhance}$ = 3 kWh/m^2). This occurs as the 5-year return period melting limit in Munich is so low that almost all snow is melted from the roof.

3.3 Net energy balance

The net influence of consumption and yield enhancement from snow melting ($E_{PV\ snow\ mitigation}$) is calculated according to Equation 3 and is shown in Figure 9.

$$E_{PV\ snow\ mitigation} = \frac{E_{enhance} - E_{cons}}{E_{prod}} \quad (3)$$

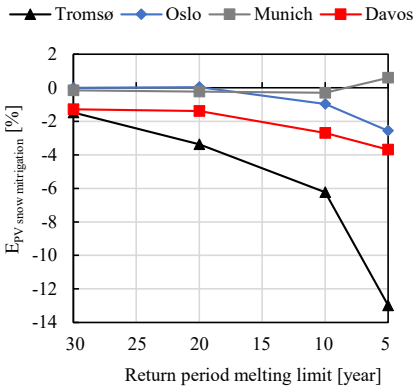

Figure 9. Simulated influence of actively mitigating snow ($E_{PV\ snow\ mitigation}$) for varying return period melting limits for the four locations.

The simulated influence of actively mitigating snow ($E_{PV\ snow\ mitigation}$) in Figure 9 is negative for most return period melting limits as the consumption exceeds the yield enhancement. The energy balance is lowest for the high snow load climates of Tromsø ($E_{PV\ snow\ mitigation}$ < -13 %) and Davos ($E_{PV\ snow\ mitigation}$ < -3.7 %) having a high energy consumption and little yield enhancement. Oslo has no energy consumption or yield enhancement for the 30-year return period melting limit due to a poor distribution fit for the high snow load data, and has a negative influence for the 20-, -10 and 5-year return period melting limits ($E_{PV\ snow\ mitigation}$ < -2.6 %). The energy balance in Munich is little influenced by the PV snow mitigation function for the return period melting limits of 30-, 20- and 10-years, but is positive for the 5-year return period melting limit ($E_{PV\ snow\ mitigation}$ < +0.6 %) as the enhancement exceeds the consumption.

4 Discussion

The results from this study show that the mechanisms which contribute to the net energy balance of PV snow mitigation systems strongly depends on the climate the PV system is situated in. For snow rich climates, the energy consumption dominates the energy balance as the yield enhancement is close to insignificant. The long-lasting winter results in that although the peak load is reduced, a significant amount of snow is still on the modules, and the influence on yield is small. Any increase in yield occurs in the spring months when the snow cover duration is shortened as less snow is necessary to be passively melted in order for the module to be cleared. However, the shortening of the snow cover duration is only in the magnitude of days and has a small total impact on the yield. The single year simulation in Figure 5 illustrates this clearly. For climates with little snow, reducing the peak load during mid-winter can significantly enhance the yield as significant snow melting can occur any month of the year, and the module surface can entirely be cleared. In this study, the system is operated to only reduce peak snow loads to ensure that the total load on the roof does not exceed the roof capacity but using the system with the intent of keeping a clear module surface may provide a larger positive energy balance. Nonetheless, the results indicate that the PV snow mitigation systems are more suitable for low snow load climates as less energy is needed to melt the snowpack and the yield can be enhanced significantly due to earlier snow clearance.

The results also indicate the suitability of PV snow mitigation systems to structures with different structural capacity here represented by the melting limit. In climates with significant snow loads, structures which are not severely lacking capacity is more suitable for PV snow mitigation systems as the melting limit strongly influences the consumption but not the yield enhancement. In low snow load climates, the differences in consumption with melting limit are smaller, and larger yield gains can be obtained for low-melting limits, resulting in melting limit having low influence on the energy balance.

To indicate the validity of the results, the simulated average energy amount per kilo of snow is compared to experimental values from previous studies of PV snow mitigation. A study from Anadol (2020) on the melting performance of PV modules with resistive wires presents the energy amounts required to melt snow. This study presents data from several melting episodes where the energy amount used to melt the snow as well as the snow depth is given, but not the density of the snow. If it is assumed that the density of the snow (which is specified to be freshly fallen) has a typical value of 100 kg/m^3 (Rohrer et al., 1994), an energy amount of 0.18-0.4 kWh/kg is calculated for snow load reduction between 4 and 9 cm and a module tilt of 10°. Aarseth et al. (2018) used payback time calculations with data from field measurements to study the energy economy of PV snow mitigation systems using the forward-bias method for modules with a tilt of 10°. In their study, an energy consumption of 0.05-0.15 kWh/kg is obtained through measurements, but no details of snow depth or density are given. In the present study, the simulated average energy amount is between 0.19-0.52 kWh/m^2 depending on the climate (Table 3). The simulated energy amount is thus similar to the values from Anadol (2020) and higher than given by Aarseth et al. (2018). Energy efficiency during melting is dependent on a number of factors including snow and air temperature, snow thickness, wind speed which can explain the range in values in both measurements and in the simulations. In order to increase the validity of the results presented here, more experimental data of the melting efficiency should be provided. In addition to the uncertainty in system efficiency, other uncertainties in the modelling approach include:

- neglecting snow erosion and roof heat loss in the energy balance snow model,
- coarse spatial resolution for the ERA5 data,
- inaccuracies in the unadapted energy balance snow model,
- suboptimal temporal resolution of snow losses in PVsyst (only monthly values).

The first three listed uncertainties have implications for the accuracy of the estimation of the SWE on the building roof for the specific locations. Neglecting snow erosion and heat loss in the energy balance snow model will contribute to an overestimation of the SWE. The impact of this simplification can be indicated by the s*hape coefficients* used in snow load design standards for buildings which are used to convert ground snow loads to roof snow loads. For flat roofs, a shape coefficient of 0.8 is used in the international, the European and the American design standards (ASCE, 2013; CEN, 2003; ISO, 2013), although this is suggested by field measurements to be a conservative estimate (Thiis & O'Rourke, 2015). Thus, the simulated SWE may overestimate the snow load by more than 20%, which can be expected to have a similar impact on the energy consumption.

Coarse spatial resolution in climate models generally leads to underestimation of climate extremes (Iles et al., 2020). However, as the average elevation of the grid cell is higher than the average location of the investigated cities, it can be argued that the coarse spatial resolution of ERA contributes to an overestimation of SWE in this study. For example, in Davos, the average elevation of the grid cell in ERA5 is 1999 m.a.s.l. when Davos actually resides at 1560 m.a.s.l. Moreover, incoming shortwave radiation in the ERA5 data might differ from actual values at Davos due to effects of orographic shadowing that are not adequately represented due to the coarse representation of topography in ERA5. Thus, the results likely overestimate the SWE for the location of the city, but may still underestimate the SWE for the area of the grid cell on average. Inaccurate simulated snow load can create biases in the energy consumption and the monthly snow losses used in the energy yield simulations. Future studies should account for the above-mentioned uncertainties to increase the accuracy of the simulating net energy balance of PV snow mitigation systems.

As research on rooftop snow mitigation systems progress, more complicated strategies for system operation than applying power when the snow load reaches the threshold limit will develop. Ideally, the strategy should take into account climatic conditions during melting as well as weather forecast to increase the chances of successfully reducing the load, minimizing the energy consumption and to achieve the desired level of structural safety (Diamantidis et al., 2018). Such strategies can involve melting during favourable conditions (i.e., in ambient temperatures above freezing) to create load buffers. This should be included in future work on PV snow mitigation systems.

5 Conclusions

Actively mitigating snow with PV systems is a measure to increase PV installation on existing roof surfaces which are indisposable for ordinary PV systems due to lacking structural capacity. The profitability of PV systems which mitigate snow is impacted by the energy used to mitigate snow, as well as how a reduced snow cover on the modules improves the yield. In this study, an adapted energy balance snow model and energy yield simulations are applied to quantify the energy consumption and yield enhancement of PV snow mitigation systems in different climatic conditions and environmental settings. To indicate the validity of the simulation method, the adapted energy balance snow model is used to reproduce a melting event with a PV snow mitigation system, showing good agreement with measured snow load data in the buildup and melting of the snow load. Simulated results with long time series of meteorological data show that in climates with significant snow loads the energy demand is high as significant amounts of snow are melted and snow losses are marginally reduced in spring, giving low yield enhancement. In climates with low snow loads, the energy demand is lower, and for low melting limits the yield enhancement is more significant. The relative influence on the energy production depends on the production of the PV system in the specific climate and is between +1% to -13% of the production of a system without active snow mitigation. The simulated energy efficiency of the active snow mitigation is compared with experimental values and exhibits a reasonable agreement, but more data on the system performance is required to increase the validity of the

findings. Future work on simulating energy consumption of PV snow mitigation with energy balance snow models should be improved to better represent the accumulated SWE on building roofs and to consider more advanced operation of the snow mitigation system.

References

Aarseth, B. B., Øgaard, M. B., Zhu, J., Strömberg, T., Tsanakas, J. A., Selj, J. H. & Marstein, E. S. (2018, 26 September 2018). Mitigating Snow on Rooftop PV Systems for Higher Energy Yield and Safer Roofs. *EU PVSEC 2018: 35th European Photovoltaic Solar Energy Conference and Exhibition*, Brusells.

Akaike, H. (2011). Akaike's Information Criterion. In Lovric, M. (ed.) *International Encyclopedia of Statistical Science*, pp. 25-25. Berlin, Heidelberg: Springer Berlin Heidelberg.

Anadol, M. A. (2020). Snow melting on photovoltaic module surface heated with transparent resistive wires embedded in polyvinyl butyral interlayer. *Solar Energy*, 212: 101-112. doi: https://doi.org/10.1016/j.solener.2020.10.073.

ASCE. (2013). *Minimum Design Loads for Buildings and Other Structures*.

CEN. (2003). *Eurocode 1, actions on structures—Part 1-3: General actions—Snow loads*. Brussels, Belgium.

Croce, P., Formichi, P., Landi, F., Mercogliano, P., Bucchignani, E., Dosio, A. & Dimova, S. (2018). The snow load in Europe and the climate change. *Climate Risk Management*, 20: 138-154. doi: https://doi.org/10.1016/j.crm.2018.03.001.

Croce, P., Formichi, P., Landi, F. & Marsili, F. (2019). Harmonized European ground snow load map: Analysis and comparison of national provisions. *Cold Regions Science and Technology*, 168: 102875. doi: https://doi.org/10.1016/j.coldregions.2019.102875.

Diamantidis, D., Sykora, M. & Lenzi, D. (2018). Optimising Monitoring: Standards, Reliability Basis and Application to Assessment of Roof Snow Load Risks. *Structural Engineering International*, 28 (3): 269-279. doi: 10.1080/10168664.2018.1462131.

Frimannslund, I. & Thiis, T. (2019). A feasibility study of photovoltaic snow mitigation systems for flat roofs. *Technical Transactions*: 81-96. doi: 10.4467/2353737XCT.19.073.10724.

Hersbach, H., Bell, B., Berrisford, P., Biavati, G., Horányi, A., Muñoz Sabater, J., Nicolas, J., Peubey, C., Radu, R., Rozum, I., Schepers, D., Simmons, A., Soci, C., Dee, D., Thépaut, J-N. (2018). *ERA5 hourly data on single levels from 1979 to present.* Copernicus Climate Change Service (C3S) Climate Data Store (CDS) (ed.).

Iles, C. E., Vautard, R., Strachan, J., Joussaume, S., Eggen, B. R. & Hewitt, C. D. (2020). The benefits of increasing resolution in global and regional climate simulations for European climate extremes. *Geosci. Model Dev.*, 13 (11): 5583-5607. doi: 10.5194/gmd-13-5583-2020.

Innos. (2022). *Innos AS*. Available at: www.innos.no (accessed: 18.01.2022).

ISO. (2013). *ISO 4355 Bases for design of structures, Determination of snow loads on roofs*: ISO. p. 42.

Jelle, B. P. (2013). The challenge of removing snow downfall on photovoltaic solar cell roofs in order to maximize solar energy efficiency—Research opportunities for the future. *Energy and Buildings*, 67: 334-351. doi: https://doi.org/10.1016/j.enbuild.2013.08.010.

Krinner, G., Derksen, C., Essery, R., Flanner, M., Hagemann, S., Clark, M., Hall, A., Rott, H., Brutel-Vuilmet, C., Kim, H., et al. (2018). ESM-SnowMIP: Assessing snow models and quantifying snow-related climate feedbacks. *Geoscientific Model Development*, 11: 5027-5049. doi: 10.5194/gmd-11-5027-2018.

Liston, G. E. & Elder, K. (2006). A Meteorological Distribution System for High-Resolution Terrestrial Modeling (MicroMet). *Journal of Hydrometeorology*, 7 (2): 217-234. doi: 10.1175/JHM486.1.

Liu, Z., Yu, Z., Zhu, F., Chen, X. & Zhou, Y. (2019). An investigation of snow drifting on flat roofs: Wind tunnel tests and numerical simulations. *Cold Regions Science and Technology*, 162: 74-87. doi: https://doi.org/10.1016/j.coldregions.2019.03.016.

Marke, T., Mair, E., Förster, K., Hanzer, F., Garvelmann, J., Pohl, S., Warscher, M. & Strasser, U. (2016). ESCIMO.spread (v2): Parameterization of a spreadsheet-based energy balance snow model for inside-canopy conditions. *Geoscientific Model Development*, 9: 633-646. doi: 10.5194/gmd-9-633-2016.

Melius, J., Margolis, R. & Ong, S. (2013). *Estimating Rooftop Suitability for PV: A Review of Methods, Patents, and Validation Techniques*. United States: Medium: ED; Size: 35 p. doi: 10.2172/1117057.

Meløysund, V., Lisø, K. R., Siem, J. & Apeland, K. (2006). Increased Snow Loads and Wind Actions on Existing Buildings: Reliability of the Norwegian Building Stock. *Journal of Structural Engineering*, 132 (11): 1813-1820. doi: doi:10.1061/(ASCE)0733-9445(2006)132:11(1813).

Meteonorm. (2020). *Features - Data sources*. Available at: https://meteonorm.com/en/meteonorm-features (accessed: 18.10.21).

Nuijten, A., Høyland, K. V., Kasbergen, C. & Scarpas, T. (2016). Modelling the thermal conductivity of melting snow layers on heated pavements. *8th International Conference on Snow Engineering*: 263-269.

Pawluk, R. E., Rezvanpour, M., Chen, Y. & She, Y. (2021). A sensitivity analysis on effective parameters for sliding/melting prediction of snow cover on solar photovoltaic panels. *Cold Regions Science and Technology*, 185: 103262. doi: https://doi.org/10.1016/j.coldregions.2021.103262.

PVsyst SA. (2021). PVsyst 7.2. route du Bois-de-Bay 107, Satigny, Switzerland.

Richards, E. H., Schindel, K., Bosiljevac, T., Dwyer, S. F., Lindau, W. & Harper, A. (2011). *Structural considerations for solar installers : an approach for small, simplified solar installations or retrofits*. United States. doi: 10.2172/1034886.

Rohrer, M. B., Braun, L. N. & Lang, H. (1994). Long-Term Records of Snow Cover Water Equivalent in the Swiss Alps: 1. Analysis. *Hydrology Research*, 25 (1-2): 53-64. doi: 10.2166/nh.1994.0019.

Sailor, D. J., Anand, J. & King, R. R. (2021). Photovoltaics in the built environment: A critical review. *Energy and Buildings*, 253: 111479. doi: https://doi.org/10.1016/j.enbuild.2021.111479.

Sexstone, G. A., Clow, D. W., Stannard, D. I. & Fassnacht, S. R. (2016). Comparison of methods for quantifying surface sublimation over seasonally snow-covered terrain. *Hydrological Processes*, 30 (19): 3373-3389. doi: 10.1002/hyp.10864.

Thiis, T. K. & O'Rourke, M. (2015). Model for Snow Loading on Gable Roofs. *Journal of Structural Engineering*, 141 (12): 04015051. doi: doi:10.1061/(ASCE)ST.1943-541X.0001286.

Urraca, R. H., Thomas; Lindfors, V. Anders; Riihelä, Aku; Martinez-de-Pison, Javier, Francisco; Sanz-Garcia, Andres. (2018). Quantifying the amplified bias of PV system simulations due to uncertainties in solar radiation estimates. *Solar Energy*, 176: 663-677.

VDMA. (2020). *International Technology Roadmap for Photovoltaic, Results 2019*.

Yan, C., Qu, M., Chen, Y. & Feng, M. (2020). Snow removal method for self-heating of photovoltaic panels and its feasibility study. *Solar Energy*, 206: 374-380. doi: https://doi.org/10.1016/j.solener.2020.04.064.

Zhao, M., Srebric, J., Berghage, R. D. & Dressler, K. A. (2015). Accumulated snow layer influence on the heat transfer process through green roof assemblies. *Building and Environment*, 87: 82-91. doi: https://doi.org/10.1016/j.buildenv.2014.12.018.

Øgaard, M. B., Aarseth, B. L., Skomedal, Å. F., Riise, H. N., Sartori, S. & Selj, J. H. (2021). Identifying snow in photovoltaic monitoring data for improved snow loss modeling and snow detection. *Solar Energy*, 223: 238-247. doi: https://doi.org/10.1016/j.solener.2021.05.023.

Paper V

Snow loss modelling for roof mounted photovoltaic systems: improving the Marion snow loss model

Øgaard, M., Frimannslund, I., Riise, H. & Selj, J.

Published in IEEE Journal of Photovoltaics 12 (2022)

https://doi.org/10.1109/JPHOTOV.2022.3166909

Supplementary paper I

A feasibility study of photovoltaic snow mitigation systems

Frimannslund, I. & Thiis, T.

Published in Technical Transactions 7 (2019)

https://doi.org/10.4467/2353737XCT.19.073.10724

TECHNICAL TRANSACTIONS 7/2019
CIVIL ENGINEERING
DOI: 10.4467/2353737XCT.19.073.10724
SUBMISSION OF THE FINAL VERSION: 14/06/2019

Iver Frimannslund orcid.org/0000-0002-7512-496X
iver.frimannslund@nmbu.no
Thomas K. Thiis orcid.org/0000-0002-0552-356X
thomas.thiis@nmbu.no
Department of Mathematical Sciences and Technology, Norwegian University of Life Sciences, Norway

A FEASIBILITY STUDY OF PHOTOVOLTAIC SNOW MITIGATION SYSTEMS FOR FLAT ROOFS

STUDIUM WYKONALNOŚCI FOTOWOLTAICZNYCH SYSTEMÓW OGRANICZANIA ŚNIEGU DLA DACHÓW PŁASKICH

Abstract

A new photovoltaic system combining electrical power production with snow mitigation intends to reduce the snow load on flat roofs. Applying electrical power to PV modules causes heat production on the module surface, allowing the ablation of snow. This study combines measurements and theoretical analysis to investigate which conditions are favourable for snow load reduction and discusses the system's feasibility to perform a controlled snow load reduction in a heavy snow load scenario for buildings with flat roofs. Both melting and sublimating of snow are investigated as means to reduce the load. The results show that the potential for load reduction is highly dependent upon weather conditions and snowpack characteristics during system operation. The refreezing of meltwater and water saturation of snow are identified as phenomena potentially preventing sufficient load reduction in cold conditions. Due to such temperature sensitivity, the system is likely to be more suitable for warm climates occasionally experiencing heavy snow loads than for climates with long and cold winters.

Keywords: snow, PV systems, load reduction, roofs, reliability, climate robustness

Streszczenie

Nowy system fotowoltaiczny łączący produkcję energii elektrycznej z ograniczaniem śniegu ma na celu zmniejszenie obciążenia śniegiem na dachy płaskie. Zastosowanie energii elektrycznej w modułach fotowoltaicznych powoduje wytwarzanie ciepła na powierzchni modułu, umożliwiając ablację śniegu. Niniejsze badanie łączy pomiary i analizę teoretyczną w celu zbadania, które warunki sprzyjają zmniejszeniu obciążenia śniegiem i omawia możliwości systemu w zakresie kontrolowanej redukcji obciążenia śniegiem w scenariuszu dużego obciążenia śniegiem dla budynków z płaskimi dachami. Zarówno topienie, jak i sublimacja śniegu są badane jako sposób na zmniejszenie obciążenia. Wyniki pokazują, że potencjał zmniejszenia obciążenia zależy w dużym stopniu od warunków pogodowych i charakterystyki śniegu podczas pracy systemu. Ponowne zamoczenie wody morskiej i nasycenie wody śniegiem są identyfikowane jako zjawiska potencjalnie uniemożliwiające wystarczające zmniejszenie obciążenia w niskich temperaturach. Ze względu na taką wrażliwość na temperaturę system może być bardziej odpowiedni do ciepłych klimatów, czasami doświadczając większych obciążeń śniegiem niż w klimatach o długich i zimnych zimach.

Słowa kluczowe: śnieg, systemy PV, redukcja obciążenia, dachy, niezawodność, odporność na klimat

1. Introduction

Due to climate change and the continuous updating of design standards, parts of the existing building stock are not well adapted to the environment in terms of reliability. Increased knowledge of the environmental loads imposed on buildings is the driving force for updating standards to better represent the actual loads occurring. The development of standards has led to many existing buildings being regarded as under-designed in the current design regulations. The temporal change of the ground snow load in Norway is an example which illustrates how increased knowledge influences our design standards. Meløysund et al. [17] describes how the ground snow load has developed from a general load with little variation, to a load varying with the local topography and the local climate. This is exemplified through the development of the ground snow load in Norway, which has evolved from being 1.5 kN/m^2 for the whole country in 1949 to ranging from 1.5–9.0 kN/m^2 in the current national annex [23]. The differentiation of the snow load results in many existing buildings being regarded as under-designed in the current regulations. Meløysund [16] states that 4.5 % of the total bulk of buildings in Norway may have too low a capacity according to current regulations.

In addition to the under-design of the existing building stock, a change in the environmental loads is expected due to climate change [3, 14, 21, 24, 25]. The global trend of climate change is that we will have increased winter temperature and winter precipitation. The increase in temperature will determine whether the precipitation falls as rain or snow, and will influence the change in the snow load [21]. For this reason, the snow cover in climates with mild winters should be more sensitive to an increase in temperature than climates with colder winters [15]. However, it is the case that even if the increased temperature leads to more precipitation falling as rain, it will not necessarily lead to a reduction of the snow load. This is due to the effect of snow absorbing the rain and increasing the load as a consequence [25]. Although it is predicted as a global trend that snow cover will reduce [11], several studies show that snowfall is expected to increase in cold areas [13, 22]. Croce [3] states that the sensitivity of snow cover to precipitation and temperature is highly related to topographic features such as the elevation aspect and terrain shading. On this basis, it is reasonable to assume that the change in snow load should be estimated on a regional scale. A report on the expected change in the characteristic ground snow load for Norway in the period 2071-2100 predicts that the snow load will be reduced for most municipalities, but thirty-four municipalities expect a significant increase in the load [14]. The authors of the report recommend that the characteristic snow load for the thirty-four municipalities should be increased.

The historical updating of standards due to increased knowledge of environmental loads together with the expected change in climate signifies a future discrepancy. Buildings are designed with a long life cycle of 50-100 years and are likely to experience a different environmental impact than what they are designed for.

If a building is under-designed with respect to snow load, there are certain measures which could be performed in order to increase the reliability of the structure. Structural health monitoring (SHM) can be performed at an early stage to determine the state of the

building and provide a basis for further improvements [4]. Retrofitting through upgrading the structural capacity of the building is a permanent measure, but often proves costly for the building owners. Manually removing snow off the roof is a measure which can be performed in the case of heavy snow loads, but relies on knowledge of the snow load on the roof and on having the available labour to remove the snow at the right time. Shovelling snow off roofs is also highly correlated with accidents [2, 12].

Buildings that are under-designed with respect to snow load are often prevented from having PV systems on the roof surface due to the additional weight. Roofs are especially suitable for having PV systems in urban environments due to them being large flat surfaces with high solar irradiation, favourable wind conditions and accessible for maintenance. Roof surfaces are often unutilised, even in densely populated areas.

2. Photovoltaic snow mitigation systems

Photovoltaic snow mitigation systems combine electrical power production with snow removal. If PV-cells are subjected to forward bias, heat is produced due to the electric resistance in the cells. The heat development on the surface of the PV-cell enables the ablation of snow and presents a new application for PV-systems. The photovoltaic snow mitigation system can serve the following three possible purposes:

- as a measure for under-designed roofs to increase snow load robustness,
- releasing roof area for PV-purposes previously indisposed due to limited load capacity,
- increasing yield of PV-systems through melting snow when the typical seasonal snowpack is present.

This study focuses on the first two purposes described above. The latter purpose has previously been briefly researched by Frimannslund [7] and more thoroughly by Aarseth et al. [1].

If the intent of the system is to reduce snow loads on flat roofs; the snow should be kept on the modules. Snow load reduction on flat roofs relies on melting the snowpack from the bottom up, and requires modules with a low angle tilt due to the sliding of snow. For increasing yield through removing snow from the modules, a tilt could be beneficial because sliding snow off the modules requires less energy than melting the entire snowpack.

Applying heat to the bottom of the snowpack will gradually increase the temperature of the snow towards 0°C. A thick snowpack reduces heat loss to the ambient environment, enabling a steady increase in temperature and a gradual melting process on the module surface. For load reduction to be effective, meltwater must be transported off the roof.

Sublimation, the instant transition from solid to vapour, can serve as another means of load reduction when melting is difficult. Sublimation occurs naturally in snow when there is a higher partial pressure of water vapour in the snowpack than in the air. The difference creates a gradient in specific humidity, causing transportation of mass from the snowpack to the air. The natural process of sublimation in the snow can simply be amplified by applying power to the modules when the conditions are right. A formula calculating latent heat flux due to sublimation illustrates the factors influencing the process:

$$Q_{BF} = \rho L_s C_E u_a \left(q_s - q_a \right) \quad (1)$$

where is the air density, is the latent heat of sublimation, is a transfer coefficient of latent heat, is the wind speed, is the specific humidity of the snow and is the specific humidity of the air. In order to induce the sublimation of snow on the PV-surface, the temperature should be close to, but never above, 0°C. Sublimation also occurs above freezing; however, this results in additional melting and necessary transportation of the meltwater. By keeping the temperature of the module close to zero, the partial pressure of water vapour in the snow increases, creating a vapour gradient and transportation of mass from the snow to the air. Sublimating snow is nevertheless far more energy consuming than melting snow. The energy required for sublimating snow at 0°C is equal to the combined energy it takes to melt and vaporise snow at 0°C [19]. The amount of energy required to induce a phase change in water is given by the latent heat constants presented in Table 1.

Table 1. Latent heat constant for phase changes in water [19, 27]

Phase change	Temperature	Latent heat constant [kJ/kg]
fusion	0°C	333.5
vaporisation	100°C	2257.0
sublimation	0°C	2830.0

The latent heat constant for sublimation is approximately 8.5 times higher than the latent heat constant for fusion. This means that it takes 8.5 times as much energy to sublimate water as it takes to melt it at 0 °C. Another way to put it is that you will have 8.5 times less ablation when sublimating compared to melting for the same energy input.

Applying forward bias to PV modules is a common way of checking the quality of the modules for defects in the manufacturing process. This is achieved with a limited electrical effect and is possible for any module regardless of the manufacturer. However, the degradation effects of applying forward bias to PV-modules over a long term is poorly documented.

In order to apply forward bias to PV-systems, rectifiers converting AC-current from the grid to DC-current are necessary. Alternatively, DC-current can be applied directly from batteries. PV modules are commonly designed with bypass diodes to only let the current pass one way, due to the unwanted effect of reverse bias. DC current must therefore be applied in the same direction as when producing power. Rectifiers are in principle the only additional component a normal PV-system needs to induce heat production on the module surface and use it for snow mitigation purposes.

In order for the photovoltaic snow mitigation system to become a widespread solution for under-designed roofs, it must be included in the framework of the international standards for structural design. The ISO standard for the determination of snow loads on roofs [10] provides a framework for reducing the design snow load based on a reliable control device or method able to reduce the snow load. The framework is presented in Annex F, entitled *Snow loads on roof with snow control*. To be able to reduce the designed snow load, the respective system's abilities for reducing the snow load for a given evaluation period must be documented.

3. Material and methods

3.1. Site description

Photovoltaic snow mitigation systems are a relatively recent invention and only a few buildings are equipped with such systems. One of the first buildings with a photovoltaic snow mitigation system installed on a flat roof was a warehouse building in Oslo, Norway. The system was designed by Innos AS and is called Weight Watcher [8]. The roof with the installed PV system is shown in Fig. 1. The system monitors the snow load imposed on modules through load sensors installed on the module rack. When the load reaches a certain limit, power is applied to the PV system and melting is initiated. The system was used for tests in this study, including a snow load reduction test and an aerial thermography of the system being applied forward bias.

The roof has a surface of approximately 1980 m^2 and is designed for a characteristic snow load of 1.5 kN/m^2. The PV system on the roof consists of 720 modules, orientated 66°/246° (East-North-East, West-South-West), each row facing the opposite direction of the previous row. The modules are tilted at an angle of 10°.

A customised drainage system is installed on the roof, designed for transporting meltwater off the roof surface. The drainage system is made of gutters between the rows of modules as

Fig. 1. The Weight Watcher system installed at the warehouse

illustrated in Fig. 1. Each gutter drains water from two rows and is heated in order to prevent the refreezing of meltwater. The gutters lead to the edge of the roof where water is disposed through scuppers.

3.2. Aerial thermography of a photovoltaic snow mitigation system

Thermography of the PV-system applied forward bias at the warehouse in Oslo was performed using a customised unmanned aerial vehicle with an infrared camera. The intent was to document the temperature distribution across the system and the location of possible hot spots and defects. The thermography was performed without an existing snow cover on the roof. Two maps were made showing the temperatures on the roof when half of the PV-system has forward bias applied. The maps were made by taking many single overlapping infrared images of the roof from heights of 50 and 30 meters. An infrared 3D-model was made by combining individual, infrared images using photogrammetric software for drone-based mapping [20]. The 3D model was then projected into the horizontal plane, creating 2D maps. The maps were calibrated for emissivity and atmospheric radiation [7, pp. 60-61] using FLIR Tools [6]. Calibration points were created on the roof surface, which was necessary to characterise individual modules on the uniform PV-system and to create the infrared 3D model.

3.3. Load reduction test of a full-scale photovoltaic snow mitigation system

A load reduction test of the full-scale facility at the warehouse was performed in February 2017. The objective was to test the performance of the snow mitigation system and to investigate the drainage system. The average snow depth on the day of testing was approximately 5 cm, which was too low to create a continuous snow cover across the modules, thus leaving the panels exposed to the wind. Due to the thin snowpack, the test cannot be said to be a true load reduction test. Load reduction is not usually necessary for snow loads less than the design snow load, which equals 75 cm of snow with an average density of 200 kg/m^3 for the warehouse roof. The test was performed not to reduce the load itself, but with the intent of documenting the physical process occurring when melting snow with PV-modules. The weather conditions on the day of the testing was partly cloudy with a temperature of -7 °C and an average wind speed of 6 m/s. The wind blew perpendicular to the rows of modules, from East-North-East. Three strings of modules were applied power for a duration of 2:00 hours. Temperature and humidity levels on the module surface and in the ambient environment were logged through the test.

3.4. Case study with single modules

In addition to testing the photovoltaic snow mitigation system at the warehouse in Oslo, a case study investigating different possible snow load reduction scenarios was performed. The purpose was to investigate the snow metamorphism occurring on the modules when applying forward bias of different intensities under varying climatic conditions. With three PV-modules, two rectifiers and the required cables, a system was setup in Nordmarka, Norway.

Fig. 2. Setup for the case study – the module to the left is a reference module, while the two to the right are active modules connected to rectifiers able to apply forward bias

Three different snow load reduction scenarios were performed:

- melting old, wet snow in ambient temperatures above freezing,
- melting fresh snow in cold conditions,
- sublimating snow in cold conditions.

The two melting cases were performed with a relatively high effect of 268.8 W/m^2 for the first case, and 762.5 W/m^2 for the second case. Both cases were conducted over the course of 3.5 hours each. Here, snow was shovelled onto the modules. The sublimation case was performed after a fresh snowfall of 14 cm. This case was conducted over a time span of 58 hours with an average effect of 29.8 W/m^2. The average air temperature was -9.3°C and the average humidity was 86.3%. The temperature of the modules was adjusted to be as close to zero as possible, without ever exceeding this limit. For all cases, temperature and humidity was logged in the top and bottom of the snowpack for both the unheated reference module and for the active modules. Ambient temperature and humidity was also logged. Load reduction was calculated using depth and density measurements both before and after applying forward bias.

4. Results

4.1. Aerial thermography of a photovoltaic snow mitigation system

The temperature maps were produced using aerial thermography of the photovoltaic snow mitigation system being applied forward bias. The thermography was conducted at the warehouse in Oslo when no snow was present. The first map provides an overview of the system with its surroundings.

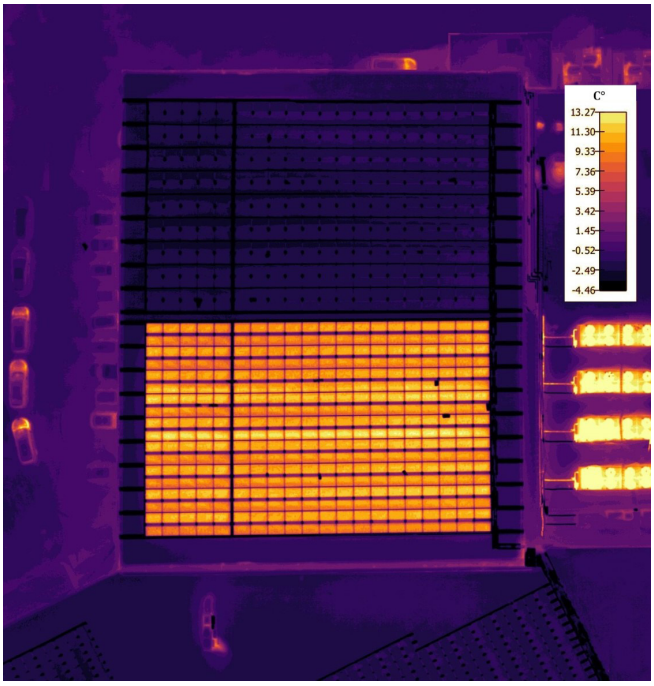

Fig. 3. Temperature map of the photovoltaic snow mitigation system; half of the system has forward bias applied

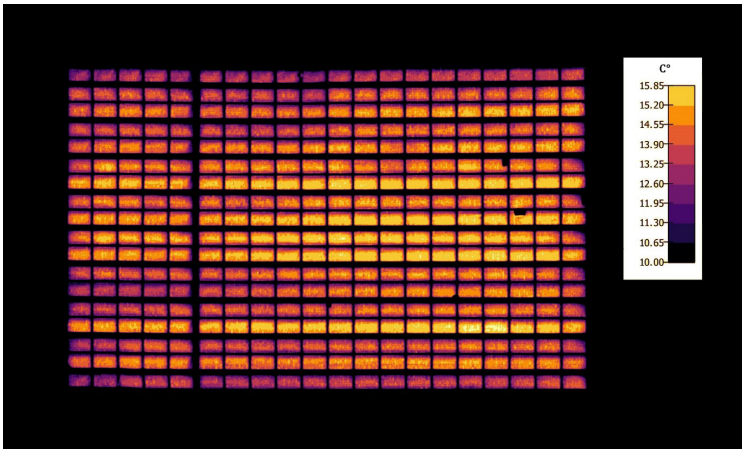

Fig. 4. Temperature map highlighting detail of the photovoltaic snow mitigation system with forward bias applied

The temperature map is created from 79 single images taken from a height of 50 m. The temperature scale is set to a wide range which includes the temperature of the surroundings. The map comprises surrounding objects such as recently used cars, smaller buildings at ground level, and the cooling system that is clearly running to the right on the map. The black dots at the modules are calibration points as described in Section 3.2.

The second map excludes the surroundings and amplifies the details of the modules emitting heat.

The temperature map is created from 68 single images taken from a height of 30 m above the roof. The temperature scale is set to a narrow range, amplifying the details and excluding the surroundings. In addition to the small temperature differences on the modules, there appears to be a pattern of equal temperatures in the strings of modules. Modules on the same string have similar temperatures, from one end to the other. The highest measured temperature on the PV-system was 15.85˚C, while the temperature of the air was approximately -4.7˚C [18].

4.2. Load reduction test of a full-scale photovoltaic snow mitigation system

Shortly after applying forward bias to the three strings, the temperature increased on the module surface. For the East-North-East rows facing the wind, the snow melted on the module surface only to be refrozen on the rim of the frame. An ice cap was created over the module, as shown in Fig. 5. Underneath the ice cap, there was liquid water, encapsulated by the module and the ice. The meltwater did not reach the heated gutters directly beneath the modules, and there was no significant load reduction. The refreezing of meltwater did not occur for the rows facing West-South-West, which were sheltered from the wind.

Fig. 5. An ice cap formed on the lower edge of the modules that were facing the wind. The heated gutter can be seen under the module, stretching towards the edge of the roof

4.3. Case study with single modules

The first case involved melting old wet snow in ambient temperatures above freezing. When forward bias was applied to the modules, the snow melted on the module surface and created a small layer of water-saturated snow on the module surface. The water drained

efficiently despite the module not having a significant tilt. In the second case, the layer of snow on the modules was from a recent snowfall and had the light, fine structure that fresh snow often has. The temperature was below 0°C when the experiment was conducted. In this case, snow melted on the module surface and a significant amount of meltwater was sucked into the capillary pores of the dry snow. At the end of this test, a 5-cm-thick layer of slush was observed at the bottom of the module as shown in Fig. 6.

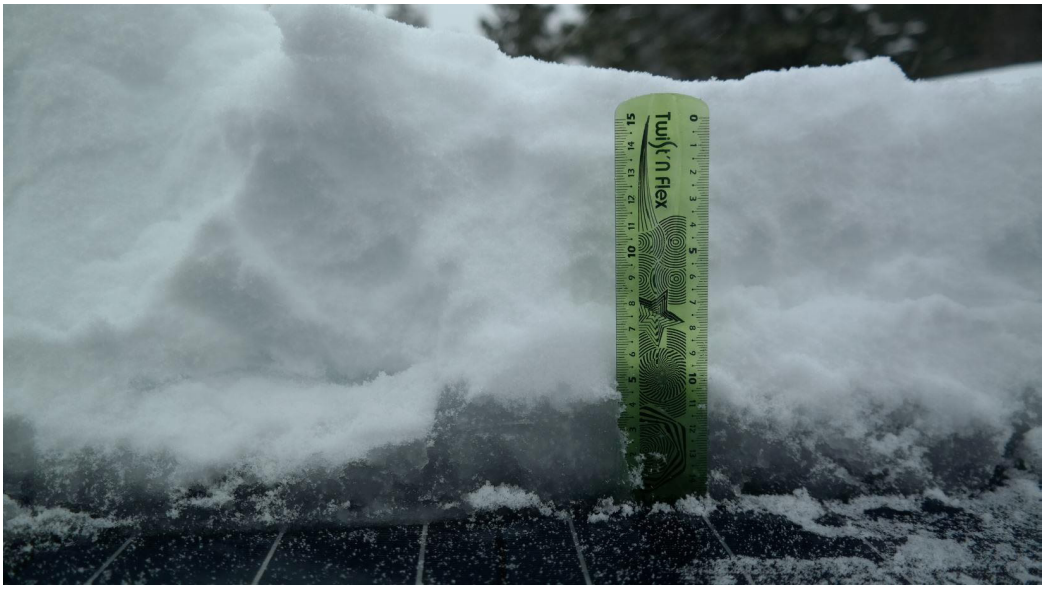

Fig. 6. A 5 cm slush layer was observed at the bottom of the snowpack at the end of the second melting test

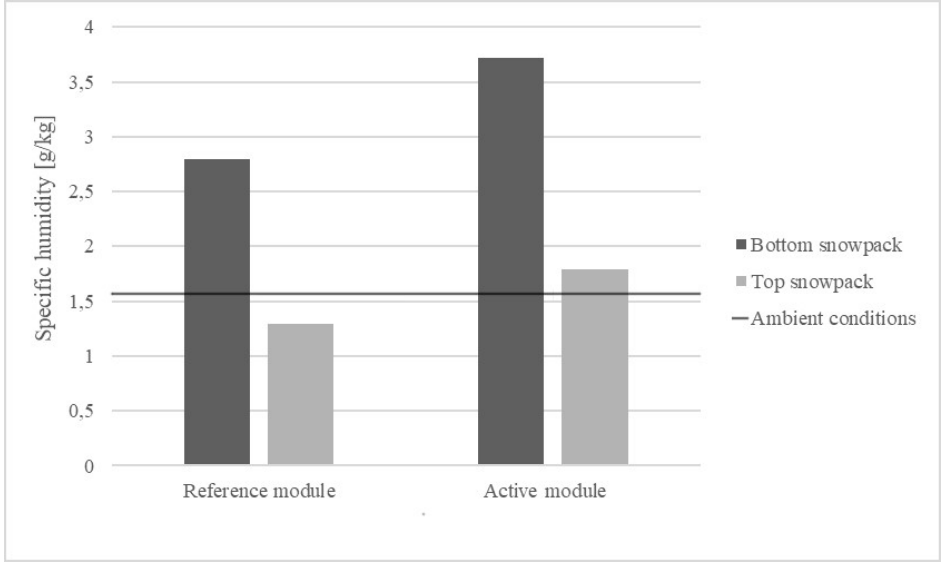

Fig. 7. Graph showing the average logged specific humidity of the reference and active module at the top and bottom of the snowpack in relation to the ambient conditions

The third case involved sublimating snow in cold conditions. At the end of the test, a clear dent in the snowpack was visible on the active modules, indicating a change in the snowpack. The temperature and humidity loggers document the change in specific humidity for the active and reference modules providing information indicative of the change in mass. Figure 7 illustrates the average specific humidity at the top and bottom of the snowpack based on the logged temperature and humidity.

The temperature and humidity loggers shows an increase in temperature on the module surface towards 0°C when forward bias is applied, and a corresponding increase in humidity in the snowpack. The partial pressure of vapour was highest at the bottom of the snowpack where heat was applied, and decreased towards the top of the snowpack. The partial pressure of water vapour for the modules applied forward bias was generally higher at the top of the snowpack than in the air, implying the transport of moisture from the snowpack to the air. For the reference module, the partial pressure of water vapour was higher for the air than the top of the snowpack, indicating condensation. This corresponds with measured changes in weight where the active module lost weight and the reference module gained a small amount of weight. The weight reduction was calculated by comparing the density and the snow depth measurements before and after the test. The average weight reduction for the active module was measured at 0.86 kg/m^2 per day. The total energy applied to the modules was 2299.2 kJ per kg of sublimated snow. At the end of the experiment, an ice sheet was uncovered on the surface of the active modules, although the loggers show that temperatures did not exceed zero. The ice sheet was thin and porous and covered the entire module surface.

5. Discussion

The results from the experiments highlight the importance and possible difficulties of transporting meltwater away from the roof due the risk of refreezing and water saturation of the snow. This is illustrated in the load reduction test at the warehouse, which resulted in meltwater freezing directly at the module. The refreezing of meltwater obviously contributes to insufficient load reduction, but it can also cause an unfavourable redistribution of load if water accumulates on the roof surface before refreezing.

However, the test at the warehouse is not entirely representative of a real snow load reduction scenario. Melting with the intent of reducing the snow load is only required for larger snow depths imposing a high load. The insulating effect of snow will increase the temperature on the module surface and will also provide shelter from the wind. Melting snow in cold conditions is therefore likely to be more easily performed for thick than for thin snowpacks.

The case study with single modules showed that the snow's capacity for being saturated with water is highly dependent on the microstructure of the snow, and is an important factor for the drainage conditions on the roof. The snow's ability to suck up meltwater on the module and roof surface inhibits the drainage of water and the subsequent load reduction. A slush layer on the module or roof surface will continue to delay the drainage until the snow is fully saturated and cannot hold more water. The case study showed that if the snow is fresh and

dry, it has a larger buffer capacity for holding water than older and more grainy snow. Draining meltwater from old and grainy snow, typically present in spring, is therefore likely to be less problematic than for snow with a fine microstructure that is typical of mid-winter conditions. Water saturation of the snow also increases the consequence for freezing of meltwater if the weather conditions change. If such a slush layer was to freeze, it could result in an ice sheet on the roof surface, further preventing drainage.

Poorly insulated roofs are subject to significant heat loss through the roof surface, increasing the temperature under a thick snowpack, favourable for drainage with respect to the refreezing of meltwater and the water saturation of snow. For roofs with significant insulation, heated gutters are recommended to improve the drainage conditions. Either way, a heat supply preventing the refreezing of meltwater in an unobstructed pitched flow path is crucial for the transportation of meltwater away from the roof when melting snow in cold conditions.

A phenomenon involving the formation of snow bridges over the PV-modules as melting is initiated was not observed in the load reduction tests, but it is a common occurrence in applications involving the melting of snow with heat cables in, for example, gutters and drains. If snow is melted from the PV-surface and the snow cover above does not collapse as the snow is melted away, a cavity can form between the PV-surface and the snow, forming a bridge of snow over the modules. The formation of such snow bridges can be reinforced by evaporating water from the roof or PV-surface condensation and freezing onto the snow. A cavity might also result in enhanced air infiltration, increasing the risk of freezing melt water. Such a phenomenon is dependent upon snowpack characteristics, weather conditions and the density of PV-modules on the roof surface.

As cold conditions can cause phenomena preventing the drainage of melt water; as revealed in the load reduction tests, the system is likely to be more suitable for warm climates occasionally experiencing heavy snow loads than for climates with long and cold winters.

The test of load reduction through sublimation indicates the potential for drainage free snow mitigation. Sublimation is conducive under cold and windy conditions, which is typically when melting is unfavourable. An amount of 0.86 kg/m^2 per day was sublimated in the case study with single modules. Although this is not much compared to the loads posing danger to roofs, the method can be improved with further knowledge of the phenomena and better control of the system, potentially resulting in more effective load reduction. Sublimation occurs naturally in snow and applying low magnitude forward bias to modules can simply amplify the sublimation if the conditions are right. This enables load reduction through cooperation with the ambient forces of nature. The amount of energy used for sublimation in the case study was calculated to be 19% lower than the latent heat of sublimation presented in Table 1, indicating a contribution of the ambient conditions. The ice sheet uncovered at the end of the experiment raises the question of whether induced sublimation on PV-modules is possible in the long term. The ice sheet indicates some sort of snow metamorphism which may prevent further load reduction. The sublimated snowpack was of a relatively shallow depth, contributing to a steep vapour pressure gradient between the snow and the air. A thicker snowpack results in a more gentle gradient and it is possible that the snow will be sublimated on the module surface only to be deposited further up in

the snowpack, never reaching the outside air. The question of whether it is possible to reduce the load by induced sublimation for thicker snow packs with photovoltaic snow mitigation systems has been poorly documented and should be further researched.

The results from the aerial thermography of the PV system with forward bias applied show that the relative temperature differences between modules and strings are of low magnitude. Temperature differences between string and modules do occur, but the relative temperature differences do not indicate any deficiencies in the system. Although highly dependent on the resolution of the map, typical infrared patterns from defects [9, 26] cannot be observed in the pictures, indicating a well-functioning system.

Reducing the snow load on under-designed roofs by applying electrical power to PV systems raises the question of how much energy is required to keep the roof safe, and whether the system is a sustainable and cost efficient solution to increase snow load robustness. The amount of energy required to keep the roof safe depends on the amount of energy used in a single load reduction, and how often it is necessary to reduce the load. The frequency of load reduction depends on what the building is designed for, hence the magnitude of under-design. The magnitude of the snow load imposed on buildings varies from one year to another, making load reduction unnecessary every year. This is one of the reasons why it is not necessary, with respect to safety, to melt the snow away as it accumulates. The long--term energy balance of reducing load and producing energy is little researched and should be investigated further. The potential for increasing the yield of PV systems through melting snow during the seasonal snowpack should be taken into account in this evaluation.

Photovoltaic snow mitigation systems are designed with the intent of reducing the snow load on flat roofs, but installing PV systems on roofs changes how snow accumulates and is distributed on the roof surface. In the design standards, different roof shapes have different shape factors determining the distribution of snow on the roof due to wind erosion and the sliding of snow [10]. A shape factor for PV systems on flat roofs is nevertheless still premature for most design standards. Research indicates that PV systems influence the friction velocity on the roof important for snow erosion, depending on the angle, height and distance between the rows of the panels [5]. The layout of the system, in combination with the prevailing wind direction on the site, can potentially result in an inhomogeneous snow load distribution compared to flat roofs without PV systems. In addition to this, having PV systems on flat roofs results in a bulk of snow laying on the module surface rather than on the surface of the roof itself. This decreases the effect of melting snow due to heat loss through the roof and increases the snow load compared to roofs without PV systems. This is especially significant for poorly insulated roofs. How PV systems change the distribution and magnitude of snow loads on flat roofs should be taken into account when assessing PV snow mitigation systems as a measure of increasing robustness to snow loads. Hopefully, future design standards will provide accurate calculation methods for how PV systems affect the snow load on roofs.

As mentioned in Section 2, Annex F in ISO 4355 presents a framework enabling a reduction in the design snow load for a reliable control device or method which slide or melt snow [10]. In order for the design snow load to be reduced, documentation guaranteeing load reduction must be provided. Such documentation is highly dependent

on the climate where load reduction is performed. The results from this study uncover phenomena important for snow load reduction that are applicable to similar climates. However, areas with very long and cold winters might experience additional problems that are not documented in this study. In general, it is necessary to conduct further studies of load reduction under varying climatic conditions before it can be used as a geographically widespread solution for snow load reduction.

Implementing a photovoltaic snow mitigation system on an under-designed roof and being dependent on a controlled snow load reduction severely influences the reliability of the roof. Building reliability is calculated to satisfy a predefined reliability level in the design standard, corresponding to the consequence of building failure. The variables used for dimensioning the structural components (e.g. resistance variables, permanent actions and climatic loads) have a certain statistical probability for occurring. When a PV snow mitigation system is installed on a roof, the dead load on the roof increases and the dependence of the controlled snow load reduction is added. The snow mitigation system itself has a certain probability for providing sufficient load reduction in a heavy snow load scenario, which must be taken into account in the reliability calculation. The probability of sufficiently reducing the load depends on the temporal efficiency of load reduction, and possible events interrupting the reduction (technical malfunctions, power outages, climatic conditions). Such risk factors must be identified and implemented in a reliability model for the structural safety of the building before the system can become a widespread solution for under-designed roofs.

6. Conclusion

The state of the existing building stock and the expected change in the future climate calls for new measures for under-designed roofs. Photovoltaic snow mitigation systems combine power production with snow removal by applying forward bias to the system. The results from this study show that reducing the snow load on flat roofs with photovoltaic snow mitigation systems is possible. The feasibility of load reduction is, however, highly dependent on the climatic conditions during system operation. The possible refreezing of meltwater and water saturation of snow are possible outcomes which can prevent sufficient load reduction and possibly result in an unfavourable load distribution. Melting in ambient temperatures above freezing is less problematic with respect to drainage of meltwater and it is naturally less energy consuming than melting in cold conditions. Melting a thicker snowpack in cold conditions is yet to be tested on a full-scale PV system. Reducing the snow load in ambient temperatures above freezing is therefore likely to be effective, while melting in cold conditions provides more risk due to the possible refreezing of meltwater and the water saturation of snow. For this reason, the system is likely to be more suitable for warm climates occasionally experiencing heavy snow loads, than for climates with long and cold winters. Tests of load reduction through sublimation indicates a potential new strategy for snow removal when conditions are cold and windy, typically unfavourable for melting. It is, however, unknown whether load reduction through induced sublimation is possible for thicker snow packs and

if it will function in the long term due to the metamorphism of snow at the bottom of the snowpack. The load reduction tests nonetheless highlight the importance of cooperating with the weather conditions to perform sufficient and energy-efficient snow removal. Before the photovoltaic snow mitigation system can become a widespread solution for under-designed roofs, it is crucial to investigate the long-term effect of applying forward bias to PV modules and provide documentation for the system's load reduction capabilities to be used in structural design standards. In addition to this, the long-term energy balance of reducing snow loads and producing energy should be researched in order to determine the system's sustainability as a measure to increase snow load robustness.

Our appreciation to Tommy Strömberg at Innos AS for welcoming us to research the Weight-Watcher system and for providing equipment for scientific measurements.

References

[1] Aarseth B.B., Øgaard M.B., Zhu J., Strömberg T., Tsanakas J.A., Selj J.H., Marstein E.S., *Mitigating Snow on Rooftop PV Systems for Higher Energy Yield and Safer Roofs*, presented at EU PVSEC 2018: 35th European Photovoltaic Solar Energy Conference and Exhibition, Brusells 2018.

[2] Bylund P.-O., Johansson J., Albertsson P., *Injuries sustained during snow removal from roofs resulting in hospital care*, International journal of injury control and safety promotion, Vol. 23, 2016, 105–109.

[3] Croce P., Formichi P., Landi F., Mercogliano P., Bucchignani E., Dosio A., Dimova S., *The snow load in Europe and the climate change*, Climate Risk Management, Vol. 20, 2018, 138–154.

[4] Diamantidis D., Sykora M., Lenzi D., *Optimising Monitoring: Standards, Reliability Basis and Application to Assessment of Roof Snow Load Risks*, Structural Engineering International, Vol 28(3), 2018, 269–279.

[5] Ferreira A., Thiis T.A., Freire N., *Experimental and computational study on the surface friction coefficient on a flat roof with solar panels*, Proceedings of the 14th International Conference on Wind Engineering, Vol. 12, 2015.

[6] FLIR, http://www.flir.eu/home (accessed: 01.02.2017).

[7] Frimannslund I., *Measurements and analysis of snow load reduction on flat roofs using a photovoltaic system in heating mode*, in *Department of Mathematical Sciences and Technology*, Norwegian University of Life Sciences, 2017, p. 157.

[8] Innos AS, www.innos.no (accessed: 18.10.18).

[9] International Electrotechnical Commission, IEC 62446. Grid connected photovoltaic systems – Minimum requirements for system documentation, commissioning tests and inspection, 2009.

[10] International Organization for Standarization, ISO 4355 Bases for design of structures, Determination of snow loads on roofs, 2013.

[11] IPCC, *Climate Change 2013: The Physical Science Basis. Report by WG1AR5*, 2013.
[12] Kamimura S., *Risk analysis on snow-related casualty cases in Niigata Prefecture, Japan*, presented at Snow Engineering V: Proceedings of the Fifth International Conference on Snow Engineering, 5–8 July, Davos, Switzerland, 2004, CRC Press.
[13] Krasting J.P., Broccoli A.J., Dixon K.W., Lanzante J.R., *Future Changes in Northern Hemisphere Snowfall*, Journal of Climate, Vol 26(20), 2013, 7813–7828.
[14] Kvande T., Tajet H.T.T., Hygen H.O., *Klima- og sårbarhetsanalyse for bygninger i Norge – Snølast og våt vinternedbør*, SINTEF Byggforsk, 2013, p. 44.
[15] Lemke P., Ren J., Alley R.B., Allison I., Carrasco J., Flato G., Fujii Y., Kaser G., Mote P., Thomas R.H., et al., *Observations: Changes in Snow, Ice and Frozen Ground*, 2007, 337–383.
[16] Meløysund V., *Prediction of local snow loads on roofs*, in *Department of Structural Engineering*, Norwegian University of Science and Technology, Trondheim 2010, p. 42.
[17] Meløysund V., Karl V.H., Bernt L., Lisø K.R., *Economical effects of differentiated roof snow loads*, [in:] *Proc. of the 6th International Conference on Snow Engineering*, Engineering Conference International, New York 2008.
[18] Meteorologisk Institutt, www.eklima.no (accessed: 24.10.18).
[19] Oke T.R., *Boundary layer climates*, Second edition, Routledge, London 1987, p. 460.
[20] Pix4D, https://pix4d.com (accessed: 30.10.2016).
[21] Räisänen J., *Warmer climate: less or more snow?*, Climate Dynamics, Vol. 30(2), 2008, 307–319.
[22] Räisänen J., Eklund J., *21st Century changes in snow climate in Northern Europe: a high-resolution view from ENSEMBLES regional climate models*, Climate Dynamics, Vol. 38(11), 2012, 2575–2591.
[23] Standard Norge, NS-EN 1991-1-3:2003+NA:2008.
[24] Steenberg R.D.J.M., Geurts C.P.W., Bentum C.A., *Climate change and its impact on structural safety*, Heron, Vol. 54(1), 2009, 3–35.
[25] Strasser U., *Snow loads in a changing climate: new risks?*, Natural hazards and Earth System Science, Vol. 8(1), 2008, 1–8.
[26] Testo, *Practical Guide, Solar Panel Thermography*, New Jersey 2014, p. 19.
[27] Tipler P.A., Mosca G., *Physics For Scientists and Engineers*, 6th ed. W.H. Freeman and Company, New York 2008.

If you want to quote this article, its proper bibliographic entry is as follow: Frimannslund I., Thiis T. K., *A feasibility study of photovoltaic snow mitigation systems for flat roofs*, Technical Transactions, Vol. 7/2019, pp. 85–100.

ISBN: 978-82-575-2030-4
ISSN: 1894-6402

Norwegian University
of Life Sciences

Postboks 5003
NO-1432 Ås, Norway
+47 67 23 00 00
www.nmbu.no

115555 / ANDVORDGRAFISK.NO